Forest&Wood Products Australia
Knowledge for a sustainable Australia

PRODUCTS & PROCESSING

PROJECT NUMBER: PNB034-0506 APRIL 2010

The durability of isocyanate-based adhesives under service in Australian conditions. The results from a 3 year exposure study and accelerated testing regime

This report can also be viewed on the FWPA website
www.fwpa.com.au
FWPA Level 4, 10-16 Queen Street,
Melbourne VIC 3000, Australia
T +61 (0)3 9927 3200 F +61 (0)3 9927 3288
E info@fwpa.com.au W www.fwpa.com.au

The durability of isocyanate-based adhesives under service in Australian conditions. The results from a 3 year exposure study and accelerated testing regime

Prepared for

Forest & Wood Products Australia

by

K. Van Langenberg, P. Warden, C. Adam and H.R. Milner

Publication: The durability of isocyanate-based adhesives under service in Australian conditions. The results from a 3 year exposure study and accelerated testing regime

Project No: PNB034-0506

This work is supported by funding provided to FWPA by the Australian Government Department of Agriculture, Fisheries and Forestry (DAFF).

This work is supported by funding provided to FWPA by the Department of Agriculture, Fisheries and Forestry (DAFF).

ISBN: 978-1-921763-00-7

Principal Researcher:

K. Van Langenberg, P. Warden
CSIRO Materials Science & Engineering
Bayview Avenue,
Private Bag 10, Clayton South, Vic, 3169

C. Adams, H. R. Milner
Timber Engineering Centre
Monash University
Clayton, Vic, 3168

Final report received by FWPA in April, 2010

Forest & Wood Products Australia Limited
Level 4, 10-16 Queen St, Melbourne, Victoria, 3000
T +61 3 9927 3200 F +61 3 9927 3288
E info@fwpa.com.au
W www.fwpa.com.au

EXECUTIVE SUMMARY

Objective

The objective of this study was to evaluate the durability of four isocyanate-based adhesives (IBAs) relative to a phenol-resorcinol-formaldehyde (PRF) control. One of the tests used to evaluate durability determined the residual bond strengths of the adhesives after 12 months and 36 months exposure in either an environmental chamber or in an outdoor field site in the tropics. Five accelerated test methods were also investigated (2 delamination tests, a cleave test, a longitudinal lap shear test and a moisture resistance test) to determine the correlation between these tests and the 12 month exposure results. Three Australian wood species Radiata Pine (*pinus radiata*), Victorian Ash (*Eucalyptus regnans*) and Spotted Gum (*Corymbia citriodora subsp. Variegata*) were studied. The hygro-mechanical responses of thin films of the adhesives were also studied to elucidate the mechanism of durability.

Key Results

The major results of the study were that:

- none of the adhesives suffered a significant strength loss after 3 years exposure in the Radiata Pine samples
- all of the adhesives suffered a significant strength loss after 3 years exposure in the Spotted Gum samples
- in general, the adhesives suffered a strength loss of between 25 and 35% after 3 years exposure in the Victorian Ash samples.
- the Darwin outdoor exposure field site provided a harsher environment than the environmental chamber
- no significant difference in the performances of the PRF and isocyanate-based adhesives was apparent after 3 years exposure
- positron annihilation lifetime spectroscopy (PALS) experiments on the exposed samples demonstrated that this technique can determine between the wood and adhesive and can detect weathering of the bondline. Further work is required to develop this technique
- the two delamination tests (taken from AS/NZS 4364:1996 and CSA O112.9-04) appeared to demonstrate differences between the adhesives. All of the adhesives performed badly with Spotted Gum, with very high levels of delamination in both tests. There was a species dependency for some of the IBAs with notable differences in performance in the Radiata Pine and Victorian Ash samples. Whereas some of the IBAs performed as well as the PRF control, others did not. There are discrepancies between the outcomes of the two delamination tests
- the cleave test (as described in AS/NZS 1328.1:1998) on Radiata Pine and Victorian Ash samples demonstrated that with the majority of the IBAs evaluated, a decrease in wood fibre failure values occurs when tested in the wet condition. The PRF control adhesive was little affected by moisture. In

the case of the Spotted Gum, all of the adhesives gave low wood fibre failure values in both the dry and wet conditions

- lap shear samples that had been exposed to either cold or boiling water soaks did not demonstrate any degradation of adhesive strength after having been redried
- there was no statistically significant difference between any of the adhesives when tested for heat and moisture resistance as prescribed in ASTM D4502
- the hygro-mechanical responses of thin films of the adhesives were outwardly different to those previously reported in the literature, necessitating both further investigation of the theoretical framework and the use of mechanical methods of controlling the relative humidity as opposed to the current method of using saturated salt solutions. There were sufficient differences in the data to indicate that the mechanical properties of IBAs and PRFs differ and that these differ from the wood substrate. Although outside the requirements of the project, based on hypothetical parameters and finite element analysis, indications are given of the type of inferences that can be drawn from such work in relation to the levels of bondline stress that can be generated under varying climatic conditions. Accurate property values for the adhesives and underlying wood substrates, described within a common theoretical framework, are required to complete this work.

Application of Results

At this stage, after 3 years exposure, the general lack of significant adhesive strength loss in the Radiata Pine and Victorian Ash samples prevents correlations being made between the likely longer-term performance of the adhesives and their performance in the accelerated tests. Differences in adhesive durability when used with these species may begin to become apparent following further exposure. The substantial losses in bond strength for all the adhesives in Spotted Gum samples during the 12 month exposure period, and their poor performance in the accelerated tests, reflects the known difficulty in achieving durable bonds with this species. The degree of strength loss and variability in the recorded data prevent specific correlations being made between test outcomes for the adhesives in this species. Based on the lack of statistically significant differences between the adhesives, it appears that there is no difference between the IBAs and the PRF after 3 years.

The results of the accelerated tests indicated differences in the relative performances of the adhesives, both between the IBAs and between the IBAs and the PRF control. Of particular concern is the difference in results obtained in the two delamination tests. The two methods have been included as alternatives in the new AS/NZS 4364 (Int):2007 and draft ISO standard on the performance of wood adhesives, and are being regarded as equivalent. In view of the questions raised by some of the data, it is recommended that further work be undertaken to determine whether other discrepancies might exist in the proposed test methods. Future work is also required in developing the theoretical framework for determining the hygro-mechanical response of thin adhesive films.

Table of Contents

INTRODUCTION

The work reported here is part of the FWPA project "*PNO05.2015 Durability of isocyanate-based adhesives in engineered wood products*", which is being conducted collaboratively by CSIRO and Monash Timber Engineering Centre, Monash University. The project was initiated to investigate if, under Australian service conditions, isocyanate-based adhesives (IBAs) are suited to use in structural wood products made from Australian timber species. There is considerable interest amongst Australian manufacturers of structural wood products in the use of IBAs as a replacement for the traditional phenolic-based adhesives. Key drivers for this include:

- IBAs are typically fast and cold curing, allowing for the potential to improve productivity and reduce product reject rates
- IBAs cure to a clear or wood-coloured bond line making the finished product more appealing to the end-user
- The potential to utilise wood species that have been traditionally regarded as difficult to glue reliably with phenolic-based adhesives
- The use of phenolic-based adhesive systems can result in the generation of effluent streams with high potential environmental impact

A further important driver for the current work is the international shift in standards for the development of adhesively-bonded engineered wood products (EWP). This has seen a change in the standards from being prescriptive with regards to adhesive type, to performance-based without any reference to adhesive type. Performance-based standards for adhesives are being developed in a number of jurisdictions (e.g. USA, Europe, Canada, Australia) and internationally (ISO) that would formally permit the introduction of IBAs subject to meeting specified performance criteria under given test conditions. Questions have been raised as to whether the proposed test methods adequately assess IBAs. This project has provided a unique opportunity to put the test methodologies and acceptance criteria under close examination.

This project is aimed at developing a level of understanding of the performance of IBAs when used to bond Australian wood species and used in Australian conditions. To achieve this, a 3 year exposure experiment using two different exposure conditions was set up to monitor any degradation of four IBAs compared to a PRF control. The adhesives were used to bond laminated beams of three wood species currently used in Australia, namely Radiata Pine (*pinus radiata*), Victorian Ash (*Eucalyptus regnans*) and Spotted Gum (*Corymbia citriodora subsp. Variegata*). Samples were taken from the exposed beams to determine whether any potential degradation of the adhesive can be detected at the molecular level before it manifests itself as a loss of adhesive bond strength. This was studied using Positron Annihilation Lifetime Spectroscopy (PALS) which has been very successful in visualising polymer fatigue long before it

can be detected on the macro scale.[1,2] The relative performances of the adhesives have been evaluated using a number of established short-term accelerated aging tests with the aim of identifying how the results from these tests correlate with the longer-term exposure results. A further part of this project is the investigation of the behaviour of thin films of these adhesives and their response to changes in environmental conditions, particularly moisture.

RECOMMENDATIONS AND CONCLUSIONS

The primary objective of this project was to determine the durability of isocyanate-based adhesives (IBAs) relative to a phenol-resorcinol-formaldehyde (PRF) adhesive after exposure periods of 1 and 3 years to two different environmental conditions. The first involved subjecting test beams to a repeating cycle of 2 weeks at 50°C and 80% RH followed by 2 weeks at ambient Melbourne conditions. The second environmental condition consisted of full exposure of test beams to tropical weather in an outdoor field trial. The outdoor exposure site was situated in Darwin, Australia. In both environmental conditions, half of the test beams were loaded in four point bending while the other half of the test beams were not loaded. Four different IBAs and a PRF were tested using three different Australian wood species. The wood species investigated were Radiata Pine (*pinus radiata*), Victorian Ash (*Eucalyptus regnans*) and Spotted Gum (*Corymbia citriodora subsp. Variegata*).

The results of the three year exposure study were found to be highly dependent on which of the timber substrates were used.

The Radiata Pine results were based on the environmental chamber site as many of the beams exposed at the Darwin site were found to be seriously degraded through decay of the timber, resulting in only a few testable samples. The few results obtained from Darwin, however, were qualitatively similar to the environmental chamber results.

There were some differences in performance between the adhesives but these appeared to be minor. There was no significant loss of strength for any of the adhesives after 3 years. Of interest to note was the fact that the PRF and one of the IBAs appeared to increase in strength. This result was a surprise and cannot be explained at this stage. Certainly, this anomalous result was not seen for the other wood species.

Whilst some difference in the percentage of retained strength was observed between the adhesives, there was no statistically significant difference between the adhesives when the mean residual strengths were compared.

---

[1] B. Tiganis, L. Burn, A. Hill, "Degradation of acrylonitrile butadiene styrene blends", *J. Polym. Degradation and Stability*, **76**, 2002, 425

[2] A. Hill, M. TAnt, L. McGill, P. Shang, R. Stockl, D. Murray, J. Cloyd, "Free volume distribution during consolidation and coalescence of latex films", *Journal of Coatings Technology*, **73**, 2001, 115

The Spotted Gum samples were found to be the other extreme case. All of the adhesives displayed significant loss of strength, with many of the specimens failing after 12 months of service.

The Victorian Ash samples were found to behave between the two extremes described above. All of the adhesives displayed a loss of strength after 3 years. The Darwin site appeared to be a harsher environment for the samples. The loss of strength was observed to be approximately 25-35% with the exception of one of the IBAs which showed only *ca* 5% strength loss. Whilst some differences between the adhesives were starting to manifest, the 3 year timeframe was too short to identify statistically significant trends.

In looking at all of the results across the three timber substrates and two exposure conditions, it appears that the IBAs are comparable in performance to the PRF. This conclusion needs to be treated with caution however, since the results are based on only three years of exposure data. It is recommended that Darwin exposure site experiment with the Victorian Ash substrate be continued and the samples tested after at least 5 years and preferably after 7-10 years. This should allow any statistically significant trends, if present, to emerge. There are currently additional Victorian Ash samples being exposed in Darwin that have already had 3 years of exposure.

The second objective of this project was to screen a number of accelerated test methods prescribed in various national standards to determine whether they could be used to effectively differentiate the adhesives on the basis of durability. These test methods would be expected to demonstrate a high level of correlation with the exposure results. Five test methods were investigated: two delamination tests, a cleave test, a longitudinal lap shear test and a moisture resistance test.

The first delamination procedure was taken from AS/NZS 4364:1996. All of the Spotted Gum samples demonstrated very high levels of delamination with no significant difference between the adhesives. A large variation existed in the results from bonded radiata pine samples. The PRF adhesive gave very low levels of delamination with an average of 0.7%. One of the IBAs was comparable to the PRF with an average delamination level of 1.6%. The other 3 IBAs all had much higher levels of delamination which lay in the range of 8.2-25.7%. The PRF adhesive also performed very well with Victorian Ash samples with a very low average delamination of 0.3%. Three of the IBAs performed very well with Victorian Ash with delamination averages ranging from 2.9-5.2%. The remaining IBA had a much higher level of delamination (12.8%) but there were some concerns regarding the validity of those results. Whilst there was no difference in the delamination results between the pine and Victorian Ash for the PRF, there was a clear species dependency for the IBAs which demonstrated better performance with the Victorian Ash substrate compared to the pine substrate.

The second delamination test was based on the procedure given in the new Canadian Standard, CSA O112.9-04. As with the previous delamination test, all of the adhesives performed poorly in the Spotted Gum samples. There was variation between the adhesive performances in the pine samples with two of the IBAs performing as well as the PRF. The other two IBAs demonstrated higher levels of delamination. There were differences found for the adhesives on the Victorian Ash substrate as well. One of the IBAs performed better than the PRF while the other three gave very high levels of delamination. A species dependency was also noted for this delamination test. Unlike the previous test (*vide supra*), samples using the pine substrate generally performed better than the Victorian Ash samples.

Both of the delamination tests are proposed in the new Australian and New Zealand standard (AS/NZS 4364 (Int):2007) and the draft ISO standard for bond performance of wood adhesives and are considered to be equivalent. Based on the finding of this project, there are discrepancies in how each of the tests ranks the adhesives. This is summarised below (Table 1) and reveals the possibility that an adhesive could pass one test and fail the other test. This situation needs to be addressed in the Australian Standards technical committee before the proposed interim standard becomes fully operational. As an important risk mitigation strategy, it is therefore recommended that the industry, as a matter of urgency, complete a rigorous and scientific evaluation of the two "equivalent" methods in the Standard.

Table 1. Comparison of the two delamination tests and whether the adhesives would pass the criteria in the proposed AS/NZS 4364 (Int):2007 standard.

	AS/NZS 4364:1996 *(Method B in AS/NZS 4364(Int):2007)*		**CSA O112.9-04** (*Method A in AS/NZS 4364(Int):2007)*	
	Pine	**Victorian Ash**	**Pine**	**Victorian Ash**
PRF	*Pass*	*Pass*	*Pass*	*Fail*
IBA A	*Fail*	*Fail*	*Pass*	*Fail*
IBA B	*Fail*	*Pass*	*Fail*	*Fail*
IBA C	*Fail*	*Pass*	*Fail*	*Fail*
IBA D	*Pass*	*Pass*	*Pass*	*Pass*

Cleavage tests were undertaken according to AS/NZS 1328.1:1998 for all of the adhesive and wood combinations. All of the IBAs and the PRF control gave very high wood fibre failure levels for the pine and Victorian Ash samples when tested dry. When the pine samples were tested wet, the PRF and one IBA showed no decrease in wood fibre failure. The other three IBAs gave much lower levels of wood fibre failure when tested wet and failed to meet the 60% average wood fibre failure requirement of the standard. Similar results were found for the Victorian Ash samples with two IBAs meeting the 60% wood fibre failure requirement when tested wet and two failing to meet the requirement. All of the Spotted Gum samples gave very low

wood fibre failure results when tested wet with average values far below the 60% requirement.

Longitudinal tensile lap shear tests were undertaken on bonded specimens that had been subjected to a cold water or boiling water soak and tested either wet or dry according to the method in AS/NZS 4364:1996. The results after the samples were re-dried demonstrated that there was no significant degree of bond degradation for any of the adhesives on Radiata Pine or Victorian Ash samples. Differences in both the strength and wood fibre failure results for the wet samples were varied and appeared to be dependent on the IBA and wood species. Similar results wee found for the Spotted Gum samples.

Both cleave and lap shear tests require a determination of the level of wood fibre failure. It is clear that some of the IBAs do not give high values of wood fibre failure when tested wet. This does not demonstrate any degradation of the adhesive as performance was regained when the lap shear samples were allowed to re-dry. Accordingly, the acceptable value of wood fibre failure when tested wet will likely need to addressed

It is interesting to note that for the delamination and cleave tests the variation in results for most of the IBAs was much wider that for the PRF. The reason for this variability is not clear but it is speculated that it may be a result of localised inhomogeneity in the adhesive layer due to, for example, the presence of voids that have been formed during the curing of the adhesive. These voids have previously been reported as occurring during the curing of one-component moisture curing IBAs.

The resistance to heat and moisture of the IBAs relative to those of the PRF control were determined from testing in accordance with ASTM D4502. A number of issues were identified in the interpretation and implementation of the test method. Dry aging of the adhesives demonstrates that all of the adhesives will last far beyond the expected service life. When tested after aging in wet or moist environments significant decreases in the expected life of the samples were indicated. No statistically significant difference either between the IBAs and the PRF or between the IBAs was detected using this test.

Investigations were undertaken to determine the response of thin films of the adhesives to changes in the environment. Whilst this work is ongoing, with further testing of adhesives required before drawing definitive conclusions, several observations can be made.

- The techniques of making PUR thin films have been mastered to the extent that it is now possible to study their hygro-mechanical response.
- The Aramis system has proven to be a useful investigative tool and early problems associated with extracting data from the system have been solved by processing it through the Microsoft Excel spreadsheet program.

- Investigation is required to identify better methods of controlling chamber RH. Muszynski claimed to have achieved rapid RH changes in his work using similar methods, but did not present any supporting data
- The data acquired to date does not indicate that any of the adhesives exhibit a mechano-sorptive response, but neither does it preclude that possibility. Since mechano-sorptive strain is associated only with moisture change, and is independent of time, the strain (ε) versus time (t) curves for relative humidity (RH) varying between 60 and 98% and 98 and 60% should flatten with time as the moisture content stabilises and $d\varepsilon/dt$ tends to zero. This has not occurred for any of the adhesives examined to date; neither did Muszynski's data for wet to dry conditions at the point where his film ruptured. The strain for wet to dry conditions appears to be more in the nature of a delayed viscoelastic response influenced by moisture change. It may well be necessary to develop alternative theoretical models to explain the hygro-mechanical response of adhesive films.
- The viscoelastic responses of IBAs are more affected by moisture change than those of PRFs.

Based on these results, it is recommended that further work to investigate the hygro-mechanical response of timber substrates be undertaken to determine whether there is an optimal combination of adhesive and timber that results in stable and durable wood adhesive bonds.

Positron annihilation lifetime spectroscopy (PALS) is a characterisation technique for materials that is sensitive to subtle changes in polymer chain packing and polymer chemistry. As such this project investigated the technique to determine whether it can be used to detect early stage changes in adhesives exposed under load, and whether it can be used to do so non-destructively.

Two sets of experiments were performed, one destructive, the joint being split and the adhesive face examined, and the other non-destructive, the joint remaining intact and the adhesive being probed from the surface.

Test specimens in the form of vertical sections were taken from locations in loaded Radiata Pine and Victorian Ash beams close to those from which the compressive block shear specimen of strength most representative of the adhesive / wood species combination was taken. Control specimens were compared to exposed specimens. The tests were performed at 20^{o}C and 65% RH.

The results show that PALS was able to detect the presence of the adhesive, differentiate between the two different woods, and detect changes in the woods on exposure.

The results also indicate that several of the adhesive/wood combinations have changed during the 3 year exposure. These changes should be confirmed with mechanical testing.

In the non-destructive tests, changes in the PALS parameters were not significant enough to allow detection of the adhesive. The destructive test is therefore required for reliable results.

In summary, attempts to make any correlation between the accelerated tests described above and the exposure test results remain difficult after 3 years. There is no significant adhesive degradation associated with the pine or Victorian Ash samples exposed in either the environmental chamber samples or at the tropical field site. It is anticipated that exposure periods in excess of 5 years may be required for any trends to become more apparent. Data from the exposure and accelerated tests clearly confirm the difficulty in achieving a durable adhesive bond for exterior conditions with Spotted Gum.

RESULTS AND DISCUSSION

Three Year Field Trials

The methodology for the exposure testing is based on the procedure described in AITC 200-92 Annex E.[3] This is a qualification test method for new adhesives that have little or no previous in-service performance data and compares the performance of any new adhesive with a phenol-resorcinol-formaldehyde (PRF) control (which is assumed to be durable and has been used in-service for many years).

Testing involved the exposure of laminated beams to both a controlled cyclic environment in a test chamber and to a fully exposed outdoor environment. Half of the beams had a load applied to them whilst the other half were unloaded. The strengths of the adhesive bonds were measured after exposure periods of 1 and 3 years and any strength losses compared to those of a PRF control. Conditions within the test chamber were alternated between 50°C and 80% RH and ambient, sheltered Melbourne conditions at 2 week intervals. A CSIRO site in Darwin, Australia was chosen for the outdoor trials. This is a tropical site, latitude 12.5° south, where the beams were fully exposed to the weather.

For this project, 5 adhesives and 3 wood species were studied. This led to 15 different wood/adhesive combinations. The list of wood species and adhesives is tabulated in Table 2. There were three 1-component (1-C) moisture curing IBAs and a 2-component (2-C) IBA which will be compared to a PRF control. It should be noted that only the PRF is identified in the remainder of this report. All other adhesives remain unidentified and are referred to by means of randomly assigned code letters A-D. The order in which the IBA adhesives are listed below has been randomised and bears no relationship to the order used later in the report.

Table 2. The 3 wood species and 5 adhesives used in the current work.

Wood Species	**Strength Rating**	**Adhesive**		
Radiata Pine	MGP10	**Name**	**Type**	**Manufacturer**
Victorian Ash	F14	AVS 301	PRF	Bostik
Spotted Gum	F27	AVS 511	1-C IBA	Bostik
		Isoset WD3-A320/CX-47	2-C IBA	Ashland
		HB110	1-C IBA	Purbond
		VN3034	1-C IBA	Purbond

Glue laminated beams were manufactured at Warrnambool Timber Industries Pty Ltd from timber of dimensions 90 x 45 mm in the case of pine and Victorian Ash and 90 x 35 mm in the case of spotted gum. Timber lengths ranged from 4.5m to 6m. Beams consisting of two laminates were prepared for each wood/adhesive combination by applying the adhesive onto one face of one of the laminates at a loading of

[3] American Institute of Timber Construction, Inspection Manual AITC 200-92 for Structural Glued Laminated Timber, October 2001

approximately 250gsm. The IBAs were applied by hand using an adhesive comb or coating rod (Figure 1). The PRF was applied using an industrial applicator. The beams were manufactured in the presence of technical representatives of each of the adhesive companies and under their supervision. Pressure in the press was applied via a hydraulic hose and maintained for at least 8 hours (Figure 2). The beams were ripped in half lengthwise, dressed and docked to give test beams of dimensions 700 x 80 x 38 mm (length x width x height) in the case of Radiata Pine and Victorian Ash and 700 x 60 x 38 mm for the Spotted Gum beams (Figure 3). Forty beams for each wood/adhesive combination were prepared for the exposure study. Eight beams were used to determine baseline strength properties, sixteen beams (8 loaded and 8 unloaded) were subjected to controlled exposure in an environmental chamber at Monash University and sixteen to full outdoor exposure in Darwin. This is summarized in Table 3.

Figure 1. Application of the IBAs was achieved by using a coating rod (*top*) or an adhesive comb (*bottom*)

Figure 2. The press at Warrnambool Timber used to manufacture the test beams (*top*) before and (*bottom*) during pressing.

Figure 3. Radiata Pine (*left*), Victorian Ash (*middle*) and Spotted Gum (*right*) test beams for the exposure study

Table 3. The number of test beams required for the exposure study per wood species.

	PRF (control)	IBA A	IBA B	IBA C	IBA D
Baseline Properties	**8**	**8**	**8**	**8**	**8**
Test chamber (Monash) total	**16**	**16**	**16**	**16**	**16**
Stressed-12 months	4	4	4	4	4
Unstressed-12 months	4	4	4	4	4
Stressed-36 months	4	4	4	4	4
Unstressed-36 months	4	4	4	4	4
Outdoor (Darwin) total	**16**	**16**	**16**	**16**	**16**
Stressed-12 months	4	4	4	4	4
Unstressed-12 months	4	4	4	4	4
Stressed-36 months	4	4	4	4	4
Unstressed-36 months	4	4	4	4	4

As discussed earlier (*vide supra*), test beams were setup both under load and unloaded at two different exposure sites. The first site was an environmental chamber at Monash University where the conditions were alternated between high temperature and humidity (50°C and 80% RH) and ambient conditions on a fortnightly basis. The outdoor exposure site was located in Darwin, Australia. The test rigs were laid out such that all of the test beams were oriented with their longitudinal axes horizontal and coincident with the North-South direction. Photographs of the Darwin test site are given in Figure 4.

Figure 4. The samples at the exposure site in Darwin; (*top left*) Looking north-west at the samples with the unloaded beams in the foreground; (*top right*) Looking south-east at the samples showing the loaded samples in the foreground; (*bottom left*) A close-up of some of the unloaded samples; (*bottom right*) A close-up of the loaded samples in the test rigs.

Some selected daily meteorological data for the 36 month period that the beams were exposed in Darwin are shown in Figure 5. This data was collected by the Bureau of Meteorology at its Darwin Airport weather station which is located only a few kilometres from the exposure site and is in a similar climatic environment. The daily maximum temperature ranged between *ca* 24-38°C and minimum temperatures between 12-28°C. The humidity varied between 30-70%RH during the dry season (May-November) and 80-100%RH during the wet season (December-April) when there was significant rainfall with the maximum daily rainfall recorded at *ca* 240mm.

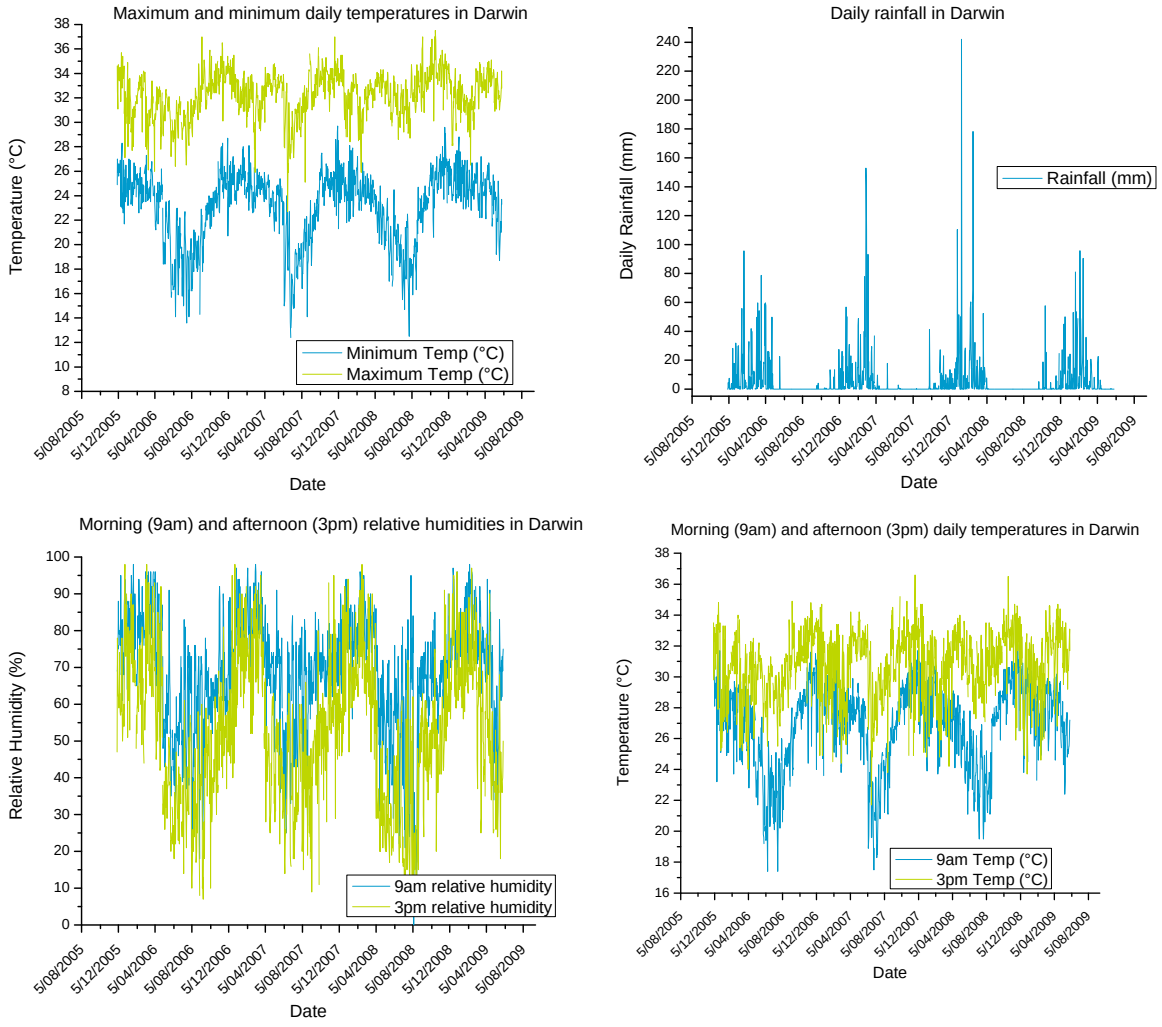

Figure 5. Selected daily meteorological data for the Darwin exposure site during the 3 year period of the exposure test.

After 1 and 3 year exposure periods to conditions in both the environmental chamber at Monash and exposure to the weather in Darwin, the adhesive bond lines of each of the wood/adhesive combinations (both loaded and unloaded) were tested for strength. This was achieved by cutting the beams into block shear samples and testing for shear strength using procedures in general accordance with those specified in CSIRO DBR Technical Paper No 31.[3] The cutting pattern for each beam is shown in Figure 6.

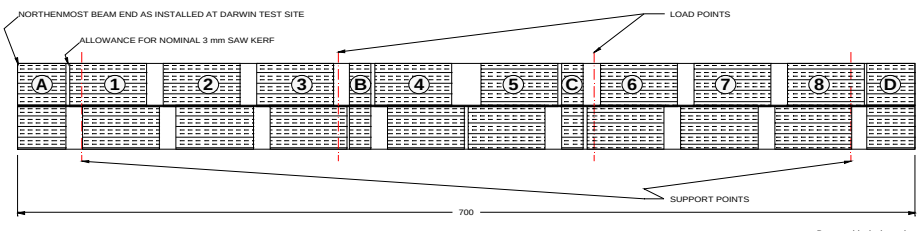

Figure 6. Cutting pattern for the test beams for the determination of shear strength.

Radiata Pine Samples

The results for the Radiata Pine samples are presented graphically in Figure 7 (environmental chamber) and Figure 8 (Darwin). The results for the loaded samples are tabulated in Table 4 and Table 5.

It is immediately noted from Table 5 that the outdoor exposure site in Darwin had very few samples remaining suitable for testing after the 3 year exposure period. This was due to many of the test beams displaying signs of severe rot or fungal attack. Some selected examples are given in Figure 9. Where some samples remained available for testing, the data is plotted in Figure 8 but is highlighted with dashed lines. The few results obtained are qualitatively very similar to the environmental chamber results. The rest of the discussion will be based on the environmental chamber results. Furthermore, based on previous work that found that adhesives under stress degrade faster, only the samples under load will be discussed further.

Each of the data sets for the loaded environmental chamber samples were tested for normality using the Shapiro-Wilk test. All of the data sets except for two displayed a normal distribution of results. The two exceptions were the IBA control results and the IBA D 3 year samples. This was due to both data sets exhibiting a skewed tail towards the lower strength results from a few data points. If these points are excluded as outliers (due to the fact they are greater than 2 standard deviations away from the mean), then the data sets show a normal distribution and can then be analyzed using Analysis of Variance (ANOVA).

One-way ANOVA (at the 0.05 confidence level) was used to compare the control and three year strength results for each of the adhesives. The PRF showed a statistically significant difference between the control and the 3 year samples. The strength appears to have increased to approximately 120% of the original strength. This result was also found for both the loaded and non-loaded Darwin samples but not for the non-loaded environmental chamber samples. The origin of this increase is unknown. It should be noted that a similar result was obtained when the PRF was subjected to an accelerated weathering regime and the fracture energy assessed.[4] IBA A displayed a small but statistically significant decrease in strength to approximately 87% of the original strength after 12 months. There was no further deterioration in strength after this time. IBA B and IBA D showed no statistically significant change in strength over the 3 year timeframe. IBA C showed no strength change after 12 months but displayed a statistically significant increase in strength after the first year. The strength appeared to increase to *ca* 120% of the original strength. It should be noted that the non-loaded samples of IBA C showed no statistically significant change in strength after 3 years. Unfortunately, there were no results for samples of IBA C from the Darwin test site to compare with.

When comparing the performance of the different adhesives, there appears to be two different possible comparisons. The first might be to look at the percentage change in

[4] K. Van Langenberg, "*New techniques for determining the mechanism of adhesive durability in engineered wood products*", Denis M Cullity Research Fellowship Report, Forest and Wood Products Australia, Report # PG07.5059, 2007

strength of the adhesives over the 3 years. This is shown in Figure 10 for the environmental chamber samples and the Darwin samples where available. It can be seen that there are some differences between the adhesives. The PRF and IBA C both appear to have increased in strength. IBA A appears to have decreased slightly in strength whilst IBA B and IBA D appear to have remained relatively unchanged.

Table 4. The mean shear strength (MPa), standard deviation (SD) and number of specimens (*n*) for the loaded Radiata Pine samples exposed in the environmental chamber.

		Mean	SD	*n*
PRF	control	8.25	1.30	32
	1 year exposure	9.04	1.34	32
	3 year exposure	9.94	1.43	32
IBA A	control	10.33	1.50	32
	1 year exposure	9.00	1.36	32
	3 year exposure	9.01	1.48	32
IBA B	control	9.05	1.21	32
	1 year exposure	8.87	1.63	32
	3 year exposure	9.20	2.52	32
IBA C	control	8.55	1.64	32
	1 year exposure	8.07	1.15	32
	3 year exposure	10.23	1.73	32
IBA D	control	10.31	1.14	32
	1 year exposure	9.47	1.29	32
	3 year exposure	9.82	3.18	32

Table 5. The mean shear strength (MPa), standard deviation (SD) and number of specimens (*n*) for the loaded Radiata Pine samples exposed in Darwin.

		Mean	SD	*n*
PRF	control	8.25	1.30	32
	1 year exposure	9.00	1.88	32
	3 year exposure	10.43	1.07	4
IBA A	control	10.33	1.50	32
	1 year exposure	10.02	1.86	32
	3 year exposure	9.16	2.27	13
IBA B	control	9.05	1.21	32
	1 year exposure	7.64	1.50	32
	3 year exposure	NA	NA	0
IBA C	control	8.55	1.64	32
	1 year exposure	9.25	1.94	32
	3 year exposure	NA	NA	0
IBA D	control	10.31	1.14	32
	1 year exposure	9.43	2.38	30
	3 year exposure	9.24	1.41	16

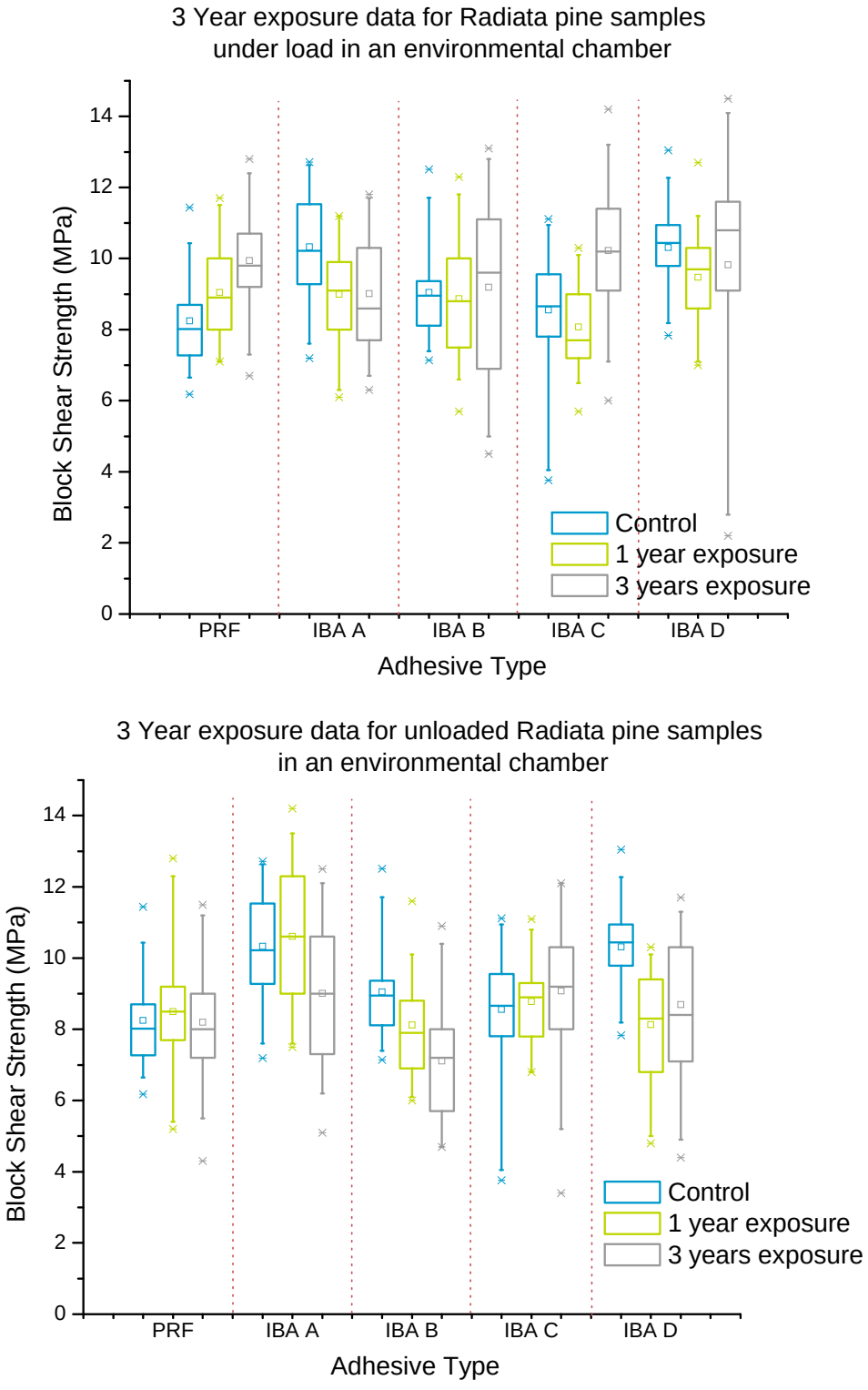

Figure 7. Shear strengths (MPa) of the adhesives bonded to Radiata Pine after 0, 1 and 3 years exposure in an environmental chamber. (*Top*) Loaded samples. (*Bottom*) Unloaded samples.

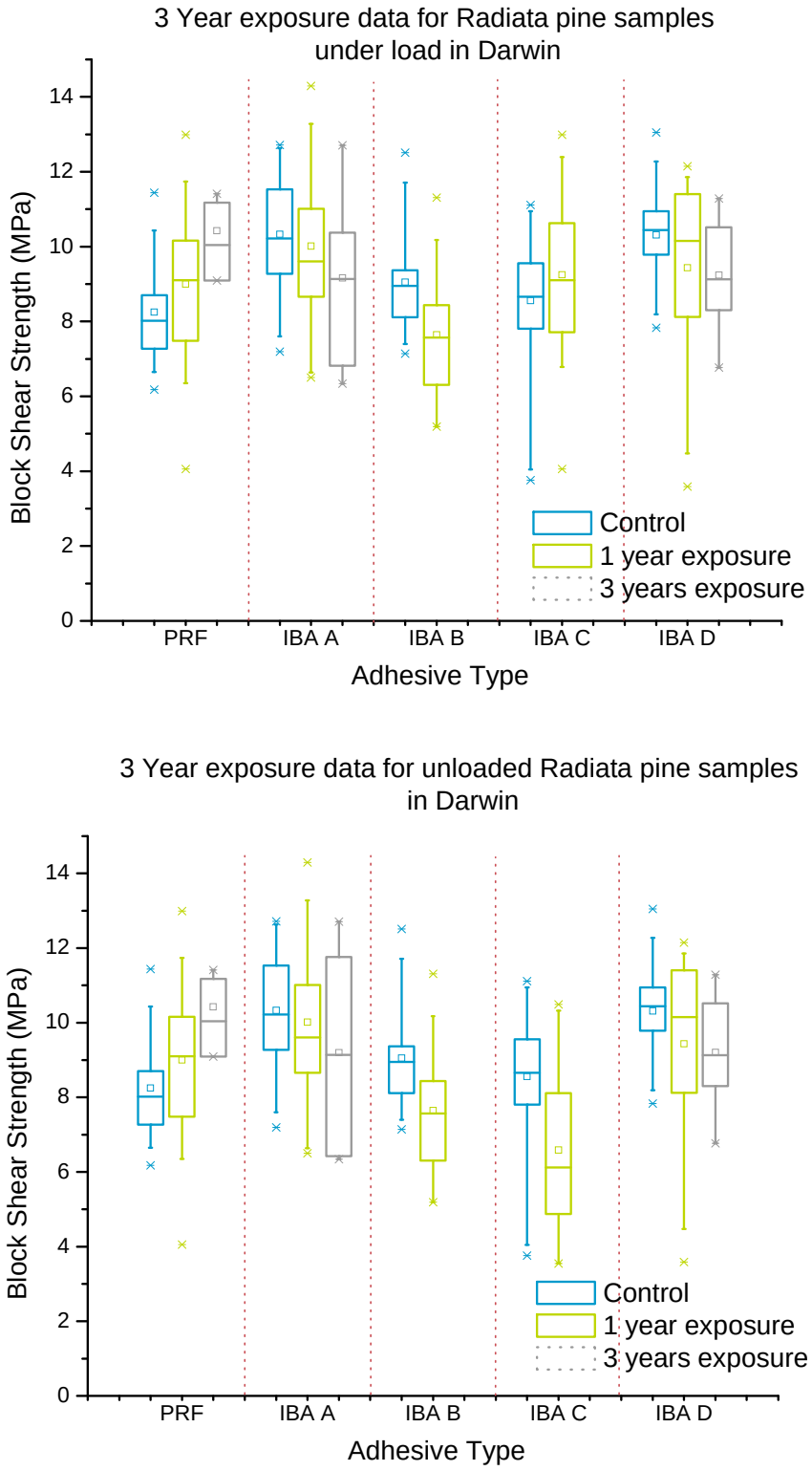

Figure 8. Shear strengths (MPa) of the adhesives bonded to Radiata Pine after 0, 1 and 3 years outdoor exposure in Darwin. (*Top*) Loaded samples. (*Bottom*) Unloaded samples.

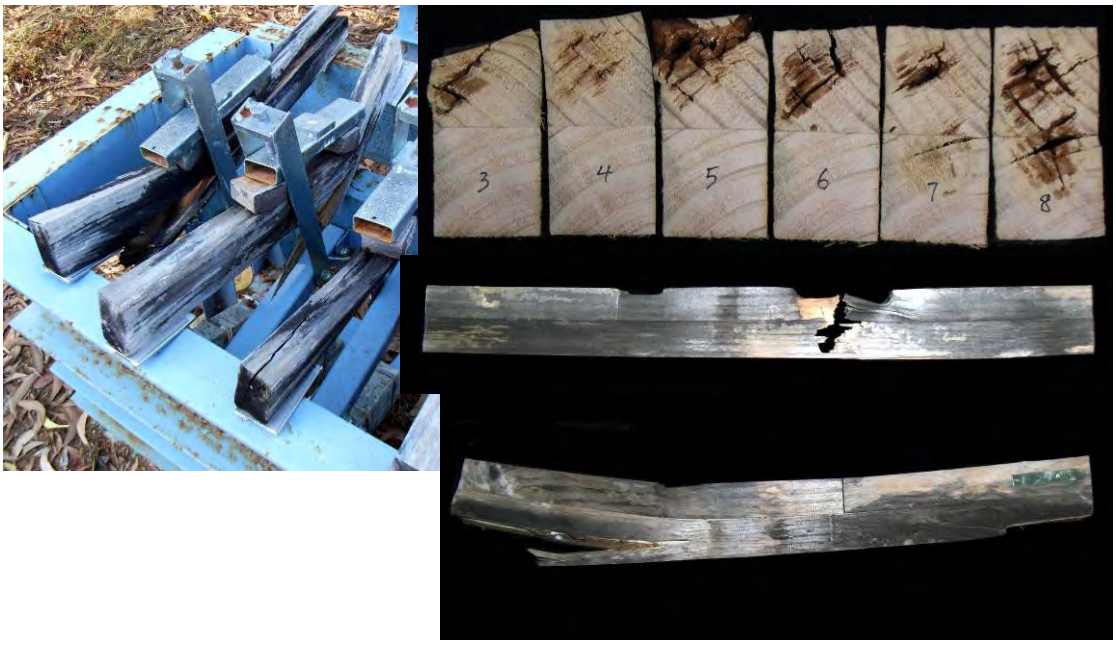

Figure 9. Examples of decay found in the Radiata Pine samples exposed for 3 years in Darwin.

This is, however, not the complete picture because when the results are plotted as the mean shear strength versus time (Figure 11), a different story emerges. It can be seen that the initial strengths of the adhesives are not identical and can be grouped into 2 subsets. After 3 years, each of the adhesives has the same retained strength. There is no statistically significant difference in the retained strength. Furthermore, the strength loss (if any) appears to occur during the first 12 months. After this period, the strength remains constant or increases slightly. For comparison purposes and a guide to industry requirements, the horizontal red dotted line in Figure 11 is the minimum shear strength required for glulam according to AS/NZS 1328.1.1998.[5]

In summary, there was no significant loss of strength for any of the adhesives after 3 years exposure for the radiata pine substrate. One of the adhesives (IBA A) showed a small (10%) decrease in strength after 12 months but did not exhibit any further deterioration. Whilst there were minor differences between the adhesives when the percentage retained strength was evaluated, there was no statistically significant difference in the mean strengths of any of the adhesives after 3 years. The Darwin results (where available) were qualitatively similar to the environmental chamber results.

[5] AS/NZS 1328.1:1998, "*Glued laminated structural timber. Part 1: Performance requirements and minimum production requirements*".

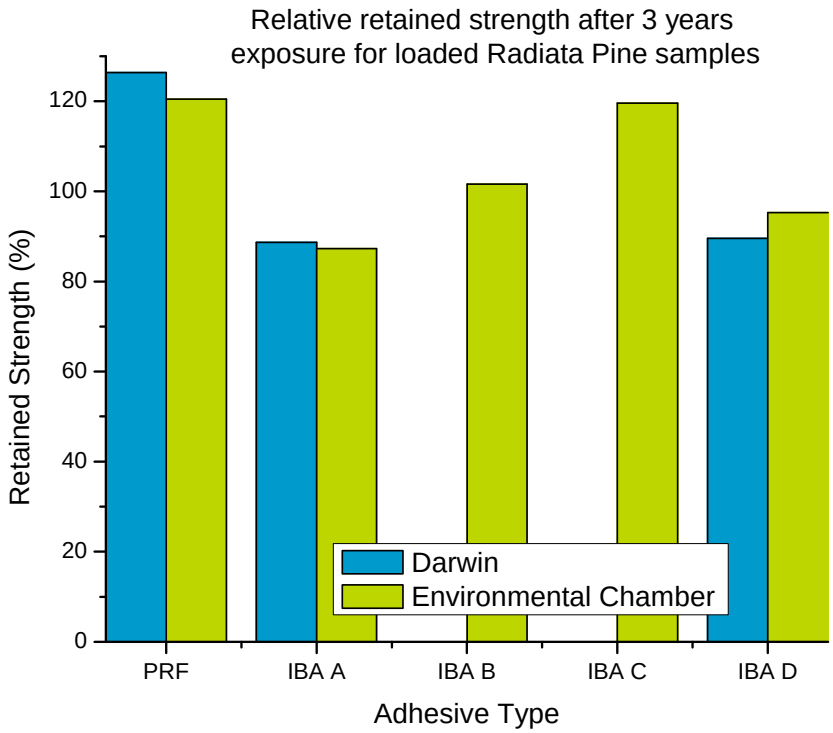

Figure 10. The relative mean retained strengths of the loaded Radiata Pine samples (expressed as a percentage of the original strength) after 3 years exposure in Darwin and an environmental chamber.

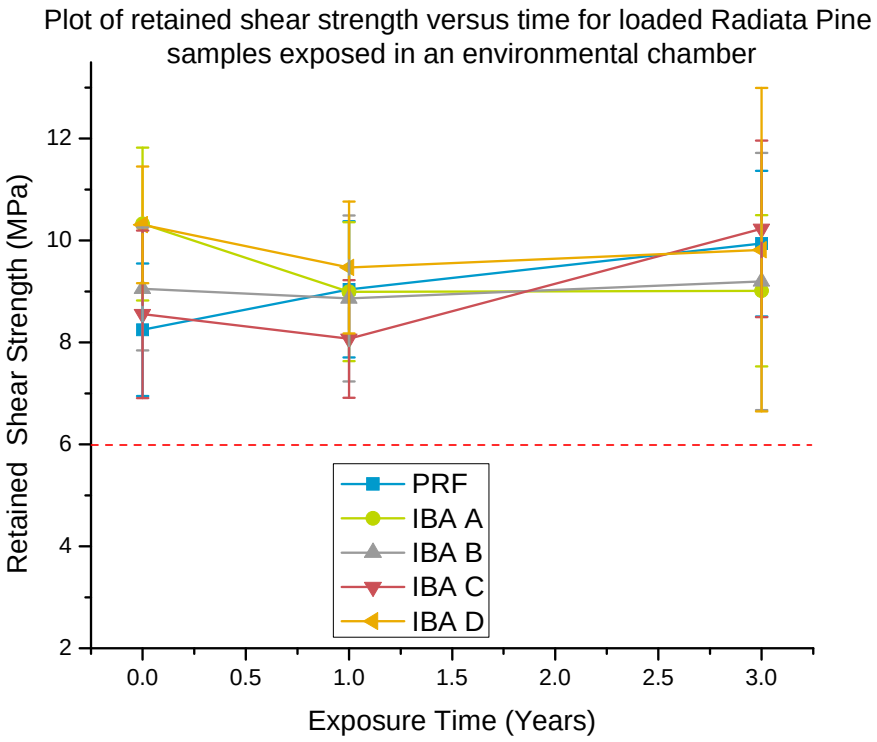

Figure 11. The shear strength (MPa) of loaded Radiata Pine samples exposed in an environmental chamber over the course of 3 years.

Victorian Ash Samples

A similar analysis to that of the Radiata Pine results can be undertaken with the Victorian Ash samples. The full results are shown graphically in Figure 12 and Figure 13 and strength results for the loaded samples tabulated in Table 6 and Table 7. Most of the datasets are normal at the 0.05 confidence level when using the Shapiro-Wilk test for normality. The only exception was the IBA C 3 year data from Darwin. This was due to a cluster of low strength values.

The data presented in Figure 12 and Figure 13 appears qualitatively very similar. The adhesives in both the loaded and unloaded samples appear to have suffered a slight decrease in strength at both the Darwin and environmental chamber sites. Comparing the 3 year strength data for the loaded samples from the environmental chamber and Darwin sites reveals that there are statistically significant differences in the cases of the PRF, IBA A and IBA D, the strengths of the Darwin samples being lesser. There is no statistically significant difference between the two sites for IBA B and IBA C. Therefore, it can be concluded that, in general, the Darwin exposure site was the harsher of the two sites. This is more clearly observed when comparing the percentage of retained strength of the adhesives across both sites (Figure 14). This difference between the sites is not as clear for the unloaded samples where only the PRF and IBA C show statistically significant differences. Comparing the loaded and non-loaded Darwin samples, it appears that the stressed loaded samples show a significantly greater degree of degradation. In light of these observations, the remaining discussion will be based on the loaded Darwin results.

Comparing the percentage retained strengths of the loaded Darwin samples after 3 years, it appears that most of the adhesives have degraded to a similar extent, that is, they have lost ca 25-35% of their original strengths. The only exception to this appears to be the IBA C adhesive which suffered little if any strength loss. This is difficult to interpret since the non-loaded IBA C Darwin samples exhibited a significant loss of strength. Regardless of this anomaly, it appears that the retained strengths of all the IBAs were no less than that of the PRF control. A similar result can be seen when the retained shear strength versus time is plotted (Figure 15).

In summary, all of the Victorian Ash samples demonstrated a loss of strength for all of the adhesives studied. The loaded samples exposed in Darwin showed the greatest loss of strength. There does not appear to be any major difference between the IBAs and the PRF control.

Table 6. The mean shear strength (MPa), standard deviation (SD) and number of specimens (*n*) for the loaded Victorian Ash samples exposed in the environmental chamber.

		Mean	SD	*n*
PRF	control	7.72	1.31	32
	1 year exposure	6.59	1.12	32
	3 year exposure	7.01	1.29	32
IBA A	control	10.95	1.12	32
	1 year exposure	7.19	1.26	32
	3 year exposure	9.23	2.16	32
IBA B	control	9.91	1.27	32
	1 year exposure	8.90	1.48	31
	3 year exposure	8.02	2.48	32
IBA C	control	9.04	1.34	32
	1 year exposure	8.08	1.29	32
	3 year exposure	8.32	1.43	32
IBA D	control	8.73	2.65	32
	1 year exposure	6.67	1.40	32
	3 year exposure	7.62	2.45	32

Table 7. The mean shear strength (MPa), standard deviation (SD) and number of specimens (*n*) for the loaded Victorian Ash samples exposed in Darwin.

		Mean	SD	*n*
PRF	control	7.72	1.31	32
	1 year exposure	6.62	1.66	32
	3 year exposure	5.84	1.42	15
IBA A	control	10.95	1.12	32
	1 year exposure	8.28	1.05	24
	3 year exposure	6.89	2.16	16
IBA B	control	9.91	1.27	32
	1 year exposure	8.67	1.79	32
	3 year exposure	7.34	1.57	28
IBA C	control	9.04	1.34	32
	1 year exposure	8.96	1.63	32
	3 year exposure	8.62	1.52	32
IBA D	control	8.73	2.65	32
	1 year exposure	7.21	1.54	32
	3 year exposure	5.74	2.37	29

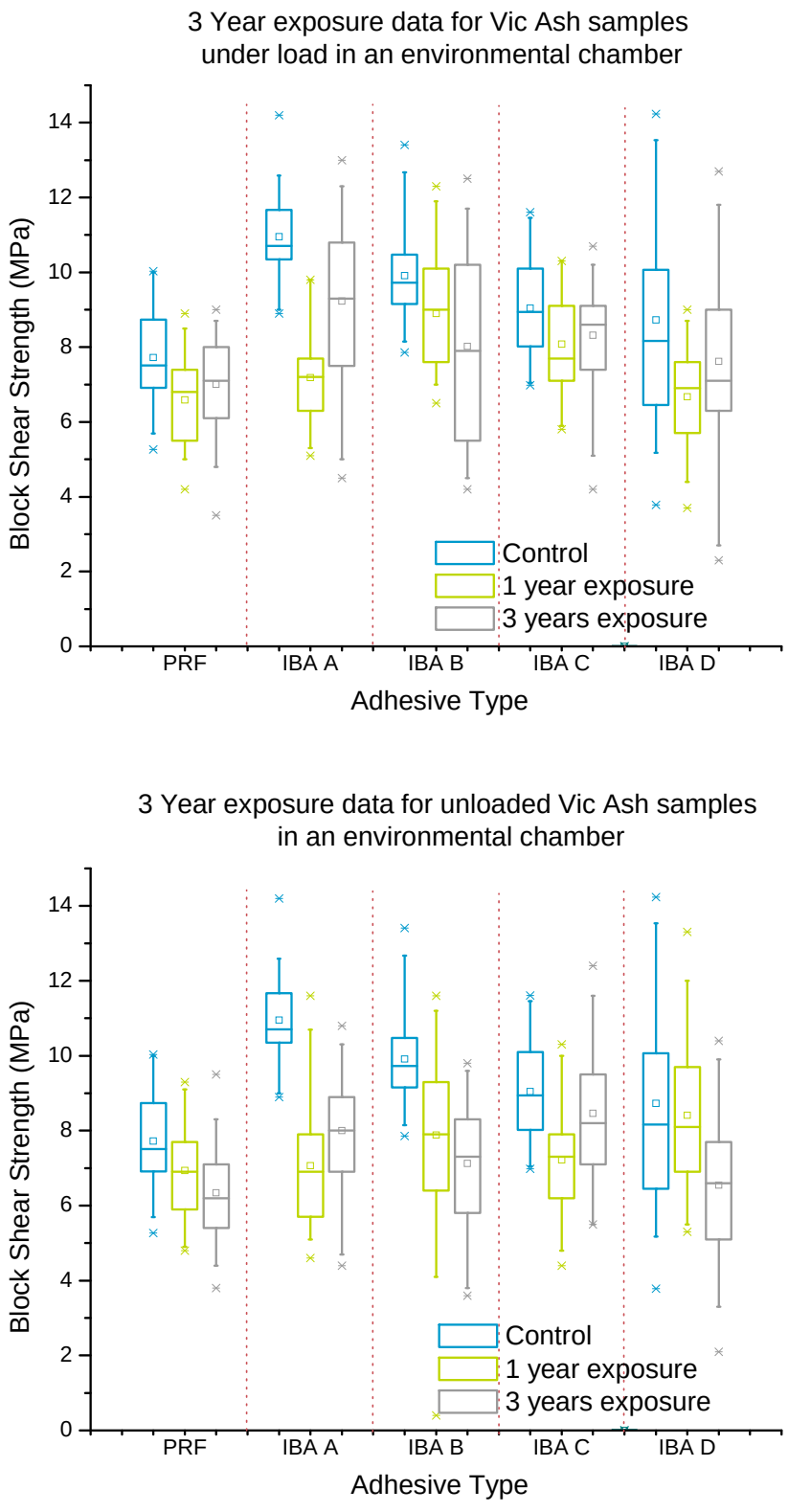

Figure 12. Shear strengths (MPa) of the adhesives bonded to Victorian Ash after 0, 1 and 3 years exposure in an environmental chamber. (*Top*) Loaded samples. (*Bottom*) Unloaded samples.

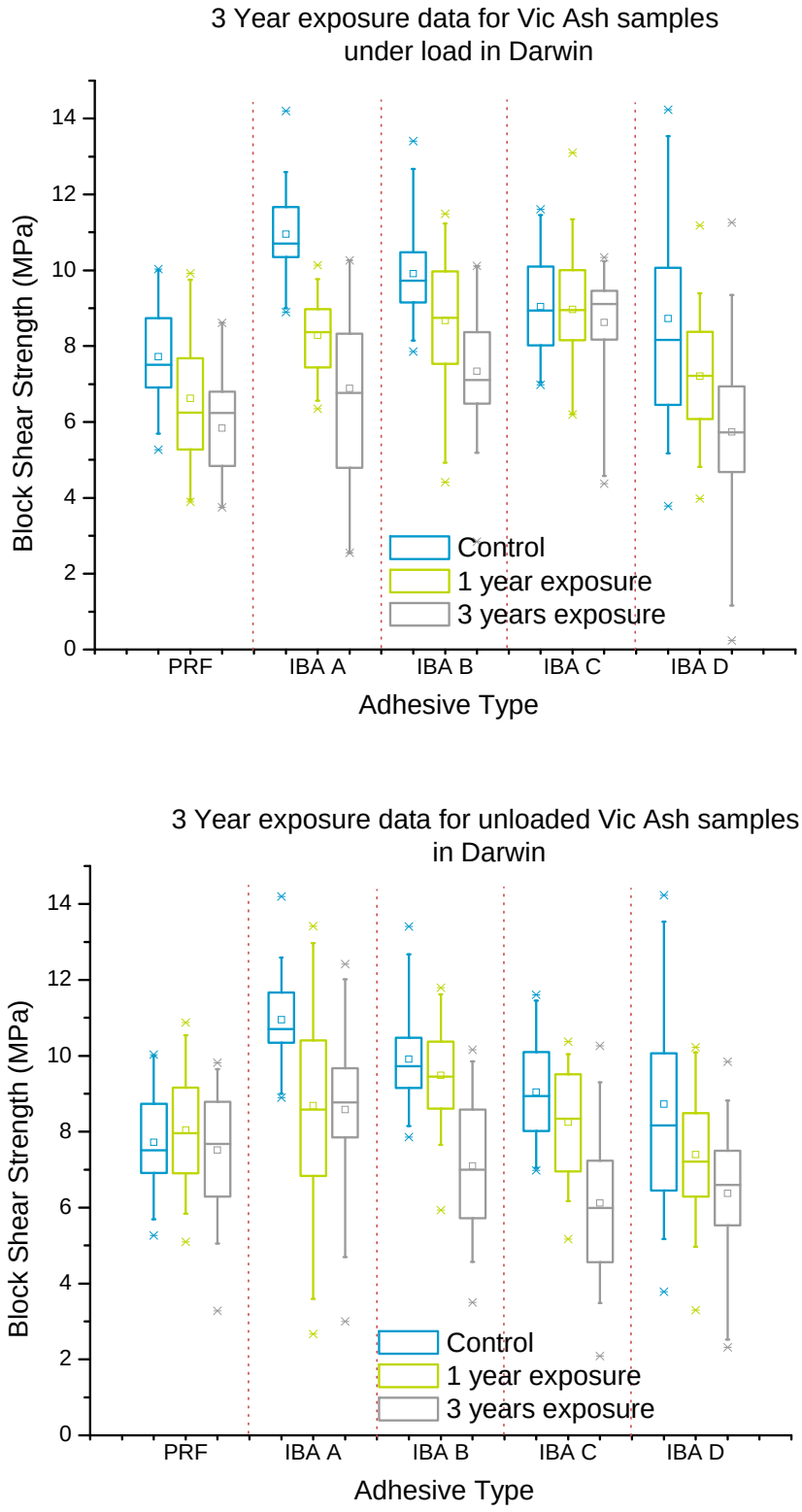

Figure 13. Shear strengths (MPa) of the adhesives bonded to Victorian Ash after 0, 1 and 3 years exposure in Darwin. (*Top*) Loaded samples. (*Bottom*) Unloaded samples.

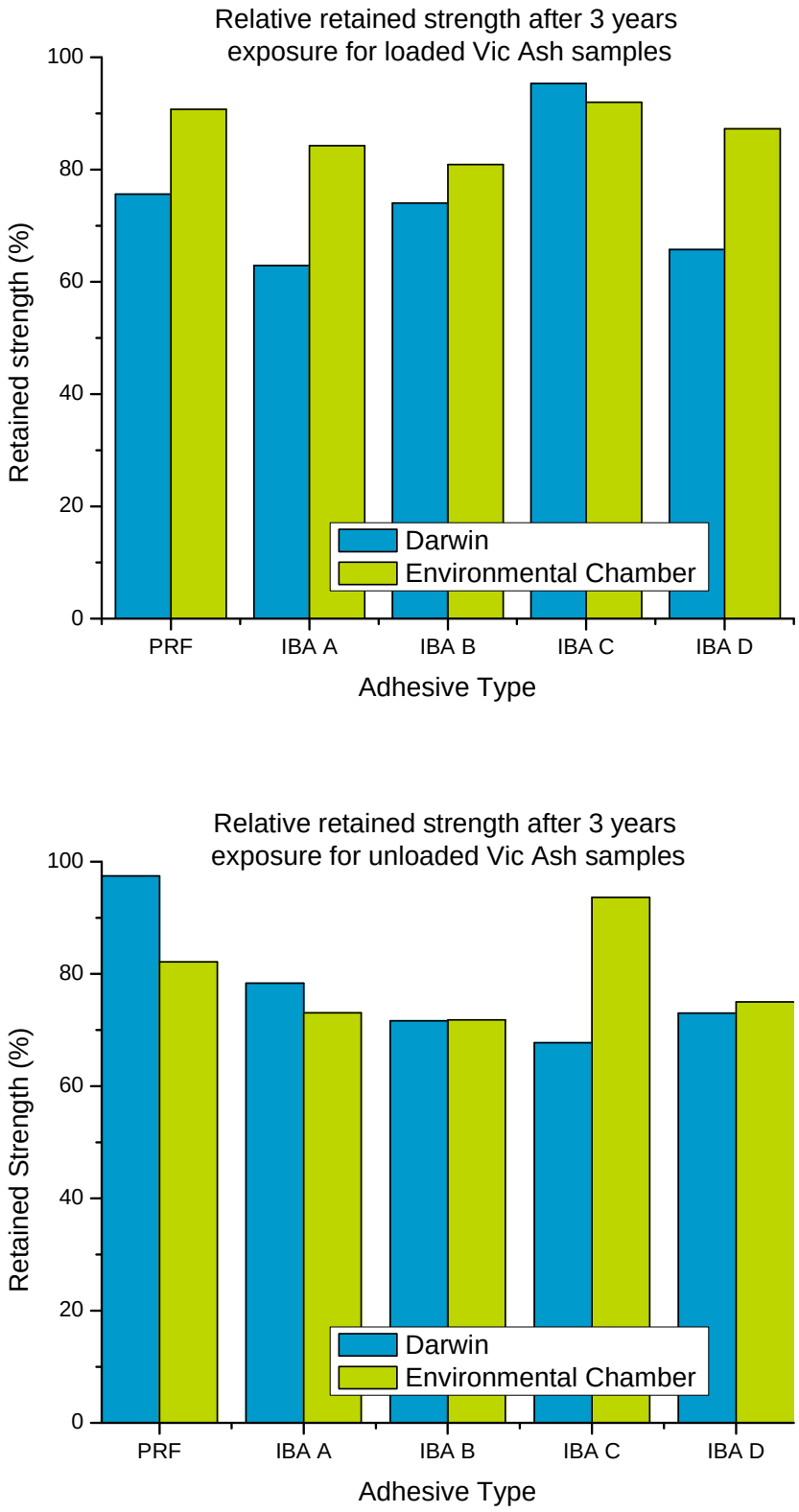

Figure 14. The relative mean retained strengths of the (*top*) loaded and (*bottom*) unloaded Victorian Ash samples (expressed as a percentage of the original strength) after 3 years exposure in Darwin and an environmental chamber.

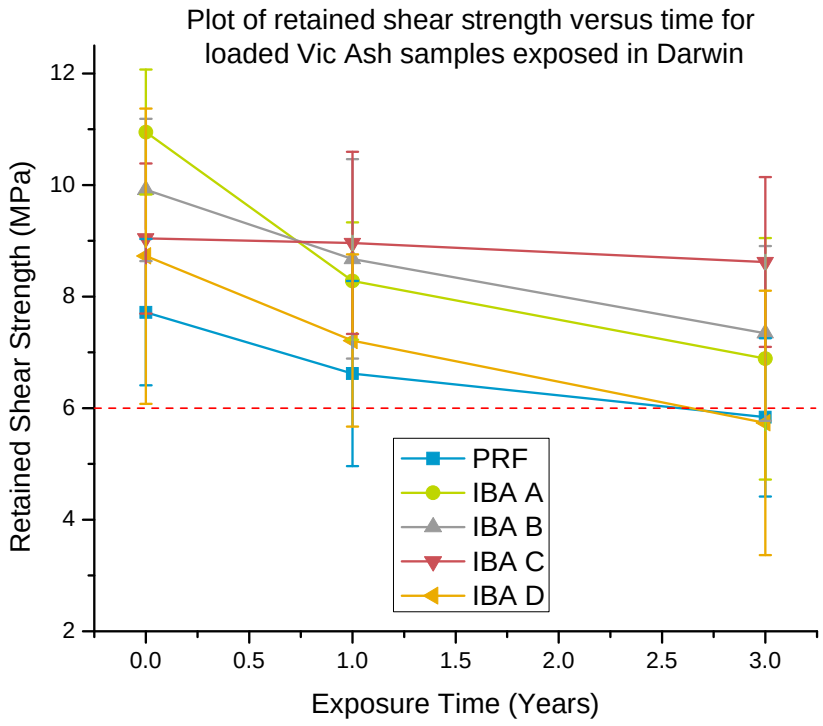

Figure 15. The mean shear strengths (MPa) of loaded Victorian Ash samples exposed in Darwin over the course of 3 years.

Spotted Gum Samples

The results for the Spotted Gum samples are shown in Figure 16 and Figure 17. Table 8 and Table 9 highlight the mean, SD and number of tests for the loaded specimens.

It is evident from Figure 17 that the adhesively-bonded Spotted Gum samples found the outdoor exposure site in Darwin an extremely harsh environment. All of the loaded samples failed within the 3 year time period, with many of the adhesives failing within the first year. An exception was IBA B in which case a few samples retained some strength after 3 years (Figure 18). It should be noted that this is at odds with the corresponding 12 month samples where the vast majority of tested samples exhibited zero retained strength.

Surprisingly, a similar result was observed for the non-loaded samples where all of the adhesives suffered significant loss of strength. The only exception was IBA D where a few samples retained some semblance of strength (Figure 19). Examples of the delamination of the non-loaded beams at the Darwin site are shown in Figure 20.

The results obtained for the environmental chamber were similar to those observed for the Darwin site, though it is clear that chamber was not as harsh an environment (Figure 16). This is evident if the retained strength (expressed as a percentage of the original strength) is plotted for each of the two sites (Figure 21), particularly for the non-loaded samples. This difference is most likely due to the different timescales

involved in the cyclic conditions. The environmental chamber operated on a fortnightly cycle, perhaps not enough time for the dense Spotted Gum substrate to significantly alter its moisture content and so induce significant stress on the adhesive bond line. In Darwin, however, the samples were subjected to half-yearly exposure to rain and high humidity's and dry, sunny conditions, allowing a significant change in the samples' moisture content, and exerting extreme stresses on the adhesive bond lines.

The non-loaded environmental chamber samples were the only samples to exhibit a significant number of non-zero strength results. Statistical analysis is difficult to undertake due to the PRF and IBA C showing a non-normal distribution of results. Qualitatively, there are differences in the performances of the IBA adhesives but none of these adhesives (including the PRF) retained any significant amount of bond strength and any comparisons should therefore be treated with caution.

In summary, the Spotted Gum samples exhibited a significant (and in many instances a complete) loss of strength for all of the adhesives. This appears to be due to the substrate exerting stresses on the adhesive bond line beyond the strength that any of the adhesives can withstand and not due to gradual degradation of the adhesives themselves. All of the IBA adhesives were comparable to the PRF. The Darwin outdoor site was a much harsher environment than the environmental chamber.

Table 8. The mean shear strength (MPa), standard deviation (SD) and number of samples (*n*) for the loaded Spotted Gum samples exposed in the environmental chamber.

		Mean	SD	*n*
RF	control	6.91	2.02	32
	1 year exposure	4.12	0.98	32
	3 year exposure	2.70	2.33	32
IBA A	control	10.07	2.56	32
	1 year exposure	1.46	1.88	32
	3 year exposure	0.88	1.73	32
IBA B	control	9.00	2.22	32
	1 year exposure	2.57	1.88	32
	3 year exposure	1.13	1.36	32
IBA C	control	4.34	1.63	32
	1 year exposure	0.73	1.19	32
	3 year exposure	0.14	0.20	32
IBA D	control	11.84	3.05	32
	1 year exposure	2.78	2.37	32
	3 year exposure	1.45	1.90	32

Table 9. The mean shear strength (MPa), standard deviation (SD) and number of samples (*n*) for the loaded Spotted Gum samples exposed in Darwin.

		Mean	SD	*n*
RF	control	6.91	2.02	32
	1 year exposure	0.00	0.00	32
	3 year exposure	0.12	0.52	32
IBA A	control	10.07	2.56	32
	1 year exposure	1.97	3.62	32
	3 year exposure	1.05	2.43	32
IBA B	control	9.00	2.22	32
	1 year exposure	1.17	2.62	32
	3 year exposure	2.08	2.85	32
IBA C	control	4.34	1.63	32
	1 year exposure	0.00	0.00	32
	3 year exposure	0.00	0.00	32
IBA D	control	11.84	3.05	32
	1 year exposure	4.22	4.69	32
	3 year exposure	0.00	0.00	32

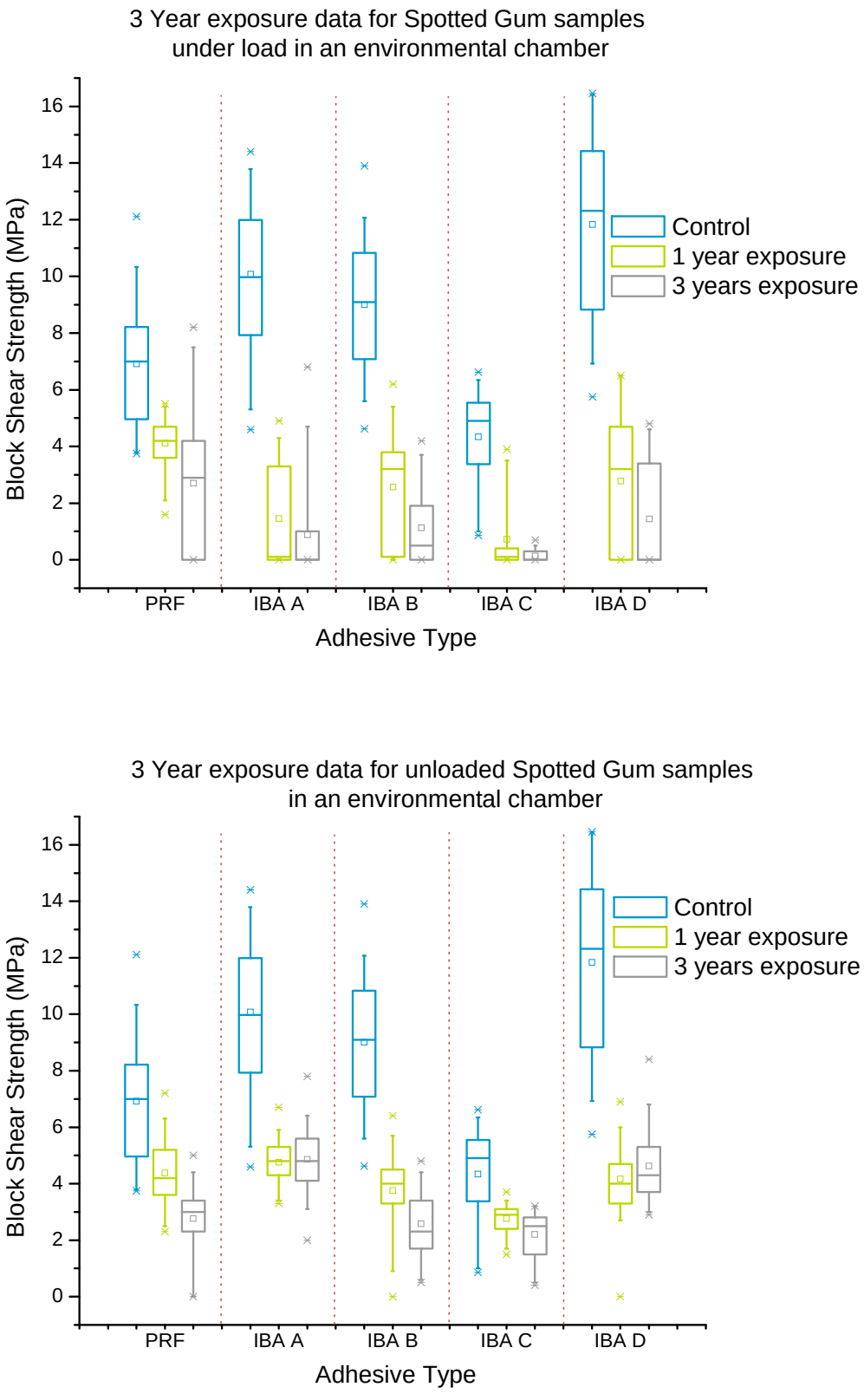

Figure 16. Shear strengths (MPa) of the adhesives bonded to Spotted Gum after 0, 1 and 3 years exposure in an environmental chamber. (*Top*) Loaded samples. (*Bottom*) Unloaded samples.

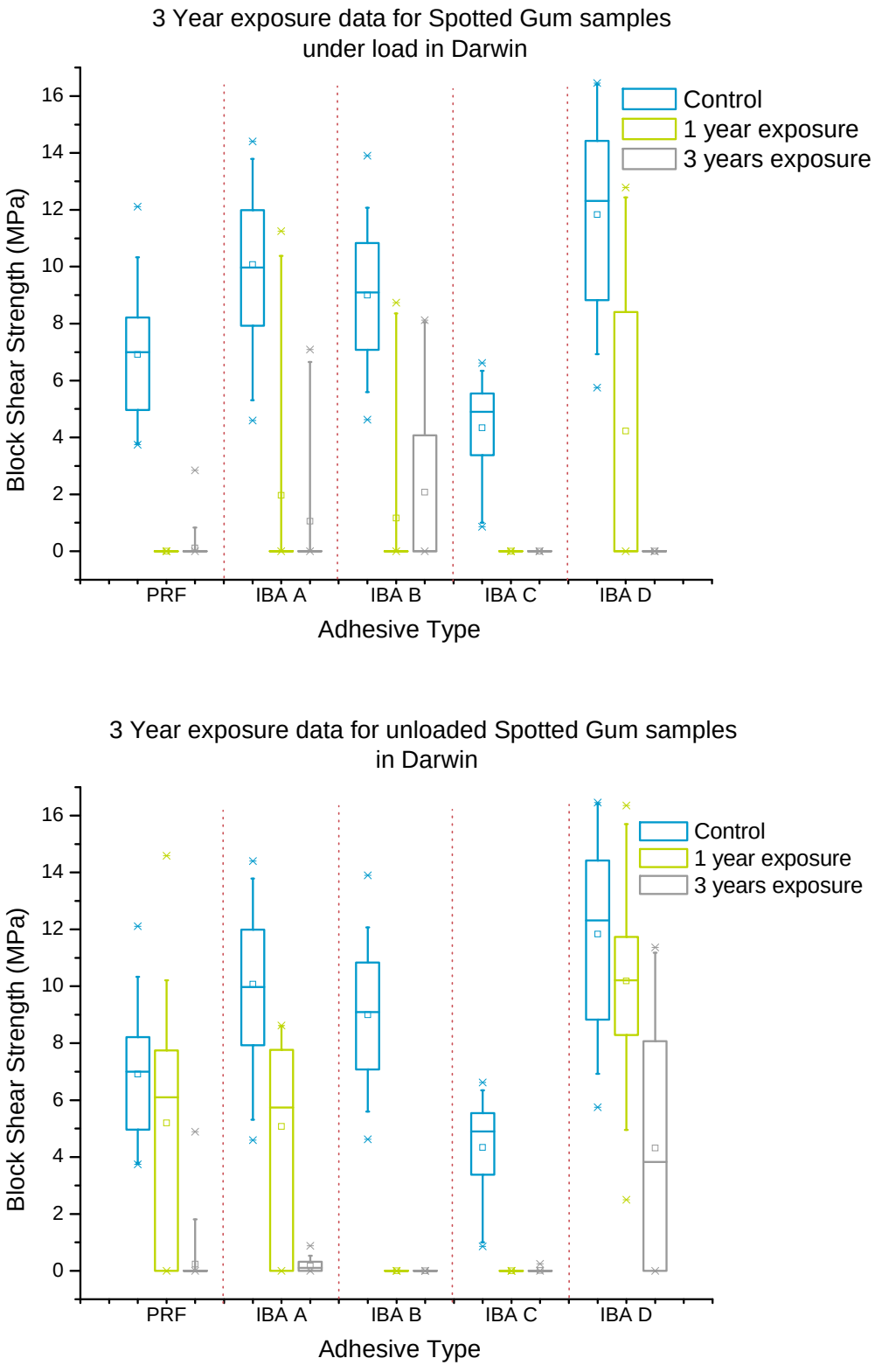

Figure 17. Shear strengths (MPa) of the adhesives bonded to Spotted Gum after 0, 1 and 3 years exposure in Darwin. (*Top*) Loaded samples. (*Bottom*) Unloaded samples.

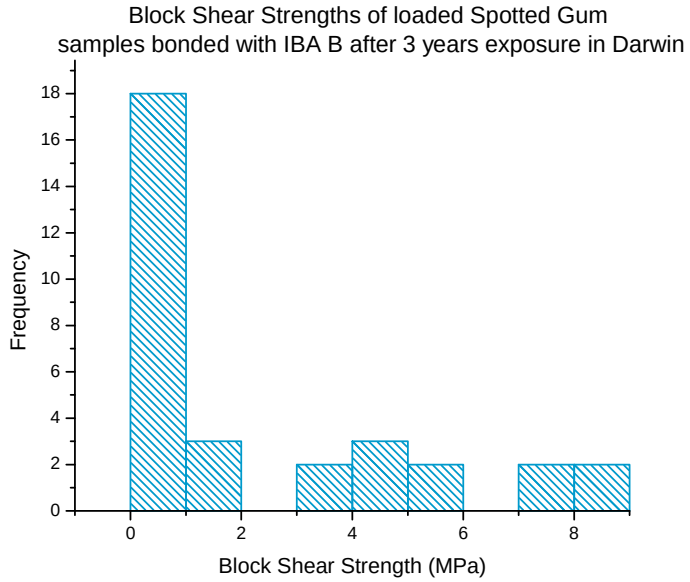

Figure 18. A histogram showing the frequency of bond strength results for the IBA B Spotted Gum samples under load after 3 years exposure in Darwin.

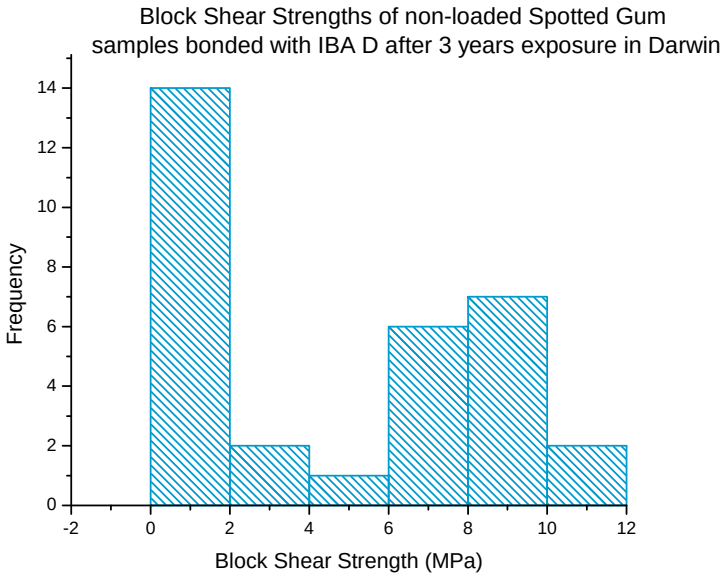

Figure 19. A histogram showing the frequency of bond strength results for the IBA D non-loaded Spotted Gum samples after 3 years exposure in Darwin.

Figure 20. Some examples of the complete failure of non-loaded Spotted Gum samples in Darwin during the 3 year exposure test.

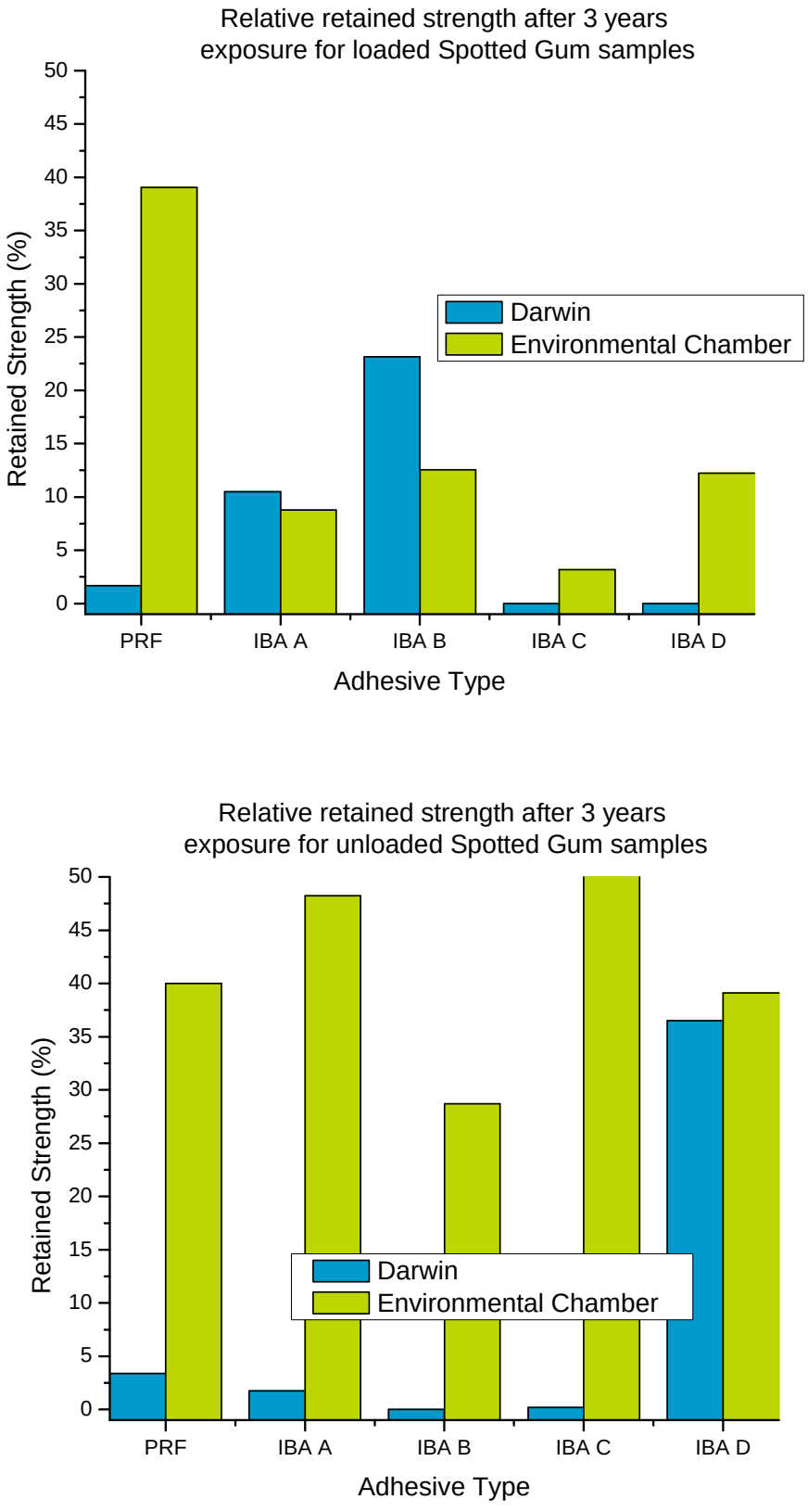

Figure 21. The relative mean retained strengths of the (*top*) loaded and (*bottom*) unloaded Spotted Gum samples (expressed as a percentage of the original strength) after 3 years exposure in Darwin and an environmental chamber.

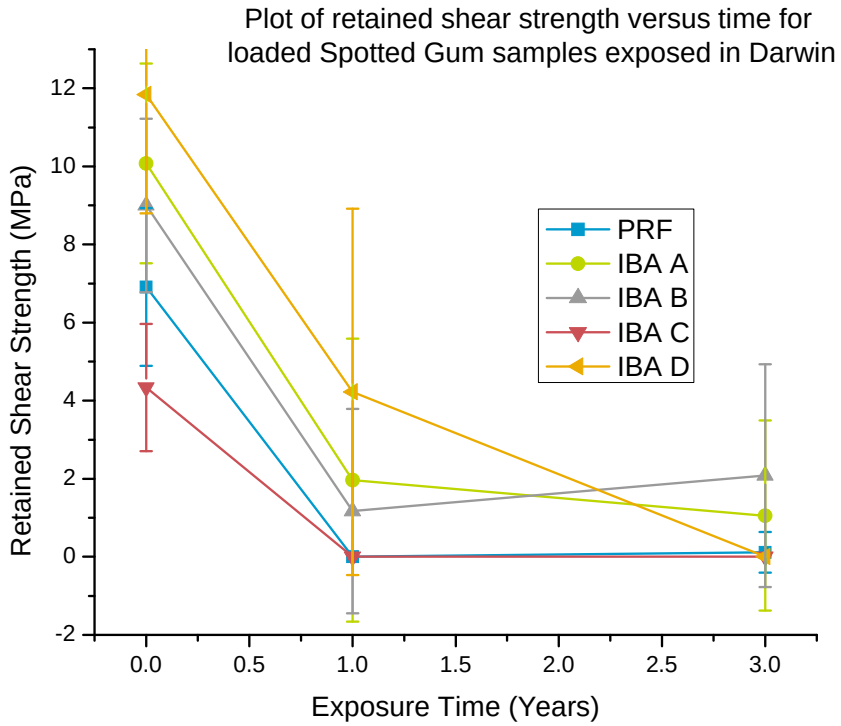

Figure 22. The mean shear strengths (MPa) of loaded Spotted Gum samples exposed in Darwin over the course of 3 years.

PALS Spectroscopy on the loaded beams after three years exposure.

Adhesives are special polymers that form a chemical bond and mechanical interlocks with the wood surface. The performance of wood adhesives can degrade with time due to the effects of both chemical aging (bond breaking) and physical aging (compaction/shrinkage). Both aging processes can lead to failure of the adhesive, and in structural applications this failure can be catastrophic.

For this reason adhesives must be tested in service conditions for extended periods of time, i.e. years. Due to the length of time required to prepare test specimens using in-service exposure conditions, accelerated weathering tests have been developed for adhesives (as well as paints and other polymers used in the outdoor environment). Previous work by CSIRO for Eastman Chemical Company showed that a non-destructive evaluation technique called positron annihilation lifetime spectroscopy (PALS) was sensitive to molecular level degradation in exterior paints one order of magnitude sooner than conventional methods. For example, if gloss loss measurements picked up macroscopic changes in the coating after 9 months exposure, then PALS detected the underlying molecular level changes after 0.9 months (in other words, ~27 days).

In light of the success in using PALS as an early warning technique for commercial coatings, the technique was included as a component of the testing regime for a series of wood beams with adhesive joints exposed under load.

The objectives of the work were to determine whether PALS can detect early stage changes in adhesives on exposure under load, and whether it can do so in a non-destructive configuration.

Approach

Samples

Wood samples as detailed in Table 10 were stored at 20^{o}C and 65%RH prior to testing by PALS. Specimens were cut from beams at locations as close as practicable to those yielding strength results most representative of the adhesive/wood species combination. PALS measurements were made at three positions on each specimen as shown in Figure 23 (glueline shown with vertical orientation). For each measurement position from six to twenty individual measurements were made in order to calculate accurate population standard deviations for the data.

Three control samples (PRF and IBA A radiata pine samples and IBA A Vic Ash) were tested after 1 year and then again after 3 years together with the exposed samples.

Table 10. Specimens examined by PALS after 3 years exposure to controlled conditions (Monash) or an unprotected tropical outdoor environment (Darwin).

Radiata Pine		**Victorian Ash**	
Control	**Exposed Samples**	**Control**	**Exposed Samples**
PRF	PRF (Monash)	PRF	PRF (Monash)
			PRF (Darwin)
IBA A	IBA A (Monash)	IBA A	IBA A (Darwin)
			IBA A (Monash)
IBA C	IBA C (Monash)	IBA C	IBA C (Darwin)
IBA D	IBA D (Monash)	IBA D	IBA D (Darwin)
			IBA D (Monash)

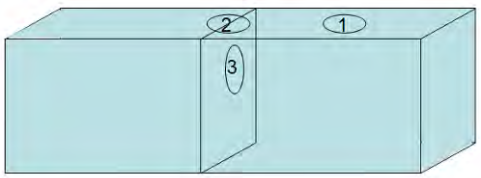

Figure 23. Specimens supplied for PALS testing were measured at three positions. The glueline was cut in half (destructive measurement) for Position 3.

PALS Measurements

Positron annihilation lifetime spectroscopy (PALS) measurements were collected in air at room temperature and 65% RH using an automated EG&G Ortec fast-fast coincidence system. The timing resolution of the system was 240 ps, determined using a prompt curve from a ^{60}Co source with the energy windows set to ^{22}Na events. A ^{22}Na source was sandwiched between two identical samples on each side, of thickness around 3 mm to ensure that all the positrons were annihilated in the sample. About 10 spectra from each sample were recorded sequentially, taking ~1 hour each and each spectrum consisted of ~1 million counts. The spectra were analysed using the program LT v.9 as the sum of 3 decaying exponentials, with the shortest lifetime (τ_1 fixed at 0.125 ns, characteristic of the para-positronium self annihilation). For the fitted lifetimes, the second lifetime (τ_2) was attributed to the annihilation of free and trapped positrons, while the third (τ_3) lifetime was attributed to the ortho-positronium component associated with the free volume in the adhesive and/or the wood.

It is the third component with lifetime τ_3 and intensity I_3 that is associated with the physical and chemical state of the adhesive and/or the wood; therefore, only the third lifetime components (τ_3, I_3) are reported here as any changes in these values reflect changes in packing and chemistry. The reported results are the mean values of these spectra. The standard deviations reported are population standard deviations for 6 to 20 repeats.

The spot size of the positron source is 2 mm such that a volume of material of about 1 mm^3 is probed when the source is placed next to a material. The configuration is shown in two dimensions in Figure 24. It is shown in Figure 24 that for the experiments performed here in the preliminary work, the positrons will always be probing some wood at the same time that they are probing the 100 µm adhesive line (positions 2 and 3). It is possible to destructively probe just the adhesive using a positron beam and the merit of this option could be the basis of further work.

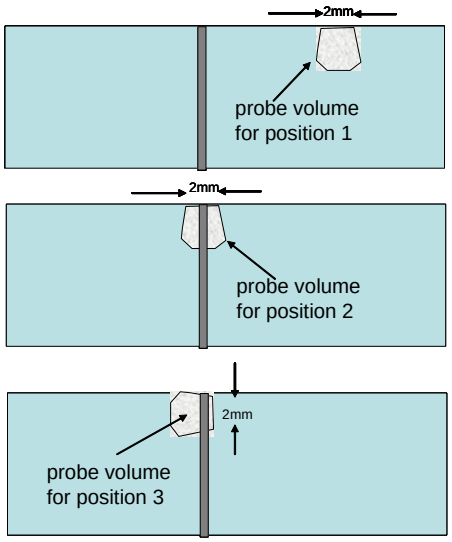

Figure 24 Two dimensional schematic of the volume of material probed by the positrons depending on the source position.

All PALS results are presented in Table 11. Each of the results will be discussed as they relate to questions that were posed for the proof of concept experiment.

Table 11. PALS data from samples exposed for 3 years.

Control Samples	Position	t_3 (ns) ± 0.03	I_3 (%) ± 0.3	Exposed Samples	Position	t_3 (ns) ± 0.03	I_3 (%) ± 0.3
Victorian Ash							
PRF	1	1.73	12.45	PRF (Darwin)	1	1.69	10.81
	2	1.73	12.19		2	1.7	11.43
	3	1.72	11.9		3	1.74	11.47
				PRF (Monash)	1	1.71	12.56
					2	1.69	11.97
					3	1.71	11.57
IBA A	1	1.74	13.19	IBA A (Darwin)	1	1.71	12.81
	2	1.76	13.45		2	1.74	13.24
	3	1.84	15.48		3	1.87	14.71
				IBA A (Monash)	1	1.73	12.94
					2	1.72	12.21
					3	1.8	13.89
IBA C	1	1.74	12.05	IBA C (Darwin)	1	1.7	13.12
	2	1.75	11.89		2	1.72	12.43
	3	1.84	13.16		3	1.96	14.38
IBA D	1	1.73	11.27	IBA D (Darwin)	1	1.69	12.19
	2	1.73	11.03		2	1.69	10.31
	3	1.76	12.94		3	1.72	12.62
				IBA D (Monash)	1	1.74	12.78
					2	1.73	12.23
					3	1.7	12.75
Radiata Pine							
PRF	1	1.64	10.5	PRF (Monash)	1	1.62	9.06
	2	1.65	10.54		2	1.63	10.33
	3	1.62	6.92		3	1.64	11.22
IBA A	1	1.63	10.78	IBA A (Monash)	1	1.65	9.7
	2	1.68	11.07		2	1.72	10.78
	3	1.72	12.37		3	1.71	12.03
IBA C	1	1.62	9.97	IBA C (Monash)	1	1.65	10.37
	2	1.65	9.98		2	1.71	10.79
	3	1.81	11.94		3	1.78	10.71
IBA D	1	1.68	10	IBA D (Monash)	1	1.63	10.79
	2	1.64	9.56		2	1.63	10.51
	3	1.67	11.41		3	1.62	11.7

Do PALS results vary in wood?

The control samples have not been exposed so variation at Position 1 in the PALS parameters reflects the packing and chemistry (cellulose/lignin) of the wood itself. It

is shown in Table 12, by comparing the control samples at Position 1, that the Victorian Ash and the Radiata Pine woods have different PALS parameters.

Each control sample was measured at Position 1 which allows a determination of the variation in PALS results between 4 pieces of the same type of wood. The lifetime measurements are very consistent for both the Victorian Ash and Radiata Pine woods.

The PALS parameters are distinctive for the two types of wood. The Victorian Ash control has an average lifetime and intensity of 1.74 ns and 12.2% compared with 1.65 ns and 10.3% for the Radiata Pine. This confirms the ability of PALS to detect the different chemistry within the two woods.

There is a considerable amount of variation with the intensity of the woods (Table 12). The Victorian Ash woods are particularly varied, with a standard deviation of 0.69%. This is approximately double the typical uncertainty for homogeneous polymers. These variations must be taken into account when looking at the changes over time.

The standard deviation in lifetime for both woods is below that of the typical standard deviation of 0.03 ns. The intensity variation for Victorian Ash is twice that of Radiata Pine indicating that the Victorian Ash is more heterogeneous in nature.

Using the variations determined in Table 12, significant changes would need to be greater than 0.7% for the intensity and 0.03 ns for the lifetime to indicate any changes or degradation with the wood/adhesive system.

Table 12. Variation of PALS results at Position 1 in four different pieces of Victorian Ash and Radiata Pine wood samples.

Victorian Ash			**Radiata Pine**		
	t_3 (ns) ± 0.03	**I_3 (%) ± 0.3**		**t_3 (ns) ± 0.03**	**I_3 (%) ± 0.3**
PRF	1.73	12.45	PRF	1.64	10.5
IBA A	1.74	13.19	IBA A	1.63	10.78
IBA C	1.74	12.05	IBA C	1.62	9.97
IBA D	1.73	11.27	IBA D	1.68	10
Average	1.737	12.24	Average	1.643	10.31
Standard Deviation	0.004	**0.69**	Standard Deviation	0.023	**0.34**

Does PALS detect the adhesive?

Looking at the PALS parameters in the control samples from Position 1 to Position 3, there are clear trends due to the presence of adhesive (Table 11).

For the PRF adhesive, for both Victorian Ash and Radiata Pine, the lifetime remains constant and the intensity drops.

For IBA A and IBA C, the lifetime and the intensity both increase for both woods.

While for IBA D, the lifetime remains constant and the intensity increases in both woods.

Despite the different lifetimes and intensity signatures for the Victorian Ash and Radiata Pine, the trends due to the presence of adhesive remain the same. This confirms the ability of PALS to detect the adhesive component amongst the background of the wood.

Does PALS detect aging of wood?

By comparing the PALS results of three control samples at 1 year and 3 years, we can determine if the wood ages when stored indoors under standard laboratory conditions of 20 ±3°C and 65 ±5% RH. The results in Table 13 show a consistent drop in lifetime (0.03 ns) and intensity (1%) for all three control samples at all positions between the first measurement in 2008 and the latest measurement in 2010. This may be due to the change in the packing density and chemistry of the wood or due to instrumental differences.

Table 13. PALS analysis of the control samples measured at 1 and 3 years.

		1 year		**3 years**		**1–3 years**	
	Position	**τ_3 (ns) ± 0.03**	**I_3 (%) ± 0.3**	**τ_3 (ns) ± 0.03**	**I_3 (%) ± 0.3**	**$\Delta\tau_3$ (ns) ± 0.03**	**ΔI_3 (%) ± 0.7**
Victorian Ash							
IBA A	1	1.8	13.6	1.74	13.19	0.06	0.41
	2	1.8	14.7	1.76	13.45	0.04	1.25
	3	1.87	15.9	1.84	15.48	0.03	0.42
Radiata Pine							
PRF	1	1.69	12	1.64	10.5	0.05	1.5
	2	1.67	11	1.65	10.54	0.02	0.46
	3	1.66	8.1	1.62	6.92	0.04	1.18
IBA A	1	1.65	11.7	1.63	10.78	0.02	0.92
	2	1.71	12.7	1.68	11.07	0.03	1.63
	3	1.73	13.6	1.72	12.37	0.01	1.23

Does PALS detect weathering of wood?

As shown in Figure 24, the PALS signal is taken from both the adhesive and the surrounding wood, therefore it is necessary to know how the PALS parameters (τ_3, I_3) behave due to the exposure of wood alone.

Table 14. The effect of exposure on PALS results from Victorian Ash and Radiata Pine wood samples by comparing τ_3 and I_3 at Position 1.

Controls	**τ_3 (ns) ± 0.03**	**I_3 (%) ± 0.3**	**Exposed Samples**	**τ_3 (ns) ± 0.03**	**I_3 (%) ± 0.3**	**$\Delta\tau_3$ (ns) ± 0.03**	**ΔI_3 (%) ± 0.7**
Victorian Ash							
PRF	1.73	12.45	PRF (Monash)	1.71	12.56	-0.02	0.11
			PRF (Darwin)	1.69	10.81	-0.04	**-1.64**
IBA A	1.74	13.19	IBA A (Darwin)	1.71	12.81	-0.03	-0.38
			IBA A (Monash)	1.73	12.94	-0.02	-0.25
IBA C	1.74	12.05	IBA C (Darwin)	1.7	13.12	-0.04	**1.07**
IBA D	1.73	11.27	IBA D (Darwin)	1.69	12.19	-0.04	**0.93**
			IBA D (Monash)	1.74	12.78	0	**1.52**
Radiata Pine							
PRF	1.64	10.5	PRF (Monash)	1.62	9.06	-0.02	**-1.44**
IBA A	1.63	10.78	IBA A (Monash)	1.65	9.7	0.01	**-1.08**
IBA C	1.62	9.97	IBA C (Monash)	1.65	10.37	0.03	0.41
IBA D	1.68	10	IBA D (Monash)	1.63	10.79	-0.05	**0.79**

Table 14 shows results for the exposed samples measured at Position 1. It is clearly observed that full outdoor exposure in the Darwin climate results in changes to the wood packing and chemistry when measured from the surface.

Four different glues were tested on two different types of wood. Therefore by comparing Position 1 for each of the controls with Position 1 from the exposed samples, the effects of exposure can be measured. From Table 14 it is evident that exposure did change the wood chemistry; however, this is not a consistent change as we see some samples increasing their I_3 value, while others reduce their I_3 value. The change in lifetime remains small for all the samples.

Figure 24 shows a schematic of the PALS experiment and the 1 mm^3 measurement volume that is probed. When the interior wood of the PRF Radiata Pine sample from Darwin was probed at a depth of 7 mm from the surface, the result showed that the wood away from the exposed surface is similar to the PRF control. This test was performed for these two samples only.

Due to the random changes from the weathering in the wood, Position 3 may offer the best spot for analysis. The wood here is not aged and can therefore be compared with the control to determine the aging of the adhesive.

If the joint is split at the adhesive, can PALS detect the adhesive?

Although this is a destructive test it is necessary to show that PALS can differentiate the 100 μm thick film of adhesive from the background wood. It is worth trying this sampling geometry (Position 3) because it may expose more volume of adhesive to

the positrons than the non-destructive Position 2 (see Figure 23), and can hence be useful in establishing the trends to watch out for when the measurement is made non-destructively. The results are measured at Position 3 (Figure 23).

For each control wood sample it is shown in Table 11 that the adhesive itself changes the PALS parameters. For the IBAs the trend is to increase the intensity, I_3, parameter. This result can be contrasted to that of the PRF control sample that shows that the adhesive decreases in I_3 in comparison to the control wood. Hence from this experiment it has been shown that PALS detects the adhesive.

It has been shown that the presence of different adhesives changes the PALS signal in a distinguishable way. Hence it has been established that PALS detects the adhesive and how the PALS parameters change when there is an adhesive layer present on the wood.

In the split joint configuration (Position 3) can PALS detect weathering of adhesive and distinguish this from weathering of the wood alone?

Due to the weathering effects at Position 1 and 2, the optimal way to determine any aging effects in the glue is to compare Position 3 on the exposed samples with the control sample. If the change from Position 1 to Position 3 on the control is similar to the change from Position 1 on the control to Position 3 on the weathered sample then we can assume that no ageing has occurred and the changes are due to the presence of adhesive only. This is equivalent to directly comparing Position 3 on the control with Position 3 on the exposed sample (see Table 15).

Table 15. The effect of exposure on PALS results from Victorian Ash and Radiata Pine wood samples by comparing τ_3 and I_3 at Position 3.

Controls	**τ_3 (ns)**	**I_3 (%)**	**Exposed Samples**	**τ_3 (ns)**	**I_3 (%)**	**$\Delta\tau_3$ (ns)**	**ΔI_3 (%)**
	± 0.03	**± 0.3**		**± 0.03**	**± 0.3**	**± 0.03**	**± 0.7**
Victorian Ash							
PRF	1.72	11.9	PRF (Monash)	1.71	11.57	-0.01	-0.33
			PRF (Darwin)	1.74	11.47	0.01	-0.43
IBA A	1.84	15.48	IBA A (Darwin)	1.87	14.71	**0.03**	**-0.77**
			IBA A (Monash)	1.8	13.89	**-0.04**	**-1.59**
IBA C	1.84	13.16	IBA C (Darwin)	1.96	14.38	**0.11**	**1.22**
IBA D	1.76	12.94	IBA D (Darwin)	1.72	12.62	-0.04	-0.32
			IBA D (Monash)	1.7	12.75	-0.06	-0.19
Radiata Pine							
PRF	1.62	6.92	PRF (Monash)	1.64	11.22	**0.02**	**4.3**
IBA A	1.72	12.37	IBA A (Monash)	1.71	12.03	-0.01	-0.34
IBA C	1.81	11.94	IBA C (Monash)	1.78	10.71	**-0.02**	**-1.23**
IBA D	1.67	11.41	IBA D (Monash)	1.62	11.7	-0.05	0.28

For the PRF adhesive there is no significant change for either of the Victorian Ash samples from Darwin or Monash, indicating that there is no degradation of the adhesive. For the Radiata Pine sample, PRF, there is a significant increase in the I_3 value for Position 3. This trend is opposite to the other PRF samples, therefore indicating a significant change to the Radiata Pine/PRF system.

For IBA A there are no significant changes for the Victorian Ash Darwin sample and the Radiata Pine Monash sample. However there is a decrease of 1.59% in I_3 for the Victorian Ash Monash sample.

For IBA C, there are some changes seen with both Victorian Ash and Radiata Pine samples. The Vic Ash sample had an increase in τ_3 of 0.11 ns and an increase in I_3 of 1.22%. The Radiata Pine sample, showed a decrease in I_3 of 1.23%.

For IBA D there is no significant change with either the Victorian Ash samples from Monash or Darwin or the Radiata Pine wood sample from Monash.

Due to the small variations of changes with the different adhesives and the different woods, (except for PRF Radiata Pine sample which has been discussed above), the data is not conclusive that the adhesives are weathering over time. The variation in weathering of the wood could be the cause of the inconsistent changes measured here.

If this is the case, it would be interesting to know if these samples were more prone to mechanical failure.

Can PALS detect the adhesive line at Position 2, non-destructively, and weathering of adhesive?

Looking at the changes in intensity from Position 1 to Position 2 of the control samples will reveal whether the non-destructive test captures enough adhesive in the probe volume (see Figure 24) to see changes in the PALS values.

Table 16. The change in Intensity and Lifetime between Position 1 and Position 2 for the Victorian Ash and Radiata Pine Control Samples.

	Position 1		**Position 2**		**Change in Lifetime**	**Change in Intensity**
Victorian Ash	τ_3	I_3	τ_3	I_3		
PRF	1.73	12.45	1.73	12.19	0.01	0.27
IBA C	1.74	12.05	1.75	11.89	-0.01	0.16
IBA D	1.73	11.27	1.73	11.03	0	0.24
IBA A	1.74	13.19	1.76	13.45	-0.01	-0.26
Radiata Pine						
PRF	1.64	10.5	1.65	10.54	-0.01	-0.04
IBA C	1.62	9.97	1.65	9.98	-0.03	-0.02
IBA D	1.68	10	1.64	9.56	0.04	0.44
IBA A	1.63	10.78	1.68	11.07	-0.05	-0.29

The results in Table 16 show that there is very little change in PALS results between the measurements taken at Position 1 and Position 2. This suggest that there is not enough adhesive in the probe volume in Position 2 to adequately test the adhesive.

It should be noted that the PALS results in Table 16 are very consistent. The changes in lifetime and intensity are well within the standard deviation of variations within the wood. This again emphasizes the reliability of the PALS measurements for the wood adhesive systems.

These results are significantly different to those measured in 2008 where there was consistently a trend between I_3 from Position 1, 2 and 3. This may indicate that the adhesive may have contracted over time, therefore reducing the volume of adhesive probed at position 2.

Can the PALS data give information on the optimum pairing of wood and adhesive?

There were small and inconsistent variations in intensity for most of the adhesives as seen in Table 15.

IBA D did not have significant changes in either Radiata Pine or Victorian Ash indicating a good pairing with both woods.

Victorian Ash also paired well with the PRF.
The Radiata Pine wood paired well with IBA A.

These are only indications, and further mechanical testing should be performed.

Conclusions

The PALS results on two different wood types, Radiata Pine and Victorian Ash, showed distinct lifetimes and intensities due to the different chain packing. By measuring the controls for each wood, we determined that the lifetime variation was within the typical bounds of uncertainty of 0.03 ns. The intensity of the wood varied more considerably at 0.7% which is more than twice the typical uncertainty for homogeneous polymers.

There was a consistent drop in lifetime (0.03 ns) and intensity (1%) for the 3 control samples that were previously measured 2 years earlier, indicating a shelf life, storage or aging effect of the woods.

Weathering at Position 1 in both woods was seen in 7 out of 11 samples due to significant changes in I_3. However these changes did not follow a particular trend for either wood. This variation is most likely due to the variable responses of the inhomogeneous domains of wood.

The adhesive was detectable at Position 3, however changes with the weathered samples were small and did not follow consistent trends. Several samples showed changes outside the accepted variations of standard deviations which may be a sign of degradation. These include Victorian Ash samples with PRF and IBA A and Radiata Pine samples with PRF and IBA C). These results should be confirmed with mechanical testing.

Changes in the PALS parameters at Position 2 were not significant enough to detect the adhesive in the control samples. Therefore the destructive test at Position 3 would be required for future testing.

Future directions

Possible future work involves measuring adhesive weathering as a function of depth from the exposed surface. This measurement is destructive and will require precision sectioning of the joints but the information gained should be useful in modelling and predicting the relationship between PALS parameters and mechanical properties of the joint. Further work will be performed to examine whether adhesive aging depends on the position in the three point bend test and if, using PALS data in conjunction with mechanical property data, it can be determined whether (and why) certain wood/adhesive combinations work better that others.

FTIR mapping would be useful on these sectioned samples to determine the chemical changes that occur in the adhesive due to weathering. The PALS data tell us when there is a change on weathering but not whether that change is physical (chain packing) or chemical (chain scission).

Positron beam experiments could be used to depth profile the adhesive face and the interface of the adhesive and wood. These results might be helpful in establishing optimum wood adhesive combinations.

Short Term Test Results

One of the important aspects of this project was to assess the suitability of a number of short term accelerated degradation tests for their usefulness in detecting differences in the longer-term performances of the adhesives. As in other aspects of this current work, the assumption has been that any new adhesive must be as durable as a PRF adhesive since PRF adhesives have a long in-service history and are regarded as being durable, that is, they degrade no faster than the wood substrate.

Five tests were chosen to broadly reflect the types of tests currently available in the various national standards. The tests were also chosen to reflect the current proposed test methods to be incorporated into a new Australian and New Zealand standard on adhesive performance (AS/NZS 4364(Int)) and the ISO standard for adhesive performance. The five test methods are shown in Table 17.

Table 17. The five accelerated tests being investigated in the current study.

Test #	**1**	**2**	**3**	**4**	**5**
Test Type	Delamination	Delamination	Cleave	Lapshear	Hydrolytic stability
Reference Standard	AS/NZS 4364:1996[6]	CSA O112.9-04[7]	AS/NZS 1328.1:1998[8]	AS/NZS 4364:1996	ASTM D4502-92[9]
Test output	% total delamination	% delamination of bond line	% wood fibre failure	Strength of bond line and % wood fibre failure	Rate of degradation

It should be noted that in this work, the five tests were performed using the same species used in the 12 month exposure study, namely Radiata pine, Victorian Ash and Spotted Gum, rather than the standardized wood species described in the respective standards. This approach was taken to allow correlation of the performance of the adhesives with the outcomes of the long term exposure study.

[6] Australian/New Zealand Standard AS/NZS 4364:1996 "*Adhesives, phenolic and aminoplastic, for load-bearing timber structures: Classification and performance requirements*".
[7] Canadian Standard O112.9-04 "*Evaluation of adhesives for structural wood products (exterior exposure)*"
[8] Australian/New Zealand Standard 1328.1:1998 "*Glued laminated structural timber. Part 1: Performacne requirements and minimum production requirements*"
[9] ASTM D4502-92 "*Standard test method for heat and moisture resistance of wood adhesive joints*".

Delamination Tests

Delamination of adhesively-bonded wood products, such as glulam, in service is a progressive rupture of the adhesive bondline causing separation of the wood laminates due to failure of the adhesive or the wood-adhesive interphase.[10] This failure occurs due to the stresses placed on the adhesive by the cyclic swelling and shrinking of the wood adherends, which can be greater than the stresses induced by mechanical loading.[10] Significant levels of delamination have been generally regarded as indicating that the adhesive bond line is not as resistant to crack growth as the wood adherend and therefore is not as durable as the wood (i.e. the adhesive or adhesive-wood interphase is weaker than the wood).

There are a number of different delamination test methods described in various national standards around the world. Two cyclic delamination test methods have been investigated in this work. The first method is based on the delamination test described in AS/NZS 4364:1996 which in turn has been derived from the European delamination method BS EN 302-2:1992. The second test method is based on the Canadian delamination test found in CSA 0112.. It was selected for investigation in this work as it has been proposed that it be incorporated into a new ISO standard on adhesives.

Cyclic delamination according to AS/NZS 4364:1996

The joint Australian and New Zealand standard subjects the adhesively bonded laminated specimens to a water soak assisted by alternate application of vacuum and pressure, followed by a rapid drying at 65°C. This wet/dry cycle is repeated twice more to give a test that comprises of 3 wet/dry cycles over a three day period. The total amount of delamination is measured immediately after the last drying cycle and is expressed as a percentage of the total length of open joints on all end grain surfaces over the total length of joints on the end grain surfaces. The level of acceptable delamination for adhesives for structural applications that are fully exposed to the weather is no more than 5% (but it should be noted that this value is for a standardized wood species, spruce).

Water uptake and loss during the delamination test

The test is premised on severe stresses being imparted on the adhesive bond line by the wood substrate as it rapidly swells in water and shrinks in the oven. To determine the level of water uptake during the test, the mass of selected samples of the pine, Victorian Ash and spotted gum test pieces was recorded at each stage of the cycle. The average percentage mass change for each of the wood species is graphed in Figure 25. It is clear that the pine and Victorian Ash samples become significantly

[10] B. River, C. Vick, R. Gilliespie, "Wood as an adherend", *Treatise on adhesion and adhesives*, Chapter 1, Volume 7, Ed. J. Minford, Marcel Dekker, 1991

saturated with water after each vacuum impregnation and returned to near their initial masses after the drying period. The spotted gum behaved very differently and was found to only take up approximately 2% of its mass by water during the water impregnation stage. This water was completely removed during the drying stage. Regardless of the low level of water uptake, there was a significant effect on all of the adhesives (*vide infra*).

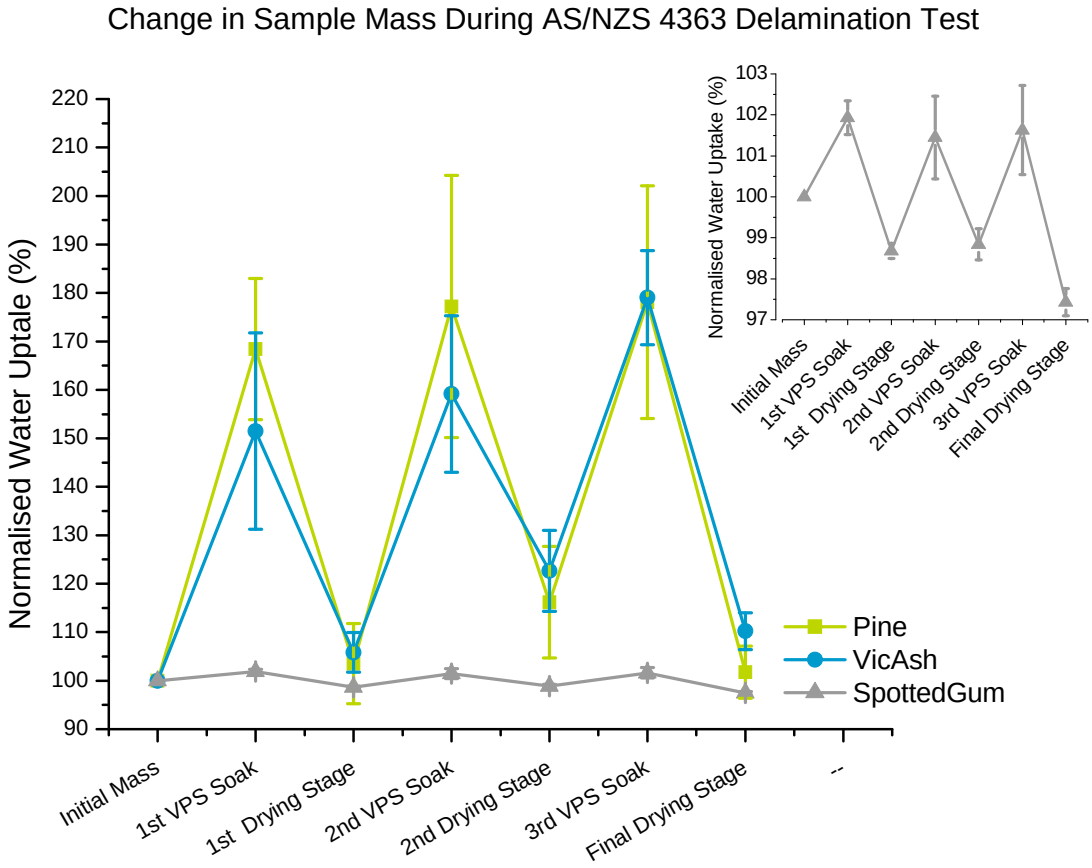

Figure 25 Variation in mass of the pine, Victorian Ash and Spotted Gum test pieces during the cyclic delamination test and (*inset*) an expanded view of the spotted gum results. Error bars represent ±1 SD.

AS/NZS 4364 Delamination Results

The results for the AS/NZS delamination test are given in Table 18 and presented graphically as a box and whisker plot in Figure 26.[11] One point that is obvious from Figure 26 is that, despite the low level of water uptake, the spotted gum specimens for all of the adhesives show almost complete delamination. This result highlights the difficulty in preparing durable adhesive bonds for this species.

[11] For more information regarding box and whisker plots, refer to Appendix C.

The results for the pine substrate show some differentiation between the adhesives. The PRF control had very low levels of delamination as did the IBA D sample. The other IBAs (A-C) had higher levels of delamination. One of the intriguing features of these results is the significant variability in the delamination results for the IBAs, particularly IBAs A-C as measured by the height of the boxes. The reason for this variability is unclear but it might reflect some level of localized inhomogeneity of the adhesive film due to, for example, the presence of voids formed during the curing of the adhesive. These voids have been detected in previous work and result from the evolution of carbon dioxide (CO_2) gas during the moisture related curing of the isocyanate adhesives.[12]

The Victorian Ash samples demonstrate results that are different to the pine samples. The PRF control samples had very low levels of delamination. IBAs B-D were very similar and a little higher than the PRF samples. IBA A shows three distinct groupings of delamination results. These appear to be related to which of the three manufactured beams the samples were taken from and may be attributable to variations in the manufacture of the beams.

One observation that should be noted is an apparent species effect with some of the IBAs (noticeably with IBAs A-C). For these adhesives, the pine samples all gave much higher delamination results compared to the Victorian Ash samples. This does not appear to occur with the PRF or IBA D.

Table 18. Average delamination values (%), standard deviation (SD) and number of tests (n) as determined by the AS/NZS 4364 delamination test.

		Average Delamination (%)	**SD**	***n***
PRF	***Pine***	0.7	0.7	*9*
	Victorian Ash	0.3	0.7	*9*
	Spotted Gum	90.2	10.7	*9*
IBA A	***Pine***	19.6	15.5	*9*
	Victorian Ash	12.8	10.8	*9*
	Spotted Gum	99.1	0.3	*9*
IBA B	***Pine***	8.2	6.2	*9*
	Victorian Ash	2.9	4.3	*9*
	Spotted Gum	94.7	6.9	*9*
IBA C	***Pine***	25.7	9.5	*9*
	Victorian Ash	5.2	5.2	*9*
	Spotted Gum	98.7	0.5	*9*
IBA D	***Pine***	1.6	2.3	*9*
	Victorian Ash	2.8	3.0	*9*
	Spotted Gum	94.4	3.5	*9*

[12] W. Tze, T. Rials, S. Kelley, S. Wang, G. Pharr, "The wood-resin interphase. Characterisation by nanoindentation and chemical imaging", *Wood Adhesives 2005 Symposium Proceedings*, Ed C. Frihart, 53

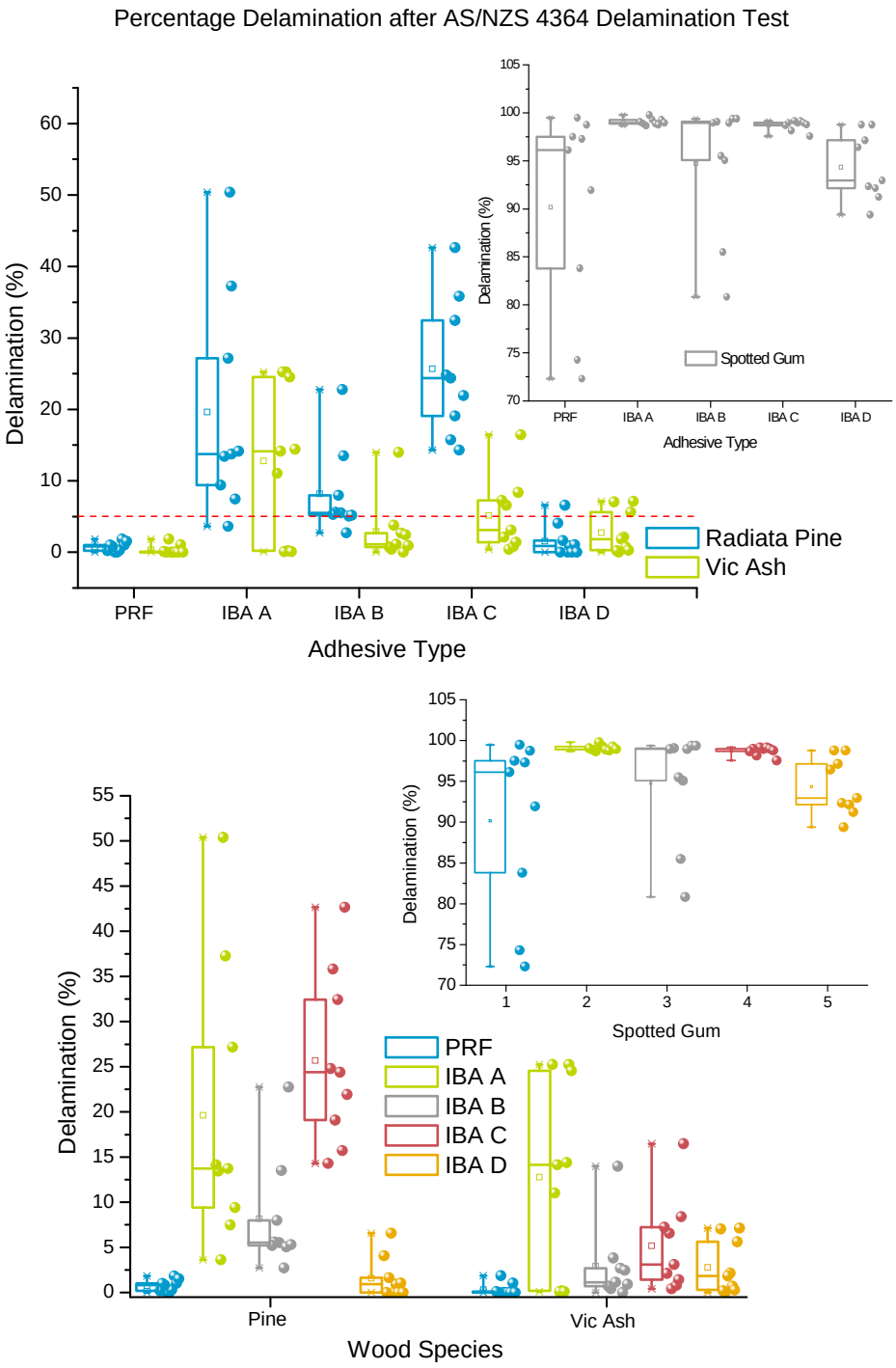

Figure 26. (*top*) A box and whisker plot (with data scatter) showing the delamination results by adhesive type for the pine and Victorian Ash (*main graph*) and for the spotted gum (*inset*). The red dashed line indicates the maximum 5% delamination allowed under AS/NZS 4364:1996 for spruce samples. (*bottom*) The same results plotted by wood species.

Cyclic delamination according to CSA O112.9

The delamination test described in the Canadian standard is based on the same principle as the AS/NZS 4364 delamination test, namely exposing the adhesive bond line to stress by the cyclic wetting and drying of the surrounding wood. One significant difference between the two tests is the exposure conditions employed.

In this test, the adhesively-bonded samples are immersed in water and subjected to an applied vacuum of 75 kPa (relative to atmosphere) for 2 hours followed by the application of pressure (540 kPa) for a further 2 hours. This impregnation cycle is repeated to give a 8 hour water soak. The samples are then dried in an oven at 28±2°C for 88 hours such that the samples dry to within 10% of their original weight. This 4 day cycle of water impregnation and drying is repeated twice more to give a 3 cycle soak/dry regime that takes 12 days to complete. The acceptance criterion for this test is different to the Australian standard and defines the maximum allowable delamination of a single bond line. The allowable delamination for a single bond line is 1% for adhesively bonded softwoods or 1.6% for bonded hardwoods with the percentage delamination being calculated as the length of the delamination of one bond line divided by the total length of end grain bond lines. The Canadian standard prescribes a group of standardized softwoods (lodgepole pine, black spruce and Douglas fir) and one standardized hardwood (hard maple) for use with the method. As a consequence of the way the result is calculated, a value of 20% delamination for a single bond line represents total delamination of that bond line.

The values of the single bond line delamination are presented in Figure 27 whilst the average results are listed in Table 19. Looking at the results for the pine substrate reveals some differences between the adhesives. IBA D had the lowest level of delamination followed by the PRF. IBA A appears to be similar to the PRF whilst both IBA B and IBA C gave higher results. These last two adhesives also had a large variation in results. The Victorian Ash samples followed a broadly similar pattern. IBA D appeared not to be susceptible to delamination whilst the PRF was the next best performing adhesive. IBA B and IBA C appear to be approximately equivalent with the highest levels of delamination while IBA A was somewhere between these two adhesives and the PRF. Finally, the spotted gum samples all showed significant values of bond line delamination with a large variation in the results.

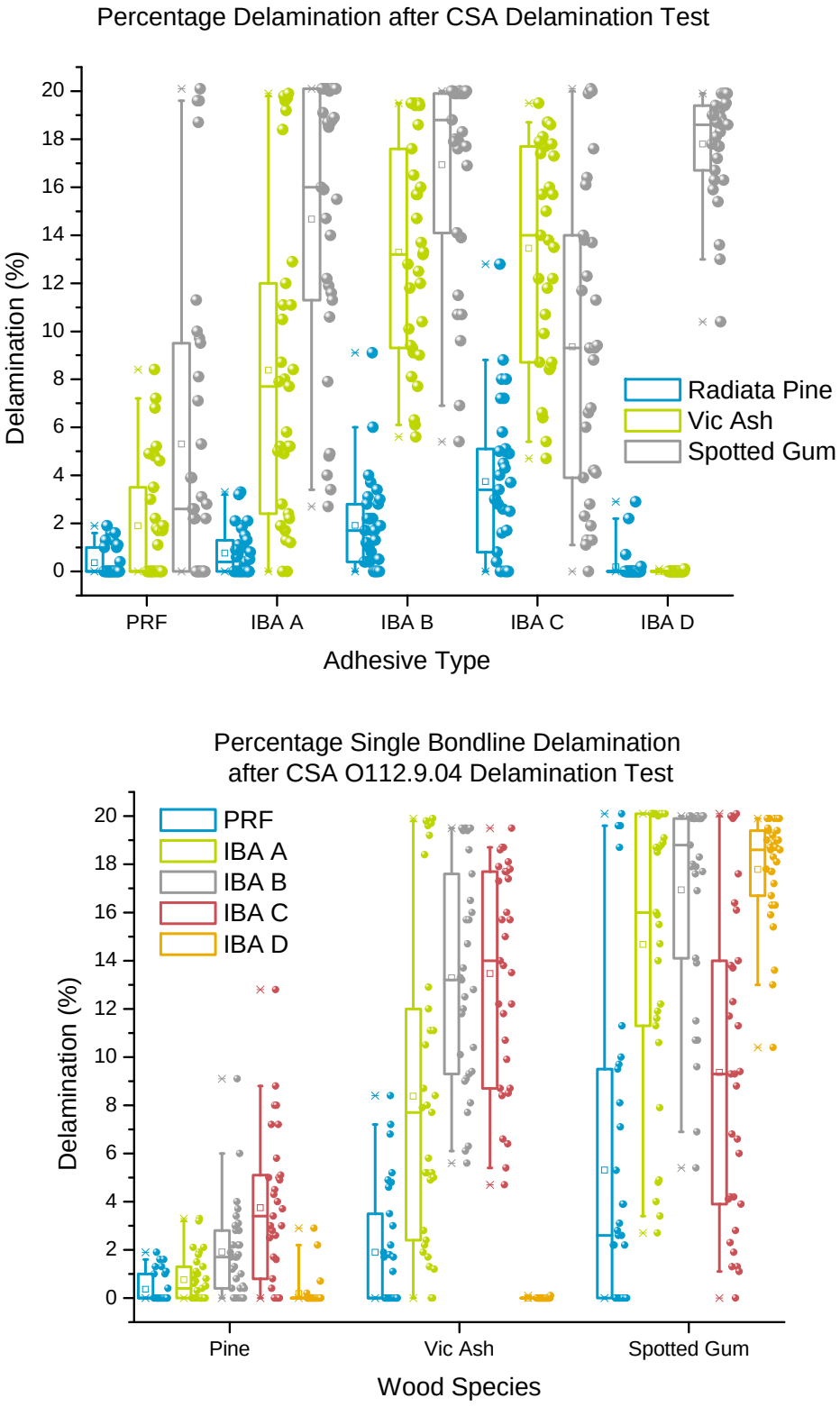

Figure 27. Box and whisker plots (with data scatter) showing the single bond line delamination results as tested according to CSA O112.9 grouped by adhesive type (*top*) and by wood species (*bottom*).

Table 19. Average bond line delamination values (%), standard deviation (SD) and number of tests (n) as determined by the CSA O112.9 delamination test.

		Average Delamination (%)	SD	*n*
PRF	***Pine***	0.4	0.6	*31*
	Victorian Ash	1.9	2.5	*31*
	Spotted Gum	5.3	6.5	*31*
IBA A	***Pine***	0.8	1.0	*31*
	Victorian Ash	8.4	6.5	*31*
	Spotted Gum	14.7	5.9	*31*
IBA B	***Pine***	1.9	2.0	*31*
	Victorian Ash	13.3	4.5	*31*
	Spotted Gum	16.9	4.3	*31*
IBA C	***Pine***	3.7	3.1	*31*
	Victorian Ash	13.5	4.6	*31*
	Spotted Gum	9.4	6.5	*31*
IBA D	***Pine***	0.2	0.6	*31*
	Victorian Ash	0.0	0.0	*31*
	Spotted Gum	17.8	2.2	*31*

Cleave Testing According to AS/NZS 1328.1:1998

One of the quality control tests listed in AS/NZS 1328.1.1998 as suitable for the continuous assessment of glulam in a manufacturing process is a cleave test. In this test, the glulam is cleaved apart parallel to the direction of the wood grain in the plane of the adhesive bond and the percentage of wood fibre failure is recorded. The cleavage is accomplished by putting a 10 mm notch in the adhesive bond line as a pre-fracture zone and splitting the adhesive bond line apart by using a thick wedge (such as a bricklayer's bolster) and a mallet. For glulam to be suitable for use in service conditions fully exposed to the weather, satisfactory results must be obtained in tests is performed on both dry and water saturated samples. The wet samples are impregnated with water in a 2 stage vacuum pressure soak (VPS) and cleaved whilst still wet. The acceptance criteria for an adhesive to pass the cleavage test is to have an average wood fibre failure of no less that 60% and no single glue line with a wood fibre failure value of less than 30%. The premise of this test is that the adhesive bond line should be at least as strong, if not stronger, than the wood itself, so that crack propagation (i.e. cleave pathway) will follow the weakest path in the wood and therefore result in a high level of wood fibre failure.

The cleave samples were taken from beams that were surplus to the 3 year outdoor exposure study and therefore representative of those that were used in the Darwin exposure testing. One point to highlight was the greater difficulty in assessing wood fibre failure for samples bonded with the IBAs, relative to the PRF control. The red colour of the PRF control assisted in the evaluation of wood fibre failure as it

facilitated differentiation of adhesive from wood. The very light colour of the IBAs made assessment of wood fibre failure a more difficult task.

Water uptake

One of assumptions of the wet cleave test was that the test requires complete penetration of the water into the wood to have an effect on the adhesive bond line. It is noted in AS/NZS 1328.1:1998 that longer VPS cycle times and higher pressures might be required to achieve full and total water penetration. To test this, the mass of the adhesively-bonded samples of the pine, Victorian Ash and spotted gum substrate were recorded prior to and after the 2-cycle VPS (Table 20 and Figure 28). It can be seen that the pine and Victorian Ash samples approximately doubled their mass with water, demonstrating full water saturation. The spotted gum samples could only achieve *ca* 5% mass increase. This did not significantly increase with extra VSP cycles. Whilst there was only a very small uptake of water for the spotted gum samples, it appears that this is still enough to affect the wet cleave results (*vide infra*).

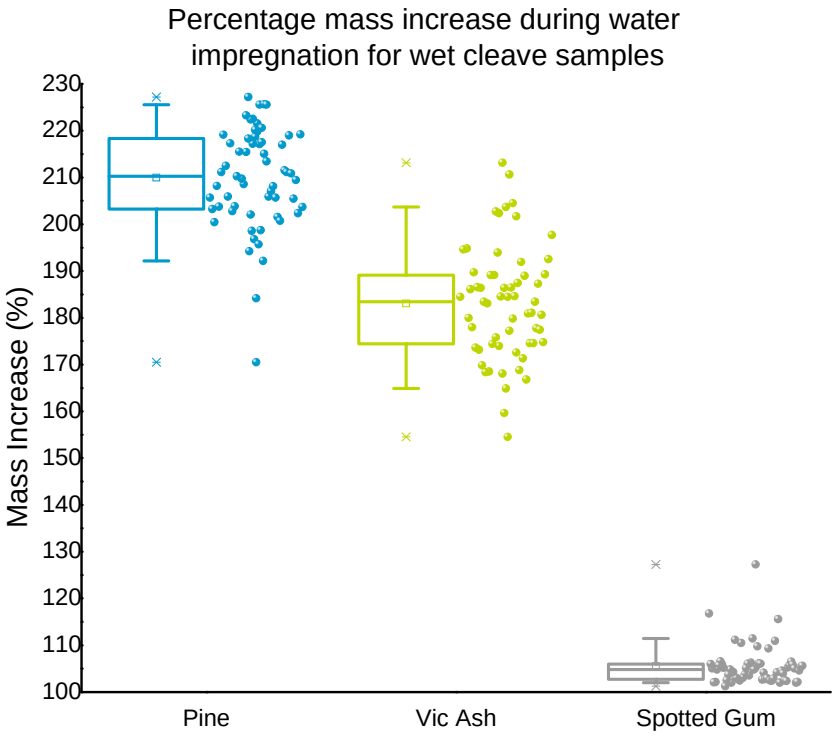

Figure 28. Normalized percentage mass increase (relative to the initial masses) of the test samples for the three wood species during the AS/NZS 1328.1:1998 wet cleave test.

Table 20. Average mass increase (%), number of samples (n) and standard deviation (SD) of the test samples for the three wood species during the AS/NZS 1328.1:1998 wet cleave test.

Species	***n***	***Mass Increase (%)***	***SD***
Radiata Pine	60	210.0	10.8
Victorian Ash	60	183.5	12.2
Spotted Gum	60	105.5	2.5

Wet and Dry Cleave Results

The wet and dry cleave results for all of the adhesives bonded to radiata pine are given in Figure 29 and Table 21. It should be noted that no attempt was made to exclude any outlier data points. It can be seen that when tested dry, all of the IBAs gave very high wood fibre failure values and are equivalent to the PRF control. It is after the samples have been exposed to water and cleaved that differences between the adhesives become apparent. The wet PRF samples still had a high level of wood fibre failure but there were a number of lower values. IBA D appeared to perform as well as the PRF control adhesive with no significant drop in wood fibre failure after immersion in water. The other three IBAs (A-C) had significantly decreased wood fibre failure values upon getting wet. IBA A suffered the greatest decrease with the average dry value of 97% falling to 19% when wet. IBAs B and C also experienced reduced wood fibre failure values upon wetting but not as great a drop as for IBA A. It should be highlighted that all of the IBAs had a wide variation in values when tested wet, the reason behind this is not clear but may be related to localized differences in the uniformity of the adhesive coverage within the small cleave area. These differences might arise from variations in the number and size of bubbles/voids in the adhesive layer due to the entrapment of CO_2 gas (a by-product of the curing reaction of some IBAs). Based on the 60% average wood fibre failure requirement of the standard, IBAs A-C would fail the test. Regardless of this, the IBAs A-C all show a lower result than the reference PRF adhesive with only IBA D appearing to be equivalent.

Table 21. The average percentage wood fibre failure values, standard deviation and number of test samples for the adhesives bonded to radiata pine.

	PRF		**IBA A**		**IBA B**		**IBA C**		**IBA D**	
	Dry	***Wet***	***Dry***	***Wet***	***Dry***	***Wet***	***Dry***	***Wet***	***Dry***	***Wet***
Average (%)	86	83	97	19	96	40	89	41	93	89
S.D.	18	22	6	24	8	24	16	30	10	17
n	30	54	30	54	30	52	30	54	30	54

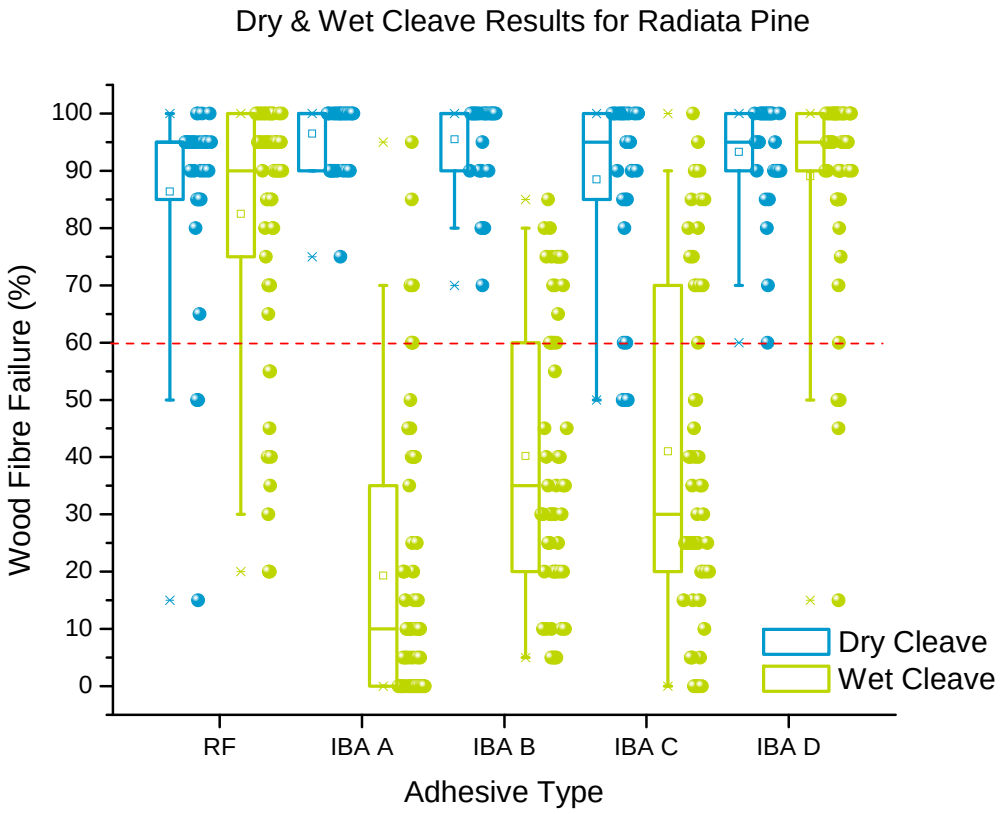

Figure 29. A box and whisker plot (with data scatter) showing the wet and dry cleave results for the adhesives on the radiata pine substrate. The red dashed line indicates the 60% wood fibre failure required in AS/NZS 1328.1:1998.

The results for the Victorian Ash substrate follow a very similar trend to those described above and are given in Figure 30 and Table 22**.** IBA D performed equivalently to the PRF control and does not show a significant decrease in the wood fibre failure values upon getting wet. IBA A again appeared to perform poorly when wet whilst IBAs B and C show smaller decreases in the average wood fibre failure upon wetting. AS was the case for the pine substrate, there is a large variation in the wet wood fibre values for IBAs A, B and C, the explanation for which is unclear. Based on the 60% wood fibre failure requirement only IBAs C and D would pass the test with IBA D appearing to perform better than the PRF adhesive.

Table 22. The average percentage wood fibre failure values, standard deviation and number of test samples for the adhesives bonded to Victorian Ash.

	PRF		**IBA A**		**IBA B**		**IBA C**		**IBA D**	
	Dry	***Wet***	***Dry***	***Wet***	***Dry***	***Wet***	***Dry***	***Wet***	***Dry***	***Wet***
Average (%)	98	84	94	17	99	49	96	66	97	95
S.D.	5	18	13	23	4	29	8	33	8	9
n	30	53	30	53	30	53	30	54	30	56

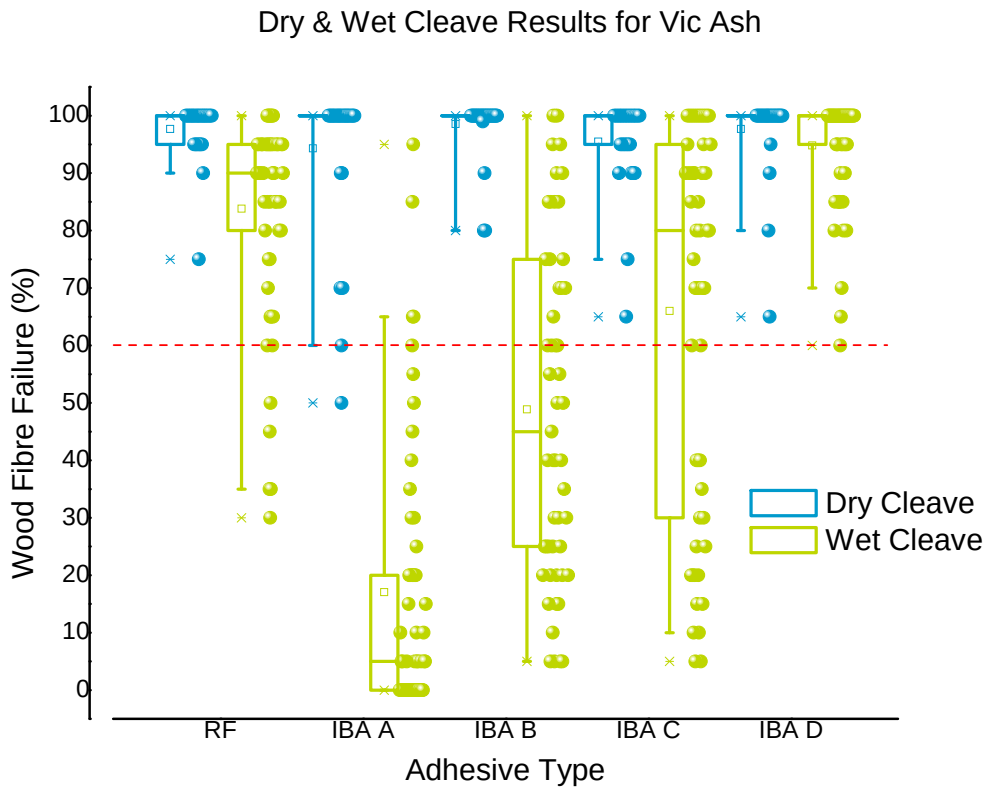

Figure 30. A box and whisker plot (with data scatter) showing the wet and dry cleave results for the adhesives on the Victorian Ash substrate. The red dashed line indicates the 60% wood fibre failure required in AS/NZS 1328.1:1998.

As discussed previously, the spotted gum samples were found to only take up approximately 5% of their mass with water, unlike the other two wood species which were found to have almost doubled their masses with water. Comparing the dry and wet cleave results for the spotted gum samples (Figure 31 and Table 23), this low mass increase apparently did not stop the water from penetrating into the wood adhesive bond line and weakening it, as indicated by a reduction in the percentage of wood fibre failure. When tested in a dry state, IBA D gave the best performance with an average wood fibre failure value of 77%. The other adhesives all gave similar values of around 14-22% except for IBA A which was marginally higher. IBA A had a number of wood fibre failure scores in the 90% region indicating that, at least in some instances, a good dry bond was established. Upon wetting, the wood fibre failure values of all the adhesives showed some degree of decrease with IBA C having an extremely low value. IBAs A and B were similar to the PRF control adhesive whilst IBA D was marginally higher. Like the other wood substrates, there was a large variation in the scatter of the results which makes comparisons very difficult. Regardless of this, the low wood fibre failure values for all of the adhesives, both dry and wet, give an indication of the difficulty in achieving acceptable bonds with this timber.

Table 23. The average percentage wood fibre failure values, standard deviation and number of test samples for the adhesives bonded to Spotted Gum.

	PRF		IBA A		IBA B		IBA C		IBA D	
	Dry	***Wet***	***Dry***	***Wet***	***Dry***	***Wet***	***Dry***	***Wet***	***Dry***	***Wet***
Average (%)	14	11	39	14	13	10	22	3	77	29
S.D.	10	13	39	26	17	18	21	12	35	29
n	30	50	30	54	30	63	30	54	30	49

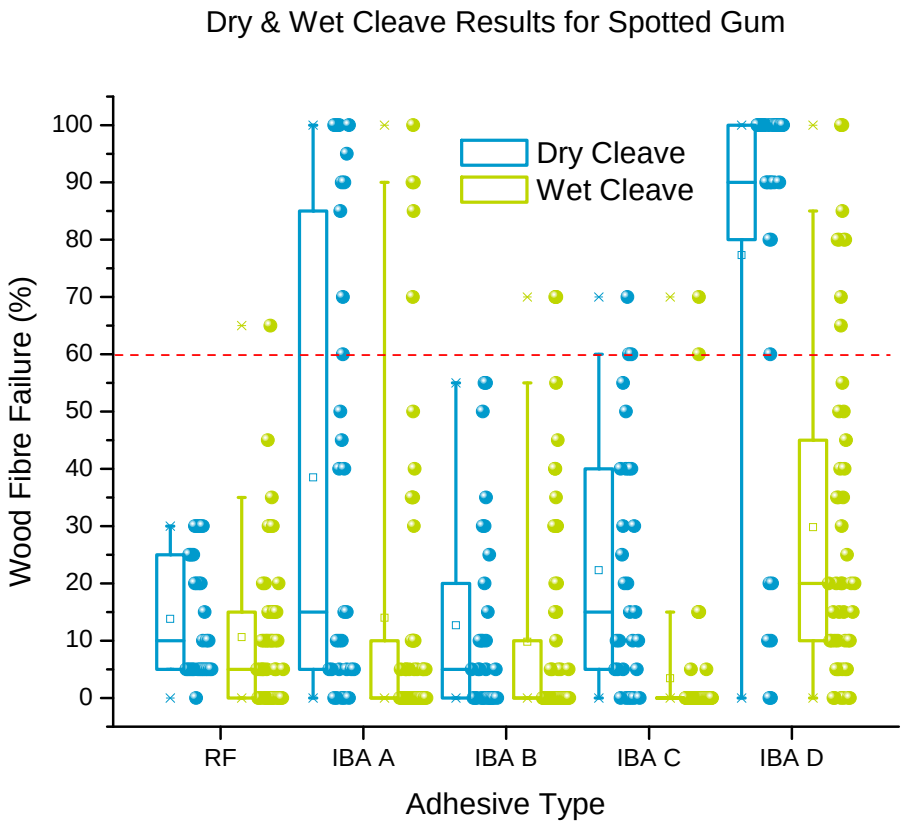

Figure 31. A box and whisker plot (with data scatter) showing the wet and dry cleave results for the adhesives on the spotted gum substrate. The red dashed line indicates the 60% wood fibre failure required in AS/NZS 1328.1:1998.

Longitudinal Tensile Lap Shear Tests According to AS/NZS 4364:1996

The longitudinal tensile shear test is described in detail in AS/NZS 4364:1996. In summary, the test consists of treating adhesively bonded lap shear specimens to either a cold water soak (treatment A2) or a boiling water soak (treatment A4) and testing the specimens in the wet state (treatments A2 an A4)and after they have been dried (treatments A3 and A5). A set of control specimens (treatment A1) are also tested.

The treatments that the adhesives are subjected to are summarised in Table 24**.** Therefore, in essence, the adhesives are subjected to two different accelerated weathering regimes, cold water and boiling water soak. Samples are tested both wet and dry to determine the effect of water on the bonding performance, with the underlying assumption that durable adhesives should be as strong as the wood substrate.

Table 24. The 5 different treatment conditions that the adhesives are exposed to prior to tensile shear testing.

Treatment Label	**Treatment Description**
A1	7 days conditioning at standard atmosphere[(1)]
A2	7 days conditioning at standard atmosphere 4 days soaking in water at 15±5°C Samples tested wet
A3	7 days conditioning at standard atmosphere 4 days soaking in water at 15±5°C Drying for 7 days at standard atmosphere Samples tested dry
A4	7 days conditioning at standard atmosphere 6 hours soaking in boiling water 2 hours soaking in water at 15±5°C Samples tested wet
A5	7 days conditioning at standard atmosphere 6 hours soaking in boiling water 2 hours soaking in water at 15±5°C Drying for 7 days at standard atmosphere Samples tested dry

[(1)] Standard atmosphere has been defined in the standard as a temperature of 20±2°C and a relative air humidity of 65±5%

The average shear strength and wood fibre failure values for each of the three wood species are given in Figures 17-21. The shear strength information is presented in two formats for each of the wood species; by adhesive type and by treatment number. Comparisons between treatments within an adhesive are best viewed when the data are grouped by adhesive type whilst comparisons between adhesives for a given treatment are best described when the results are presented by treatment type.

Looking at the radiata pine data grouped by adhesive type (Figure 32 (*top*)), several features become apparent. The PRF control values for all of the dry tests (treatments A1, A3 and A5) appear to be equivalent. One-way analysis of variance (ANOVA) of the means for each of these treatments reveals no statistically significant differences at the 0.05 confidence level. These results suggest that there is no discernible degradation of strength of the PRF adhesive (when tested dry) after either the 4 day cold water or the 6 hour boil soak.

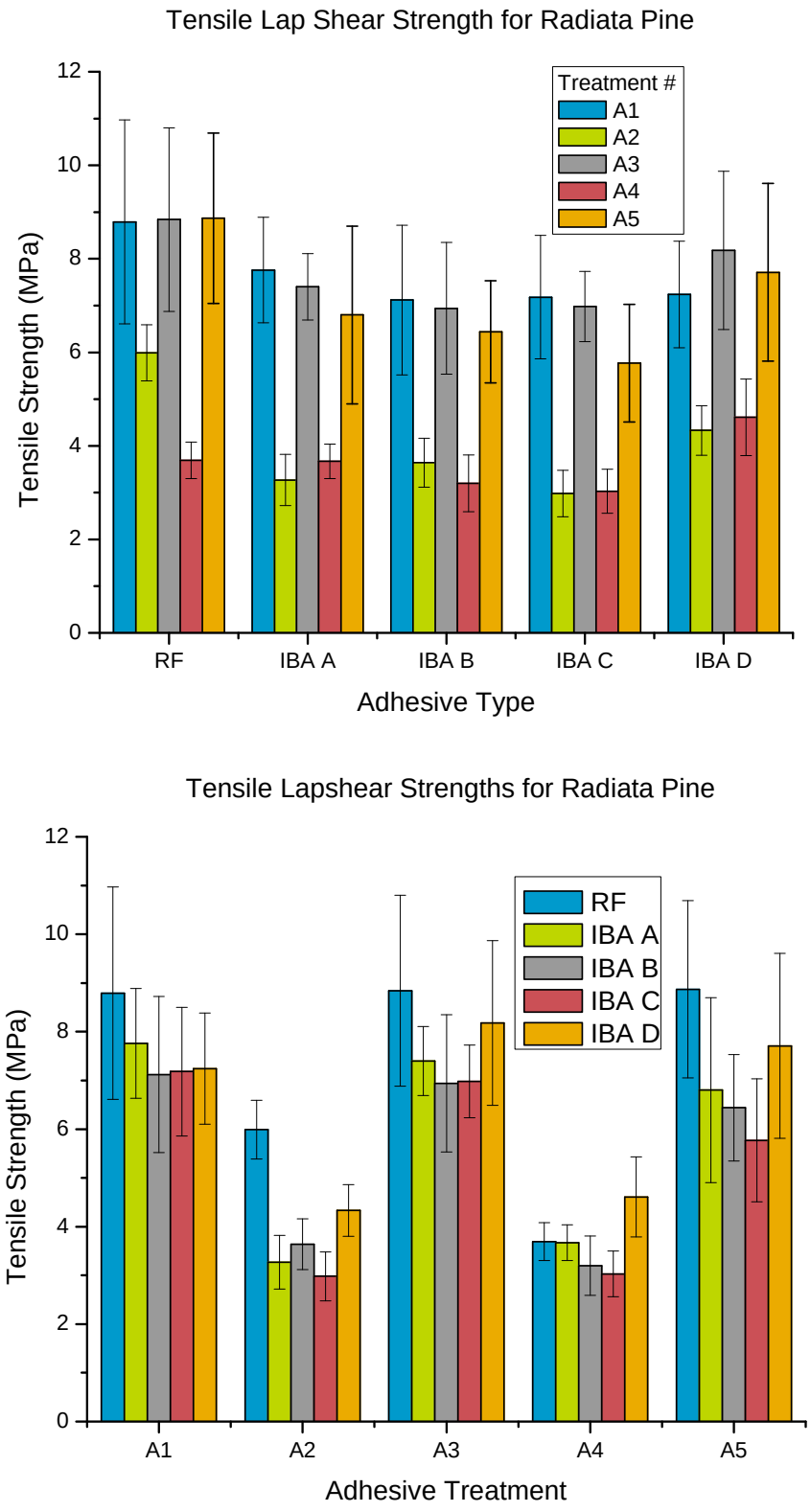

Figure 32. Average tensile lap shear strength results for the radiata pine samples by adhesive type (*top*) and adhesive treatment regime (*bottom*). Error bars represent ±1 SD.

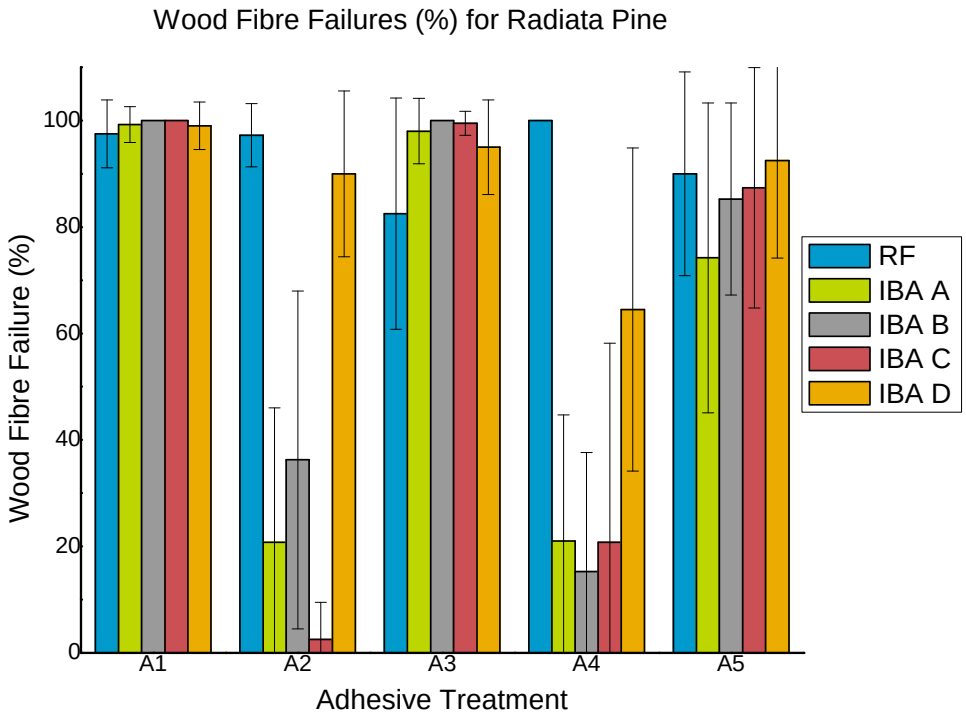

Figure 33. Wood fibre failure results for the radiata pine lapshear tests grouped by treatment. Error bars represent ±1 SD.

Similarly, one-way ANOVA testing of the dry test means for each of the IBAs indicate that, with the exception of the decrease in mean strength of IBA C following the boil treatment, there are no statistically significant differences (at the 0.05 confidence level). These results suggest that there is no degradation of these adhesives during this test. The other interesting feature of this graph is that all of the adhesives show a significant decrease in strength when tested wet but that this strength is recovered once the sample is re-dried for the majority of the adhesives.

Comparing the graph of shear strength by adhesive treatment (Figure 32 (*bottom*)) shows the comparative performance of each of the IBAs versus the PRF control for each of the 5 treatments. The PRF adhesive appeared to have the highest dry initial strength (treatment A1) of all five adhesives. However, one-way ANOVA (at the 0.05 confidence level) suggests that its strength is no greater than that of IBA A. There is a statistically significant difference between the strength of the PRF and the strengths of IBAs B-D.

Treatment A2 shows a significant difference between the PRF adhesive and all of the IBAs. Within the IBA group there are also statistically significant differences with IBA D being significantly stronger than IBA B which is in turn significantly stronger than IBAs A and C. There is no difference between IBA A and C. The adhesives recovered their original strengths when dried prior to testing after treatment (treatment A3).

Similar analysis proved that after treatment A4 (the boil test), the apparently greater strength of IBA D, relative to the other adhesives is statistically significantly. The next highest result is for both the PRF and IBA A (which are not statistically significantly different). IBAs B and C are equivalent and gave the lowest values. When allowed to dry before testing, the PRF and IBA D gave the highest values. IBAs A, B and C were found to not be statistically significantly different to each other but significant different to the PRF and IBA D.

Comparing the wood fibre failure values for each of the treatments is also illustrative of the difference between the PRF and IBAs (Figure 33). The PRF adhesive maintained very high wood fibre failure values in all the tests indicative that the failure occurred predominantly in the wood. The IBAs showed differences based upon whether the samples were tested wet or after having been dried. Wet samples, except in the case of IBA D, displayed very low levels of wood failure when tested wet except for IBA D, indicating that the failure occurred in the adhesive layer. After drying, these IBAs regained their strength and the failure occurred in the wood, resulting in high wood fibre failure values.

Similar comparison can be undertaken for the Victorian Ash samples. Comparing the treatments by adhesive type (Figure 34 (*top*)) highlights the following results. For the PRF adhesive, shear strengths following A1 and A3 are equivalent and grater than that following A5. The performance of IBA A and B were similar to each other, with the A1 and A3 treatments giving equivalent results and A5 significantly lower. Treatments A2 and A4 are not equivalent for each adhesive. For IBA C, the results are a little complicated but treatment A1 and A3 are equivalent, A3 and A5 are equivalent but A1 and A5 are statistically different. The wet tests (A2 and A4) yielded equivalent strengths significantly lower than those from the dry tests. Finally, for IBA D, treatments A1 and A3 are equivalent but A5 is significantly lower in strength. There was a statistically significant difference in the mean wet strengths following treatments A2 and A4.

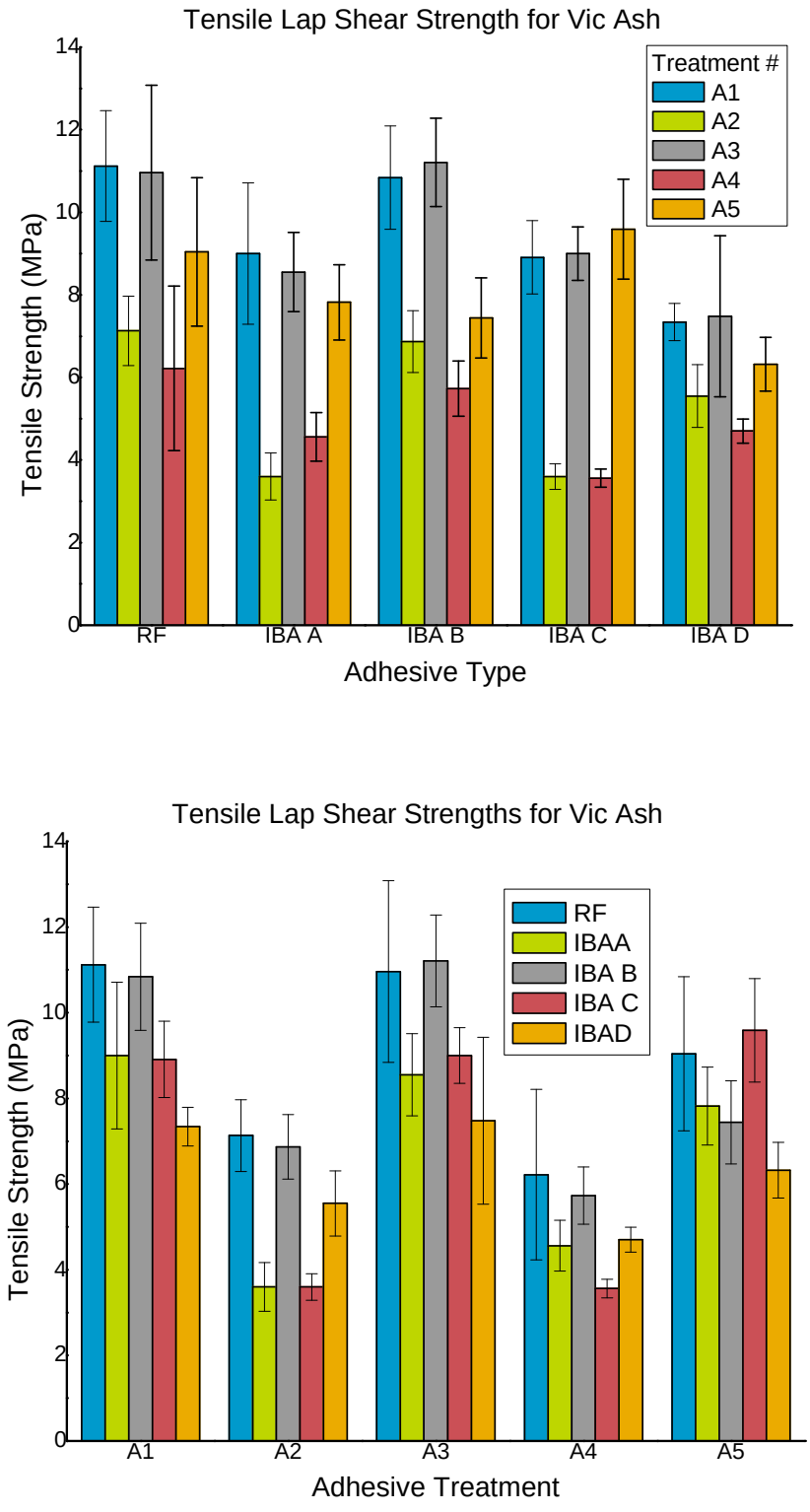

Figure 34. Average tensile strength results for the Victorian Ash samples by adhesive type (*top*) and adhesive treatment regime (*bottom*). Error bars represent ±1 SD.

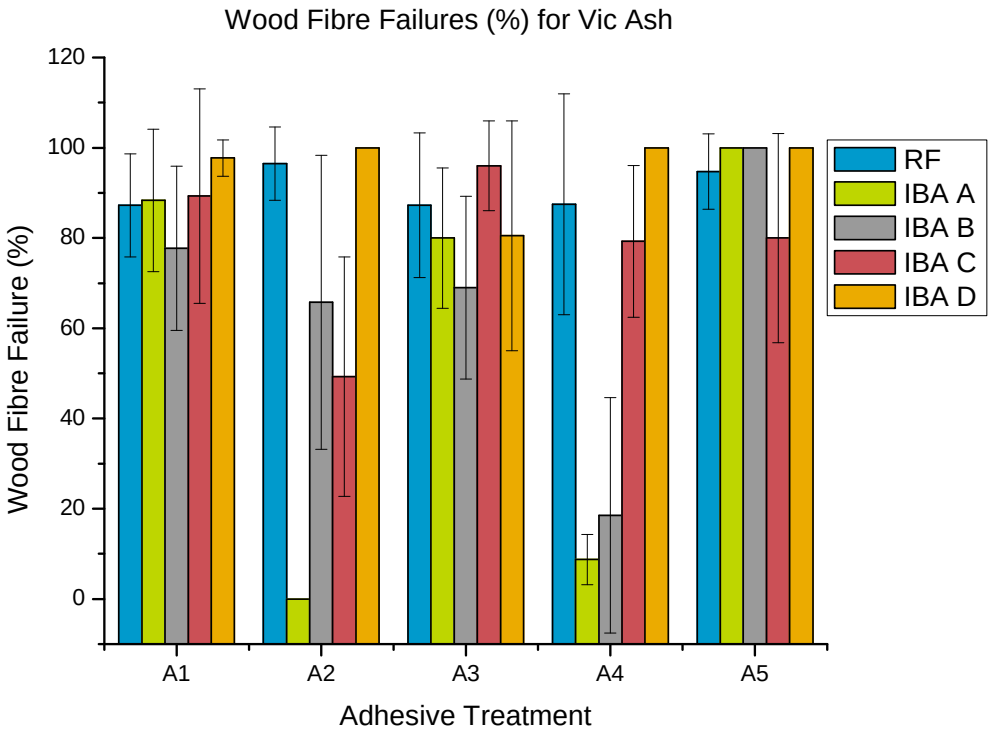

Figure 35. Wood fibre failure results for the Victorian Ash lapshear tests grouped by treatment. Error bars represent ±1 SD.

The relative performances of the adhesives following the different treatments (Figure 34(*bottom*)) can be summarized as follows. For treatment A1, both the PRF and IBA B are equivalent and gave higher strength values than IBA A and C which were equivalent. IBA D was the weakest. This same pattern was observed for treatment A4. Treatment A2 again ranked the PRF and IBA B as equivalent and significantly stronger than IBA D. Both IBA A and C were equivalent and were much lower in strength than the other adhesives. Finally, treatment A5 ranked IBA C and the PRF as equivalent and stronger than IBA A and D which were also equivalent. IBA D was the weakest following this treatment.

Comparing the wood fibre failure values for each of the treatments is also illustrative of the difference between the PRF and IBAs (Figure 35). The PRF adhesive maintained very high wood fibre failure values in all tests indicative that the failure occurred in the wood. The IBAs showed difference based upon whether the samples were tested wet or allowed to redry. IBAs A-C showed varying low levels of wood failure when tested wet after treatments A2 and A4, with IBA A giving the lowest wet values whereas IBA D gave consistently high results. The relative strengths of IBAs B and C gave depended on whether the soak was in cold water or boiling water. When allowed to dry, these IBAs regained their strength and the failure occurred in the wood, resulting in high wood fibre failure values.

The results for spotted gum are given in Figure 36. There is some difficulty in interpreting the results for the PRF adhesive as there was a very large variation in the data for the A1 treatment with a number of very low results. These results appear to have all originated from the same panel. If these results are ignored, then the average for this treatment becomes 11.6 MPa with a standard deviation of 1.6. The large variations in the results for the PRF adhesive following the other treatments arise from variations between samples within the same panel.

Comparing the results by adhesive indicate that the PRF adhesive appears to recover most of its original strength when dried after wetting. However, the large variation in the data precludes any definitive statement being made in this regard. The strength of the adhesive bond does decrease when the samples were tested wet. The IBAs all showed significant and dramatic loss of strength when they were tested wet, the relative decrease being much greater which occurred for the PRF control. The IBAs appear to regain some of their initial strength when the samples are allowed to dry before testing but only IBA D fully regained all of its original strength.

Looking at the adhesives by treatment highlights the difference in performance of the IBAs compared to the PRF. Difficulties exist in comparing the original strengths amongst the adhesives due to the large variation in the results. The other treatments are much more definitive. The cold water soak (treatment A2) reduced the strength of IBA D to a level comparable to that of the PRF. The strengths of the other IBAs were drastically reduced strength values. When allowed to dry after the cold water soak (treatment A3), all adhesives regained some strength but only that of IBA D returned to near its initial value. The boil treatment (treatment A4) caused a slight reduction in the strength of the PRF but it appeared to be very harsh on all of the IBAs. Amongst these, IBA D again retained the greatest strength. When the adhesives were tested after being dried (treatment A5), all of the adhesives regained some strength but again, only IBA D returned to its original strength.

Comparing the wood fibre failure values for each of the treatments is also illustrative of the difference between the PRF and IBAs (Figure 37). The adhesives gave very low values of wood fibre failure, the only exception being IBA D which significantly outperformed the other IBAs and, surprisingly, the PRF when tested in the dry condition. An interesting result is the apparent increase in wood fibre failure of the PRF adhesive after the boil treatment. This may indicate that further curing of the adhesive occurred during the treatment.

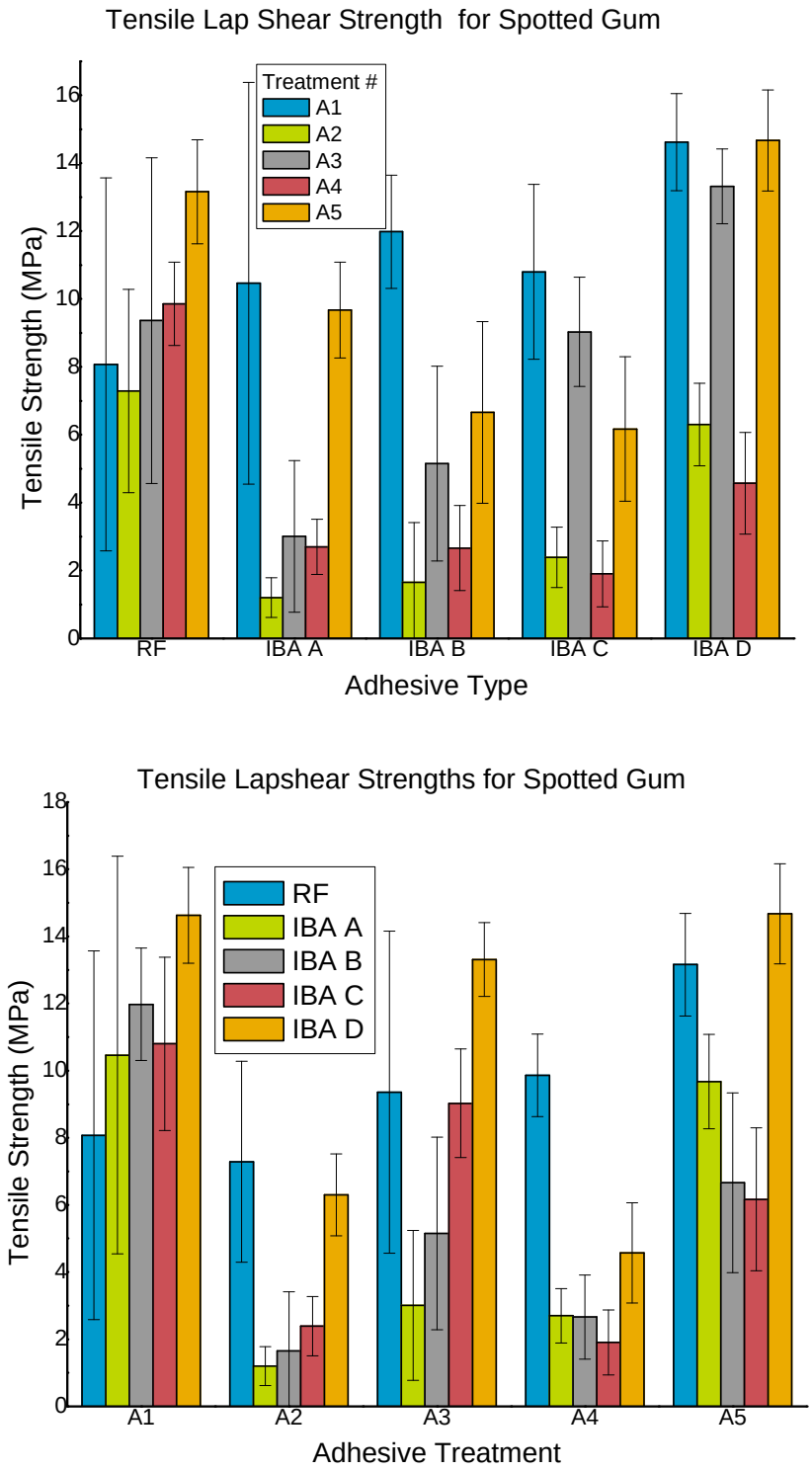

Figure 36. Average tensile lap shear strength results for the spotted gum samples by adhesive type (*top*) and adhesive treatment regime (*bottom*). Error bars represent ±1 SD.

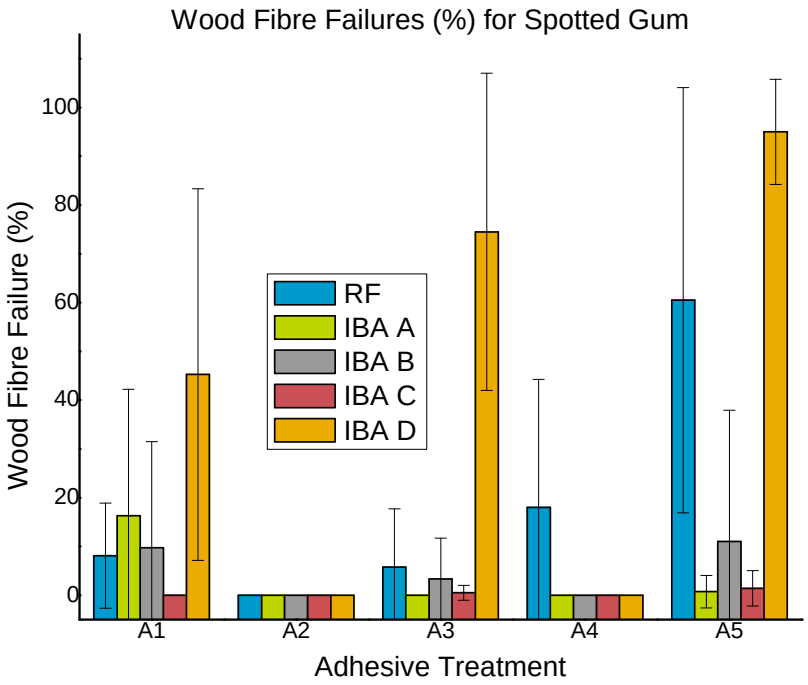

Figure 37. Wood fibre failure results for the spotted gum lapshear tests grouped by treatment. Error bars represent ±1 SD.

In summary, these tests do not appear to have demonstrated any obvious degradation of the adhesives after either the cold water or boiling water soaks since of bond strengths (compared to the baseline results) were largely regained when samples were allowed to dry before testing. One point of note is the loss in adhesive strength when the samples were tested in the wet state. Here, differences in the relative performances of the PRF reference adhesive and the IBAs become apparent. This is highlighted in the wood fibre failure results where failure in the PRF is in the wood (as signalled by the high levels of wood fibre failure) whilst the IBAs A-C give much lower values. IBA D appears to behave at least equivalently to the PRF. Again, there appears to be a species effect on the performance of the IBA adhesives.

Hydrolytic stability tests to ASTM D 4502

Purpose of tests

ASTM D4502 states that the "…degradation of adhesive joints is a physiochemical process. The speed of degradation is related to the levels of temperature, moisture (and other chemicals), and physical stress to which the joint is exposed. This test method is based on the principles of chemical kinetics and uses the Arrhenius temperature dependence relationship to estimate the long-term effects of heat and moisture at the service temperature." While the 3 year field and environment chamber trials described above can evaluate this strength loss they do not provide a practical screening method due to the long exposure times involved. By raising bond line temperatures and moisture conditions, it is assumed that the rate of chemical degradation of the adhesive will be accelerated which will manifest itself as a rapid

degradation of the joint strength as measured by compressive blockshear testing. This test does not take into account that degradation of wood adhesives is accelerated by both external loads placed on the bond line and the effect of cyclic stresses caused by the repeated wetting and drying of the wood substrate. Both of these have been demonstrated to accelerate degradation.[13] The D4502 protocol does not require the application of externally applied stress.

Outline of test method and issues arising

Temperature and humidity at which the tests are conducted

ASTM D 4502 leaves critical details to the discretion of the testing laboratory or client requesting the test. There are no firm statements in D4502 on the temperatures and moisture conditions under which aging shall be undertaken, only conditions under which the aging might be undertaken. Thus so-called wet aging can involve placing specimens in water baths at temperatures in the range 60 - 100ºC, the latter constituting a boil test, or in humid environments where the RH is unspecified. The selection of these conditions is left to negotiation between the testing laboratory and the client.

Temperature/moisture combinations

The strength degradation is tracked over time using block shear specimens or other shear specimen types.

1. Twenty (20) specimens for each adhesive-species combination are tested and used to establish base-line (un-degraded) block shear strength values.

2. D4502 Clause 10.2.1 states that for "a given temperature/moisture condition, mount five groups (10 specimens per group) on suitable racks for dry aging, place in jars for moist aging". Clause 10.2.2 states that five aging intervals are used for each aging temperature. It can be construed that the 5 groups are spread over wet and dry testing but it is not clear that that this means 5 groups for wet and 5 groups for dry testing, 10 groups in total if both a wet and dry test series is undertaken. If both the wet and dry series were to be undertaken this would have meant (10 groups x 10 temperature/moisture conditions x 5 aging conditions x 3 species x 5 adhesives =) 7500 specimens if all species and adhesives were to be involved. This number would increase to over 10000 specimens or more depending on how the wet tests were undertaken. Consequently it was decided that spot tests only would be undertaken with a view to clarifying the test conditions that are most appropriate for inclusion in a test standard rather than undertake simple parametric studies. The actual test series undertaken to date is given in Table 25.

[13] A. Kinlock, "Introduction" *Durability of Structural Adhesives*, Ed. A. Kinlock, Applied Science Publishers Inc, 1983, 1

Table 25. Temperature/moisture conditions used to degrade bond lines. A total of 3260 test specimens were involved in the study.

Adhesive	Wet test conditions		Dry test temperatures (˚C)
	Temperatures (˚C)	Relative humidity (%)	
Victorian Ash			
RF	60, 70, 85	Water bath	130, 160
IBA C	60, 70, 85	Water bath	130, 160
IBA A	60, 70, 85	Water bath	130, 160
IBA B	60, 70, 85	Water bath	130, 160
Radiata Pine			
RF	70,77,85	95,97,98	120,140,160
IBA C	70,77,85	95,97,98	120,140,160
IBA A	70,77,85	95,97,98	120,140,160
Qld Hwd			
RF	70,77,85	95,97,98	120,140,160
IBA C	70,77,85	95,97,98	120,140,160
IBA A	70,77,85	95,97,98	120,140,160

Acquisition of the basic degradation data – stage 1, time to lose 25% of initial strength

The data from the degradation are collected at specific times after subjecting the specimens to the degradation environment. As an example, for wet tests conducted at 85ºC lots of 10 specimens were removed at time intervals of 5, 10, 15, 20, 25 days but for 70ºC, because the degradation is slower, at 24, 48, 73, 96, 119 days. The time intervals are increased as the tests progress if the strength loss is not as rapid as anticipated. After conditioning, the block shear testing produces 10 strength results which are frequently scattered over a wide range. Prior to numerical processing all values are normalised by dividing the strengths by the mean strength of the base-line strength values and then computing $\ln\left(\tau/\tau_{0,mean}\right)$, where τ = shear strength of a degraded specimen and $\tau_{0,mean}$ = mean shear strength of base-line specimens. A least squares fit is then made of the $\ln\left(\tau/\tau_{0,mean}\right)$ versus time (t) in days forcing the curve to pass through the origin; see Figure 38. The vertical diamonds represent at different time intervals represent the individual block shear test data. The time to lose 25% of the base-line strength occurs when $\ln\left(\tau/\tau_{0,mean}\right)=\ln\left(0.75\right)=-0.288$ which, in the case shown occurs at $x=-0.288/-0.0101=28.5$ days which is marked off in the plot. The typical plot shown in Figure 38 is prepared for each of the temperature/moisture conditions. These plots are not reproduced in the report given the large number involved – 56 in total. What is simpler to present is the information in Table 26 which represents the degradation rates.

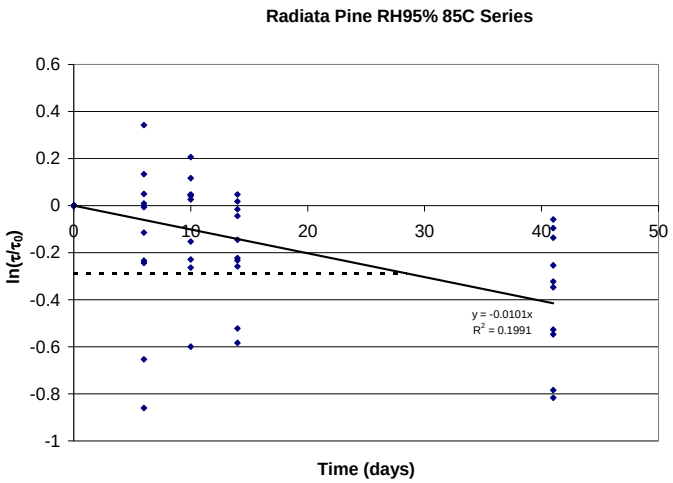

Figure 38. ln ($\tau / \tau_{0,mean}$) versus time for 85ºC and high relative humidity.

Table 26. Degradation rates extracted from strength loss data such as is shown in Figure 38.

	Water bath raw values $k(m,T)$			**Dry series**	
Victorian Ash	**60ºC**	**70ºC**	**85ºC**	**130ºC**	**160ºC**
RF	0.0042	0.0097	0.02	0.0106	0.1653
IBA A	0.0063	0.0053	0.0114	0.0279	0.3674
IBA B	0.0012	0.007	0.0049	0.0108	0.1606
IBA C	0.0042	0.0143	0.0304	0.0092	0.1272

	Water bath moisture adjusted values $k(T) = k(m,T)/m$			**Dry series**	
Victorian Ash	**60ºC**	**70ºC**	**85ºC**	**130ºC**	**160ºC**
RF	0.0007	0.001617	0.003333	0.0106	0.1653
IBA A	0.00105	0.000883	0.0019	0.0279	0.3674
IBA B	0.0002	0.001167	0.000817	0.0108	0.1606
IBA C	0.0007	0.002383	0.005067	0.0092	0.1272

	High humidity series			**Dry series**		
Radiata	**70ºC**	**77ºC**	**85ºC**	**120ºC**	**140ºC**	**160ºC**
RF	0.0034	0.0062	0.0089	0.0076	0.0231	0.1379
IBA A	0.0039	0.0118	0.0177	0.0066	0.0375	1.2808
IBA C	0.0033	0.0065	0.0101	0.0065	0.0172	0.6248

	High humidity series			**Dry series**		
Qld Hardwood	**70ºC**	**77ºC**	**85ºC**	**120ºC**	**140ºC**	**160ºC**
RF	0.0205	0.0139	0.0286	0.0113	0.0353	0.2583
IBA A	0.0242	0.019	0.0213	0.0231	0.1235	1.2264
IBA C	0.039	0.0385	0.0425	0.0125	0.0923	1.2942

Processing results, stage 2 – adjusting temperature back to normal temperatures (20ºC)

The degradation rate data detailed in Table 26 are used to prepare Arrhenius plots; logarithm of the time to reach 75% of initial strength against the inverse of the degradation temperature. A typical plot is shown in Figure 39. The wet and dry series results are separated and give sharply different results. For each of the dry and wet series tests a line of best fit is placed through the test data. Of necessity it is necessary to extrapolate this to determine the adhesive life at 20ºC = 293.15ºK. This means that 1000/293.15 = 3.411. This result is substituted into the regression equation to predict the life under the moisture content within the test aging environment. The regression equation for the damp test series is $y = 9.1217x - 22.176$ which means that $\ln(life_{25^\circ C}) = 9.1217 \times 3.411 - 22.176 = 8.94$ and $life_{25^\circ C} = \exp(8.42)/365 = 20.9$ years. The particular Arrhenius plot shown was obtained from data where the environmental conditions were RH = 95-97% and the temperatures used were 70, 77, 85ºC which led to moisture contents that approximated 20%. The dry results typically indicate service lives at 20ºC of many thousands of years which fits in the fact that timber maintained ion a dry condition will last more or less indefinitely. The particular Arrhenius plot shown is "well behaved" with a linear fit of ln(time to reach 75% of initial strength) against 1000/T being very plausible. This does not always occur.

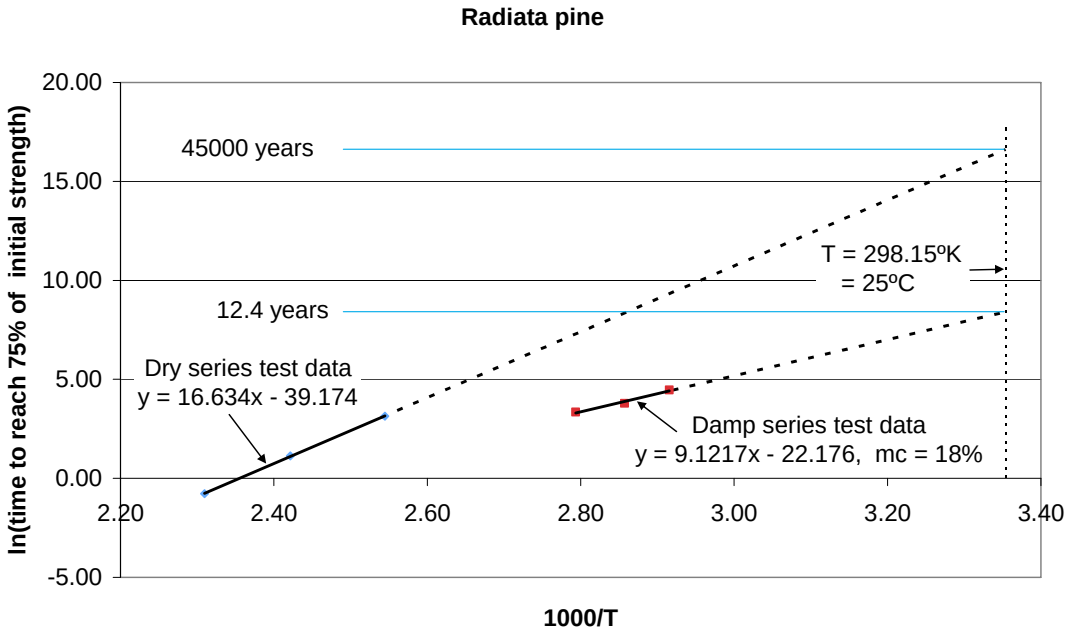

Figure 39. Arrhenius plot for dry and wet aging used to demonstrate the effect of temperatures on the adhesive bond line. The plot also demonstrates how test data are extrapolated to predict performance at typical service conditions.

Arrhenius plots

The Arrhenius plots are identified on each chart; the plots are only allocated group figure numbers, i.e., for each adhesive.

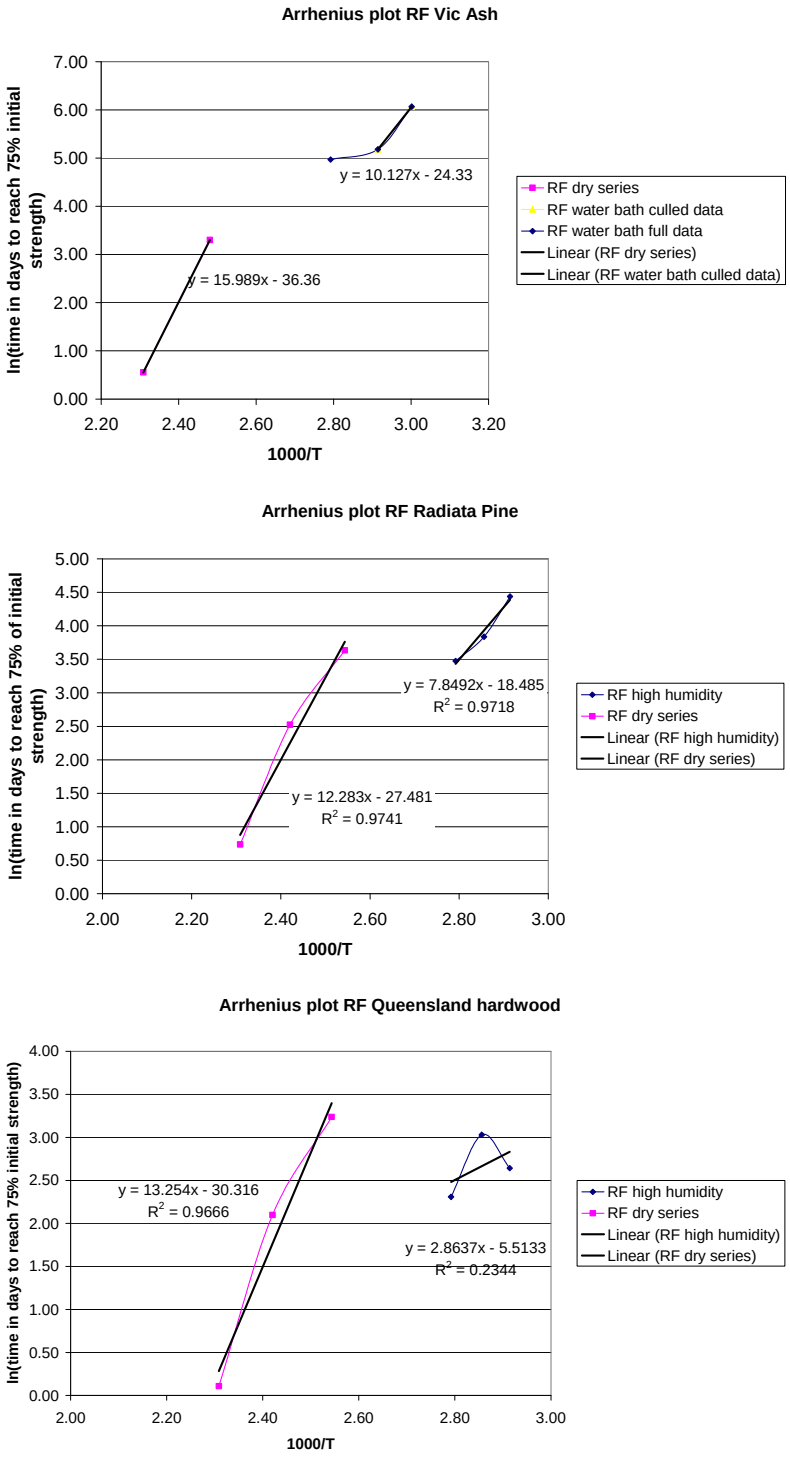

Figure 40. PRF Arrhenius plots.

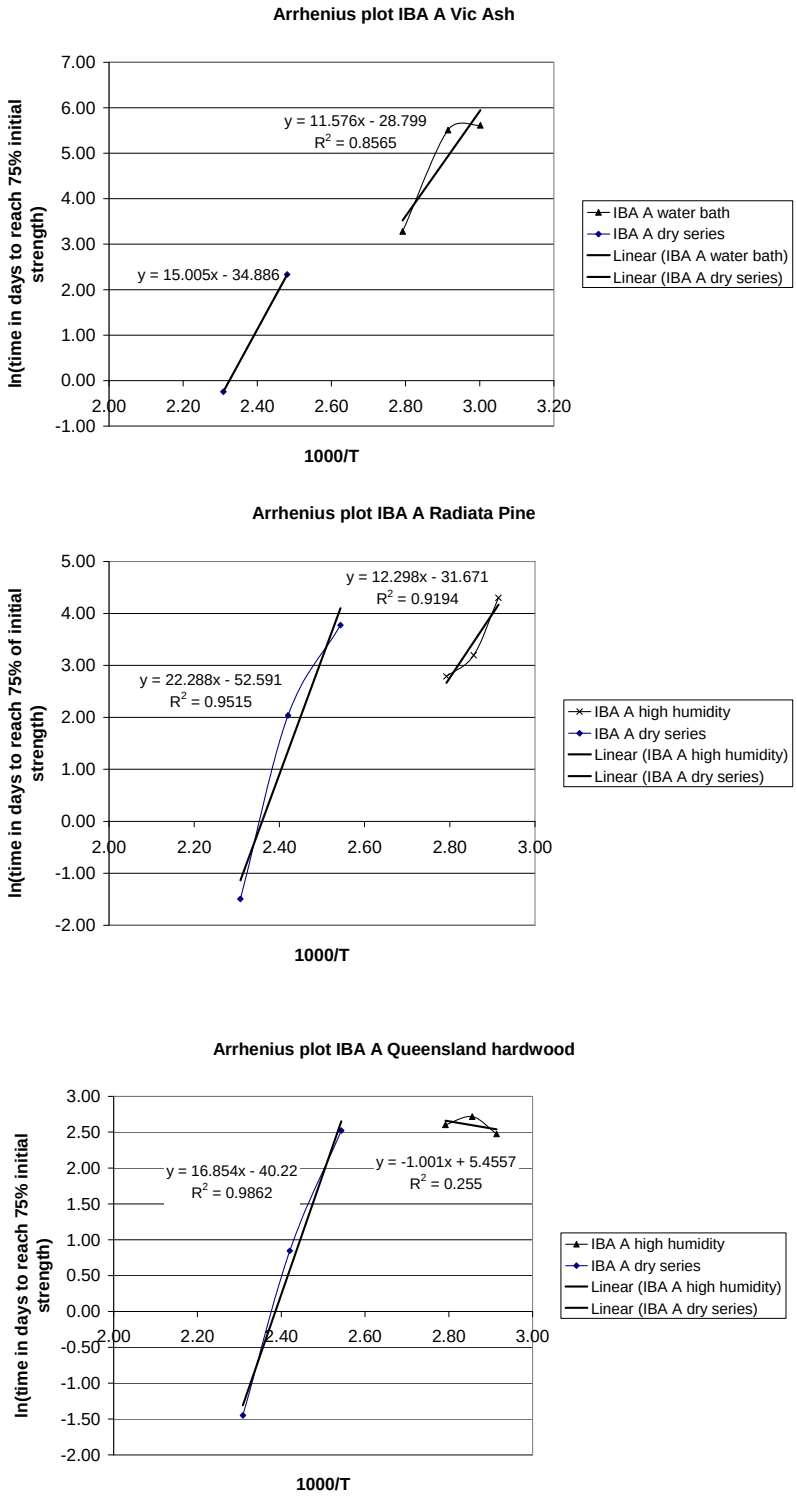

Figure 41. Arrhenius plot for IBA A.

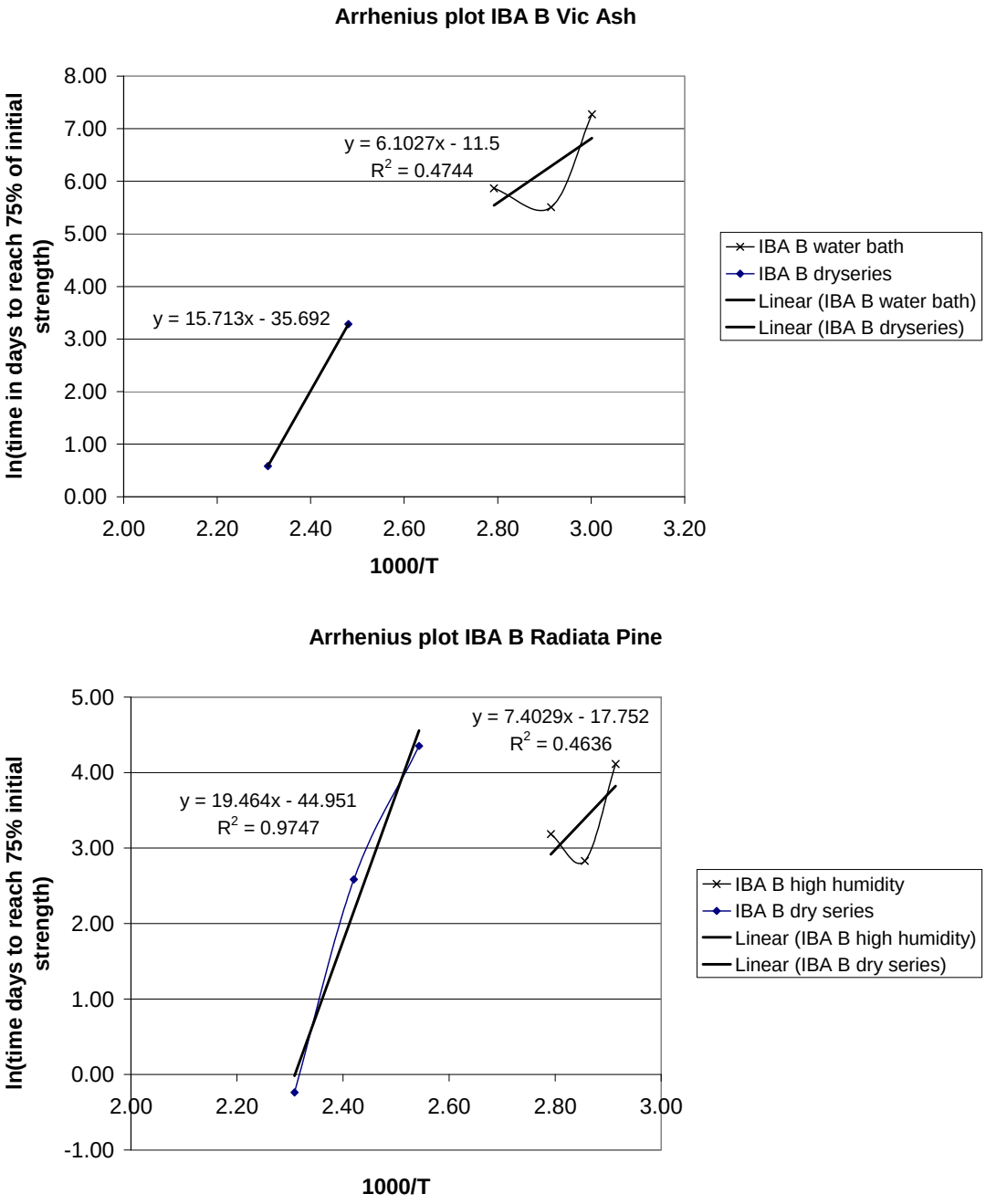

Figure 42. Arrhenius plots for IBA B.

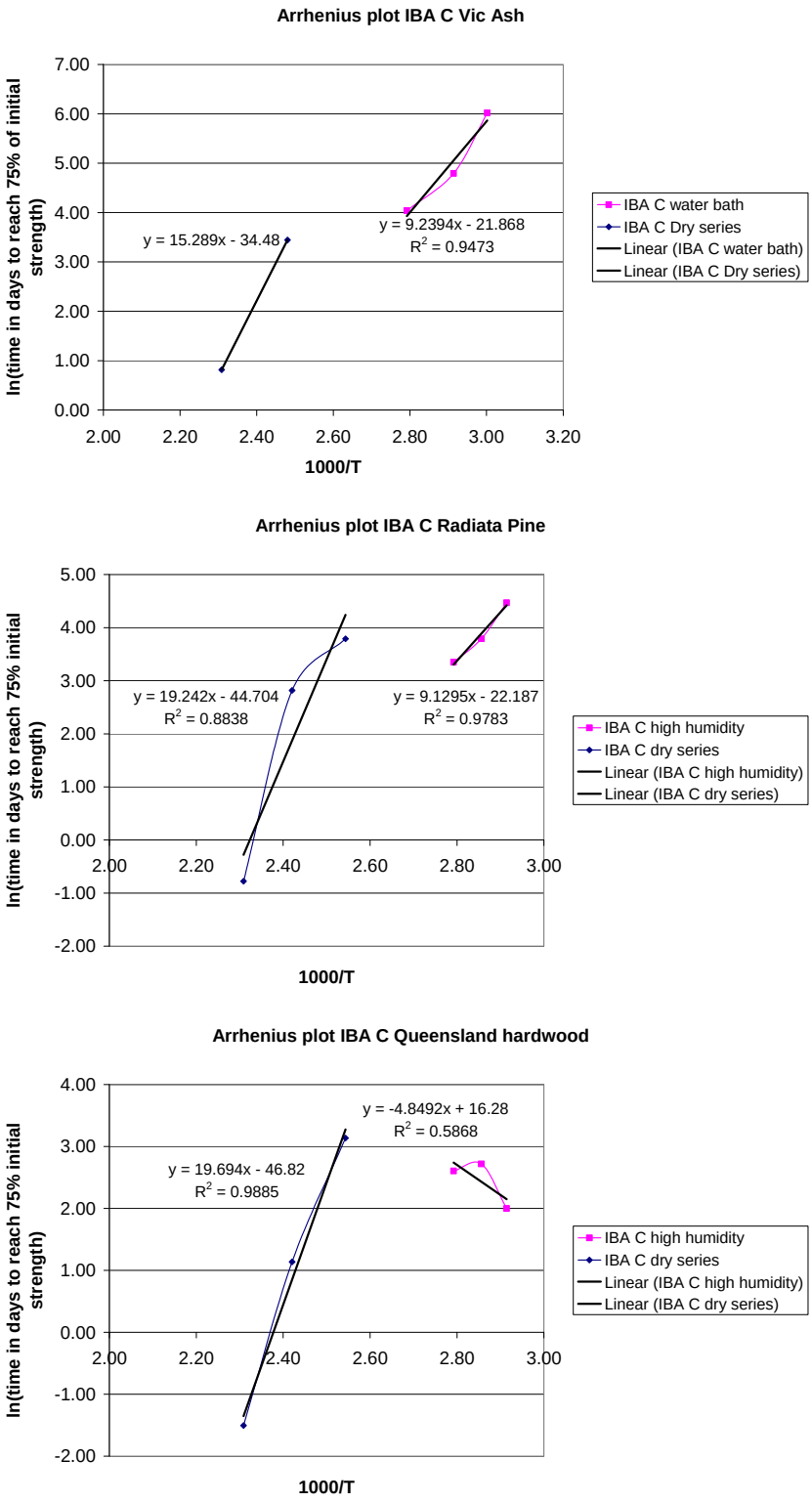

Figure 43. Arrhenius plots for IBA C.

Table 27.

Adhesive	Species	Wet series				Dry series			
		a	b	$\ln(life_{0.75}$ in days)	Life (years)	a	b	$\ln(life_{0.75}$ in days)	Life (years)
RF	Victorian Ash	10.127	-24.33	10.2	74.9	15.989	-36.36	18.2	215808
	Radiata Pine	7.849	-18.49	8.3	10.9	12.283	-27.481	14.4	5010
	Qld Hwd	2.864	-5.513	4.3	0.2	13.254	-30.316	14.9	8074
IBA A	Victorian Ash	11.576	-28.80	10.7	120.2	15.005	-34.886	16.3	32843
	Radiata Pine	12.298	-31.67	10.3	79.9	22.288	-52.591	23.4	41385418
	Qld Hwd	-1.001	5.456	2.0	0.0	16.854	-40.22	17.3	86930
IBA B	Victorian Ash	6.103	-11.50	9.3	30.5	15.713	-35.692	17.9	164168
	Radiata Pine	7.403	-17.75	7.5	5.0	19.464	-44.951	21.4	5638596
IBA C	Victorian Ash	9.239	-21.87	9.6	42.5	15.289	-34.48	17.7	129870
	Radiata Pine	9.130	-22.19	9.0	21.2	19.242	-44.704	20.9	3384965
	Qld Hwd	-4.849	16.28	-0.3	0.0	19.694	-46.82	20.4	1906399

Comments

1. A general observation that is in keeping with comments made by the originators of the chemical kinetic approach, is that the predicted lives should not be interpreted too literally. Millet and Gillespie[14], point out that "one is assuming that the mechanism of degradation remains constant over the entire temperature range; and this may not be true. Secondly, every bit of data collected via an experimental measurement represents not a point but a circle of uncertainty whose diameter reflects the cumulative errors associated with each step of the data-generating process, i.e., from adherend selection and preparation to testing of the aged specimens in tensile compression (*sic*) shear in the case of adhesive evaluation." The scatter in the raw data seen in Figure 38 is typical of and consistent with the scatter shown by Millet and Gillespie.[14] Further sources of error are cited in ASTM D4502 itself. A further and highly noticeable source of error relates to the fact that heating may cause adhesives to strengthen relative to their base-line values due to promoting further curing.

2. The dry test series indicates that the lives of adhesives under dry conditions are lengthy, in the order of thousands of years. This fits with the observation that unbonded wood, in dry conditions, has unlimited life. There is perhaps little point in performing the dry test series from the hydrolytical stability viewpoint.

3. The wet test series can be performed under water bath or high humidity conditions. The high humidity tests are carried out under conditions that are not especially easy to achieve. Ideally the wood moisture content should be constant for the different aging temperatures. While the Thermoline ovens have excellent temperature and humidity control it is desirable that the temperatures be kept relatively high so that the aging periods are not excessively lengthy; the higher the temperature the faster the degradation. It is also desirable that the moisture content of timber aged at such temperatures be maintained at around 20% and reference to Figure 44 shows that, at temperatures of 85˚C, this requires RHs in excess of 95% which is not easy to achieve from a thermodynamic perspective. The use of saturated salt solutions is another technique used to control relative humidity. Potassium sulphate, K_2SO_4, can achieve RH values around 98% at 0ºC dropping down to 95% at 50ºC with no data given for higher temperatures. The specimens are placed in sealed jars and the specimens on wire netting with the saturated salt solution below. This technique is therefore not useful.

4. The results themselves show relatively short lives under wet aging conditions. The mean moisture content was, for the water bath series, 120%, and, for the high humidity series, approximately 20%. Given that both the wood substrate and the adhesive itself are degrading with time it is best to simply argue that it

[14] M. Millet, R. Gillespie, "Precision of the rate process method for predicting bond line durability", *Report for Department of Housing and Urban Development under agreement No. 1AA-H-71*, Amendment No. 1 on Adhesives, 1978.

is the life of the bond line that is measured. Some specific observations are as follows.

5. The Victorian Ash/RF result indicates a life of 75 years based on the water bath method provided the extrapolation is made through the 60˚C and 70˚C results. If a line of best fit also includes data from the 85˚C this is sharply reduced. Further testing is required before more can be said. The Radiata Pine/RF result was obtained by the high humidity method and indicates a shorter life of 11 years. However, the data fit is much better. The result for Queensland hardwood is much poorer.
6. IBA C exhibited a life of 43 years on Victorian Ash (water bath method) and 21.2 years on Radiata pine using the high humidity method. This same trend of a longer life with Victorian Ash and shorter life with Radiata Pine occurs with all adhesives, including the PRF. There is one of three possible explanations for this result.
    - Victorian Ash is the easiest of our species to glue, which is a view of glulam manufacturers.
    - The high humidity technique is a more severe test.
    - The adjustment in the degradation rate for the water bath method whereby $k(m,T) = k(T)/m$ is not valid. Writing $k(m,T) = k(T)/m$ amounts to saying that the degradation rate is linearly dependent on the moisture concentration which may or may not be the case. The relationship might be quite complex.
7. The results for Queensland hardwoods indicate very short lives based on a least squares fit but the raw data itself is so unsatisfactory that no firm conclusion can be drawn. It is also pertinent to point out that Queensland hardwoods are not a species that is included in AS/NZS 4364 (Int) or in ISO 20152 against which wood adhesives are to be evaluated. It is of concern that none of the wood adhesives perform well on Queensland hardwoods.
8. No statistically significant differences exist between the performance of any of the adhesives.

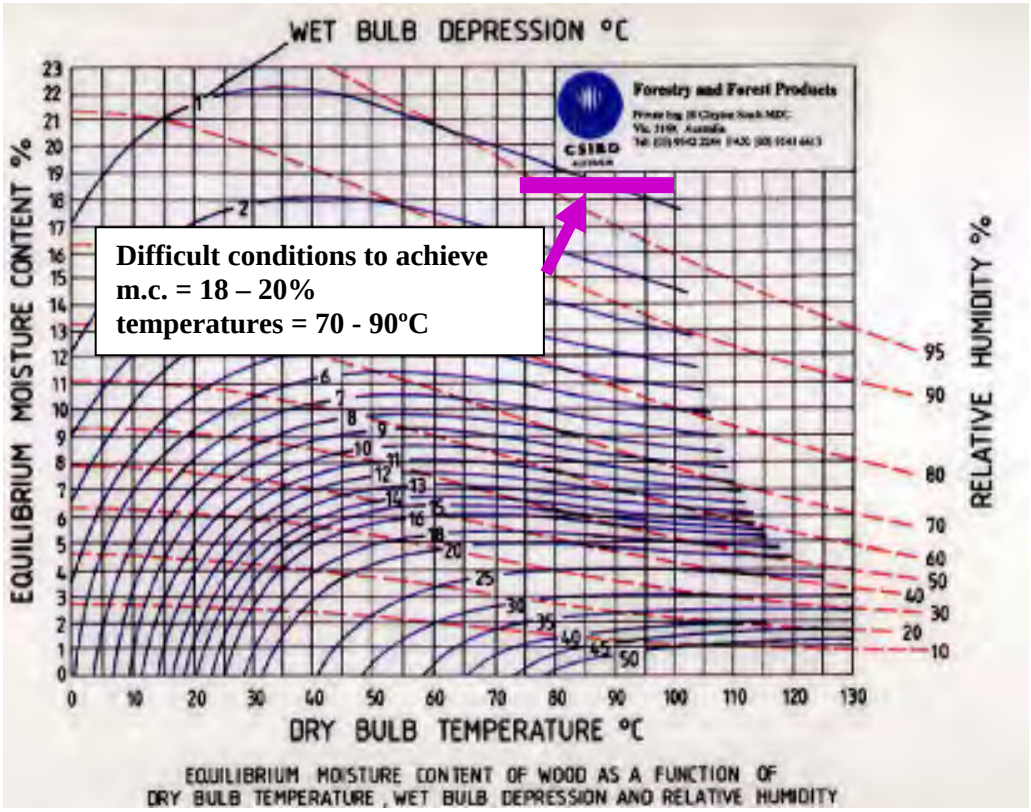

Figure 44. Equilibrium moisture content of wood as a function of dry bulb temperature, wet bulb depression and relative humidity.

Concluding remarks concerning hydrolytic stability test

While the estimates of structural life have some appeal to those persons who have numerical estimates the results obtained from the tests themselves are simply not plausible. It is for this reason that the hydrolytic stability test has been removed from the current draft versions of both ISO 20152.1 and AS/NZS4364 (Int). The same results are achieved through the boil-dry-freeze tests in both of these documents.

Thin Film Studies

Purpose of studies

The motivation for studying the physical response of adhesives to changes in moisture content is to determine if these characteristics can explain differences in service performance, especially among chemically-stable adhesive types. Chemical breakdown is still possible with some adhesives and well known as in the case of UFs but both PRFs and PURs are thought to be chemically stable.

It is a matter of observation with wood products that the likelihood of debonding increases under exterior exposure conditions. Since the adhesive is shielded from sunlight changes in moisture content and chemical breakdown are the only possible reasons for this response. It is also known that the application of stress in the absence of moisture change appears not to present problems as is noticeable that, for products kept in an air-conditioned environment at relatively low temperatures, most adhesives will last more or less indefinitely even though the stress levels may be high. Because

isocyanate based adhesives (IBAs) and phenolic adhesives are both thought to be chemically stable in the presence of water it is natural then to focus on the physical response of the adhesive to moisture change. Temperature also plays a role above 50˚C as indicated by the provisions of the European standard EN301 but not in the majority of applications this is not an issue.

Theoretical framework

A study of physical characteristics cannot be undertaken in the absence of a theoretical framework that measures the adhesive response in terms of widely accepted physical parameters and models allowing for such effects as free shrink-swell, visco-elastic response to applied stress and time and mechano-sorptive response to applied stress and moisture change. One issue that has come to the fore in the current study is the difference in the free shrink-swell characteristics of PRFs on the one hand and PURs on the other. The former has, for the.

Muszynski el al framework

One framework model has been proposed by Muszynski et al and takes the following form.[15] "Total deformation of thin films subjected to sustained load under constant temperature and non-equilibrium ambient humidity is believed to be a sum of three theoretically separable components, specifically: viscoelastic (ε_{ve})- including the immediate or elastic and the delayed response; free shrinkage or swelling (ε_{sw}); and mechano-sorptive deformation (ε_{MS}). Mechano-sorptive deformation is defined as that portion of the total strain that cannot be expressed as a simple super-position of the previous two.[16] Total strain is thus expressed as:

$$\varepsilon(\sigma, t, MC, \Delta MC) = \varepsilon_{ve} + \varepsilon_{sw} + \varepsilon_{MS}\text{"} \qquad \mathbf{1}$$

σ = stress level, t = time, MC, ΔMC = moisture content, moisture content increment, ε = strain, ε_{ve} = visco-elastic strain, ε_{sw} = free shrink-swell strain, ε_{ms} = mechano-sorptive strain.

The laws adopted by Muszynski et al are stated in strain velocity form but are presented here in incremental form as

$$\Delta\varepsilon_{ve}(t) = a(m)b(m)t^{b(m)-1}\Delta t \qquad \mathbf{2}$$

$$\Delta\varepsilon_{sw} = k_{sw}\Delta m \qquad \mathbf{3}$$

$$\Delta\varepsilon_{ms} = k_{ms}\sigma|\Delta m| \qquad \mathbf{4}$$

where it is acknowledged that the constants *a* and *b* are themselves functions of moisture content.

Muszynski et al appear to have a limited agenda in their investigations of PRF adhesives, namely, to establish that PRFs possessed a mechano-sorptive component of

[15]. Muszynski, F. Wang, S. Shaler, "Short term creep tests on phenol-resorcinol-formaldehyde (PRF) resin undergoing moisture content changes", *Wood and Fiber Sci*., **34(4)**, 2002, 612.

[16] J. Dinwoodie, "Properties and performance of wood adhesives", *Wood Adhesives. Chemistry and Technology*, Ed. A. Pizzi, Marcel Decker Inc, New York, 1983.

strain. While it is interesting that thin films of adhesive possess a mechano-sorptive component of strain it does not, on its own, provide any explanation as to why this affects adhesive durability. A complete description of its physical properties followed by stress analyses is required to determine if these affect bond durability characteristics.

Irle and Bolton framework

Bolton and Irle[17,18,19] used a simple 4 element creep model in describing the behaviour of formaldehyde resins (PF, LAPF and UF) which takes the form

$$\varepsilon = \frac{\sigma}{E_1} + \frac{\sigma}{E_2}\left[1 - \exp\left(\frac{E_2 t}{\eta_2}\right)\right] + \frac{\sigma t}{\eta_3} \qquad \textbf{Equation 5}$$

This is a simpler expression and it is an easier task to fit experimental data to their model. What it fails to say is anything about free shrink-swell which is clearly required if mathematical analysis is to be used in conjunction with the model.

Results for IBA A

Relative humidity and the specimen moisture content

The gain and loss in weight to 0.001gm was used to obtain the film moisture content. Notice how the increase of relative humidity in the first 24 hours (K_2SO_4 saturated salt) occurs at a faster rate than the decrease during the 24 to 48 hour period (NaBr saturated salt). It is relatively simple to increase RH rapidly by using a water spray but to subsequently decrease the RH mean that the moist air must be removed by suction or absorbed by the NaBr. This raises issues of how much NaBr should be used, what about the effect of K_2SO_4 that has adhered to the specimen, the chamber walls and the humidity sensor itself? What is much more desirable is have two mechanical air conditioning systems that store air at the two required relative humidity and temperature conditions so that the conditions can be changed rapidly and to remove any elements of doubt. Unfortunately, this was not anticipated at the outset and budget limitations were placed on the project that mitigated against using such equipment.

[17] A. Bolton, M Irle, "Physical aspects of wood adhesive bond formation with formaldehyde adhesives. Part 1. The effect of curing conditions on the physical properties of urea formaldehyde films", *Holzforschung*, **41(3)**, 1987, 155.
[18] A. Bolton, M Irle, "Physical aspects of wood adhesive bond formation with formaldehyde adhesives. Part 2. Binder physical properties and particleboard durability", *Holzforschung*, **42(1)**, 1991, 53.
[19] A. Bolton, M Irle, "Physical aspects of wood adhesive bond formation with formaldehyde adhesives. Part 3. The creep behaviour of formaldehyde based resins at different relative humidities", *Holzforschung*, **45(1)**, 1991, 69.

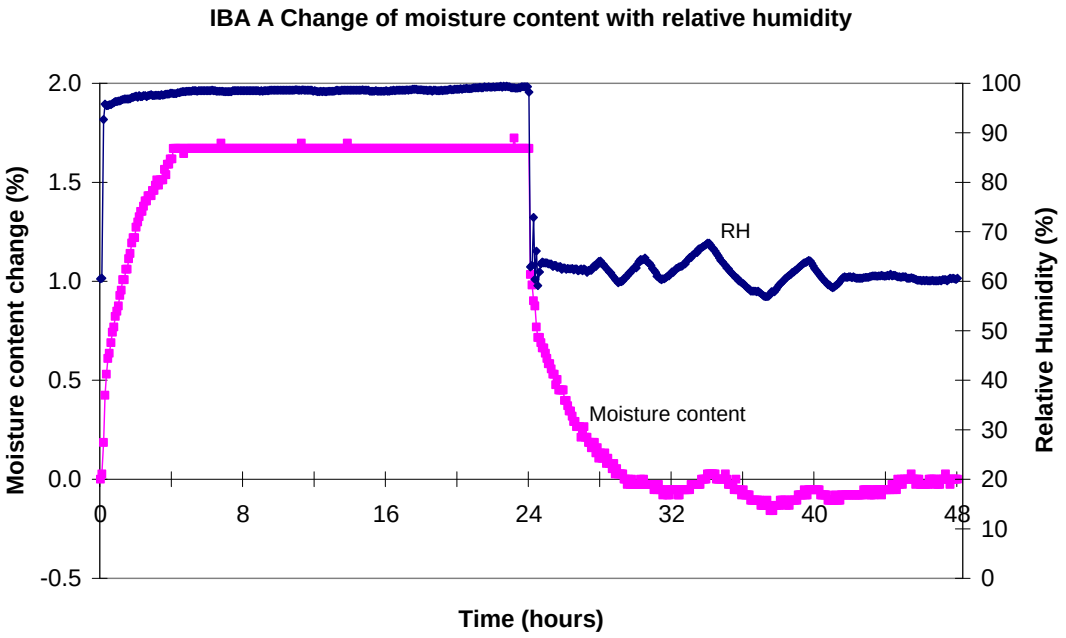

Figure 45. Variation of film moisture content with relative humidity.

Free shrink swell with RH and moisture content changes

The free shrink and swell strains as functions of time and moisture content are given in Figure 46. The procedure relies on raising and lowering the moisture content at the same rate during the separate measurements of moisture content when using the AND GX-400 weigh balance and the GOM Aramis system. The expectation is that the shrink and swell rates will be linear functions of moisture, that is, governed by a linear law of the form $\Delta\varepsilon_{sw} = k_{sw}\Delta m$. From Figure 48 and Figure 49 the shrinkage and swell rates are given in Table 28. It is a matter of concern that these two rates differ by such a large margin implying that free shrink-swell is not reversible as would be anticipated. It is relevant that IBA A was tested after IBA B and that, in its case (see 0), the shrinkage rates were very nearly equal. There is a strong possibility that the problems lay with salt contamination but the failure of the Aramis equipment prevented this being further investigated. This matter requires further investigation using mechanical air conditioning systems or at least simultaneous weighing and Aramis observations.

Table 28 Shrink and swell constants.

	Shrink/swell rate, k_{sw} (%Strain/m%)
Drying	0.267
Wetting	0.450

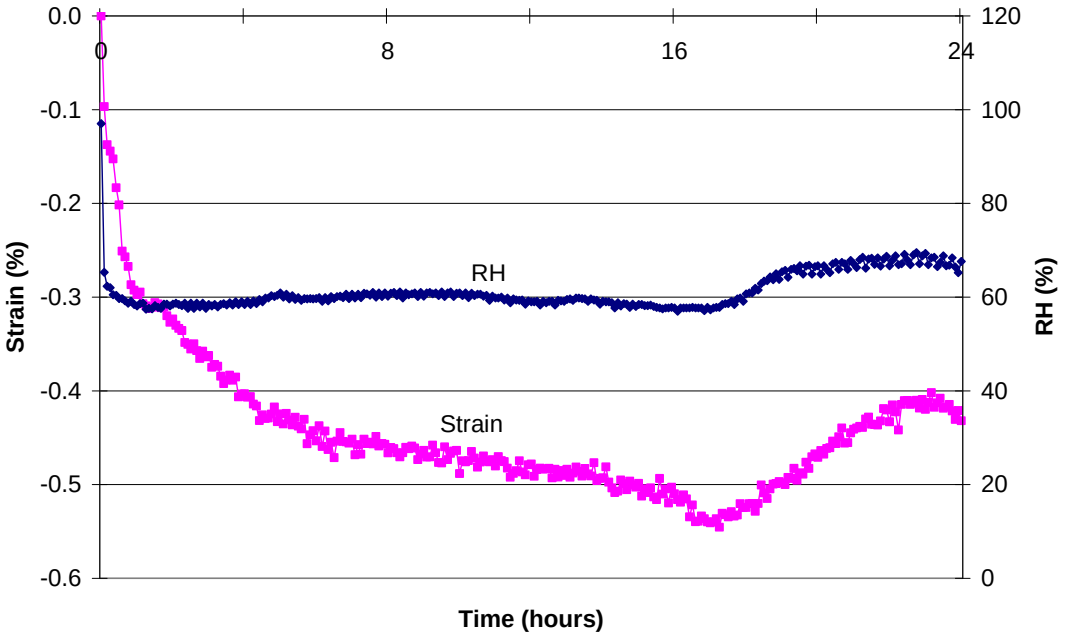

Figure 46. IBA A variation of shrinkage with time.

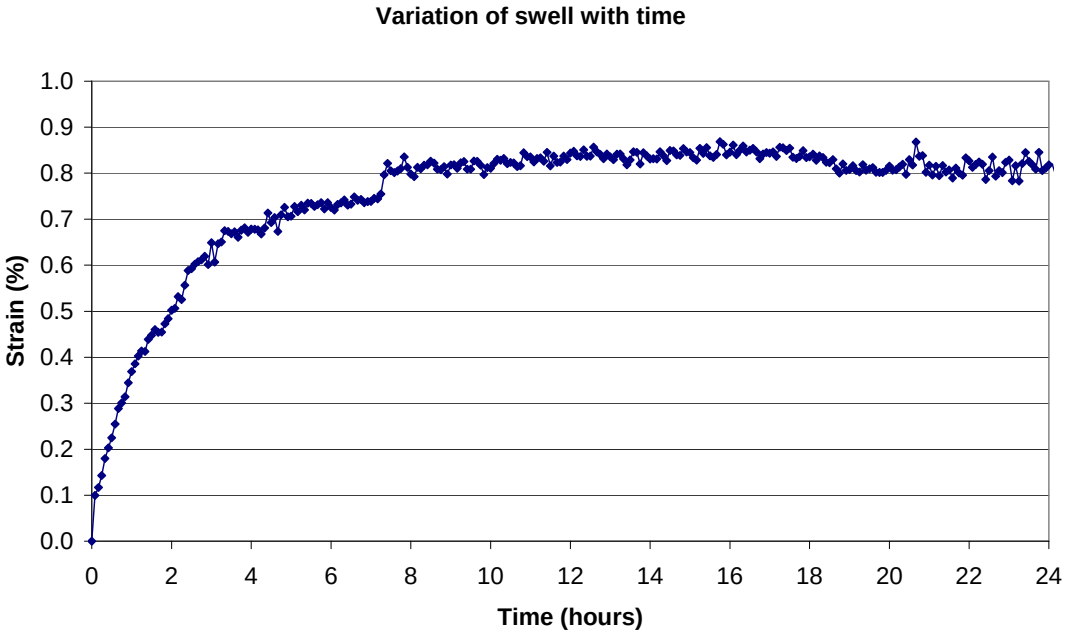

Figure 47. IBA A variation of swell with time.

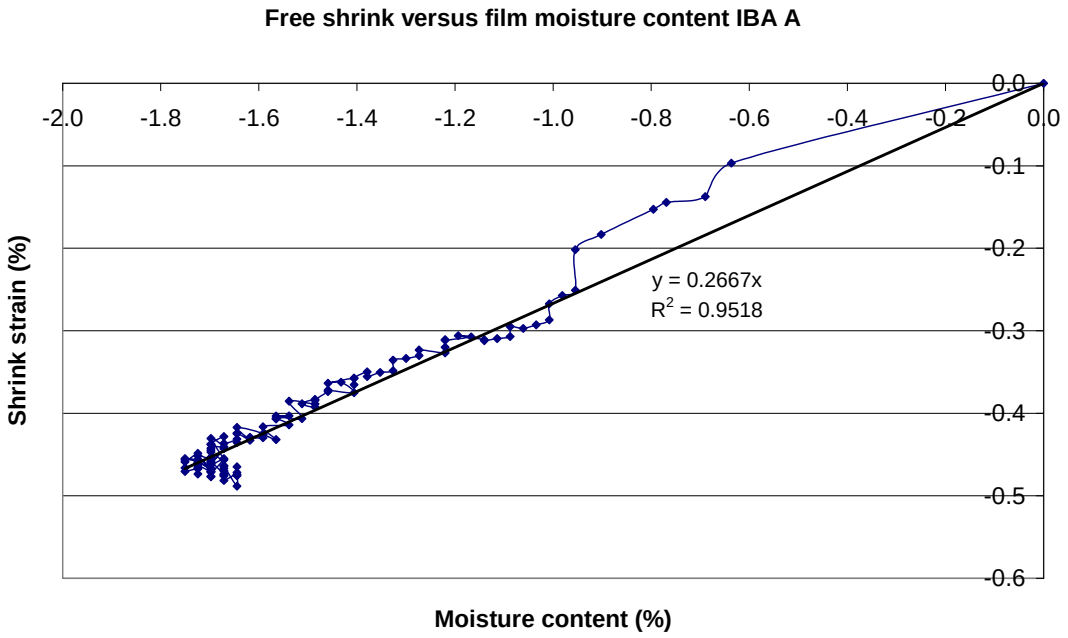

Figure 48. IBA A variation of shrinkage with moisture content.

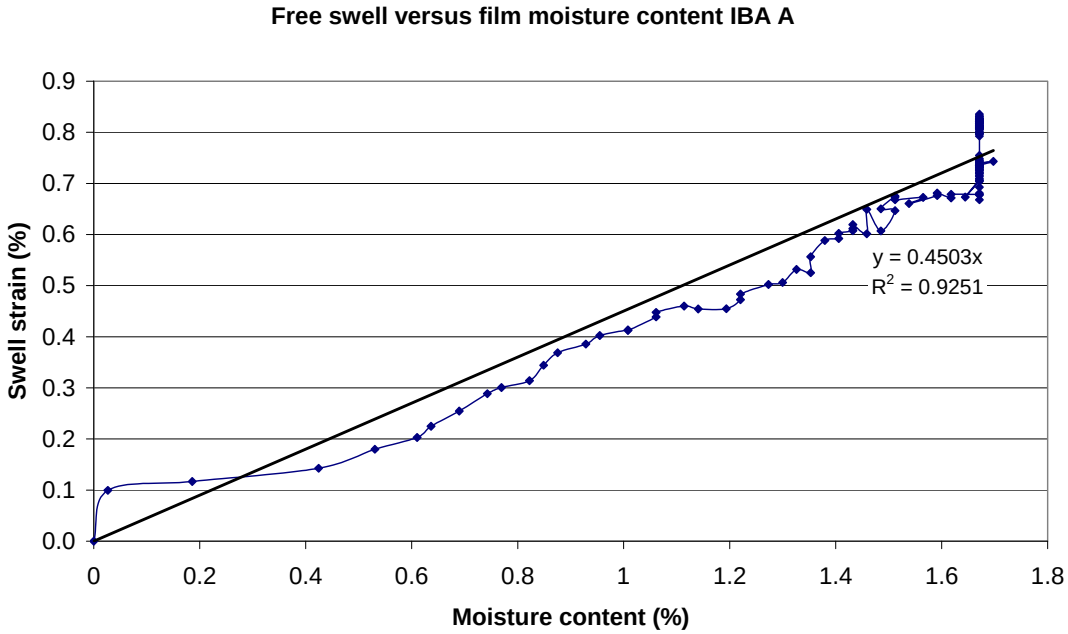

Figure 49. IBA A variation of swell with moisture content.

Viscoelastic creep at test and intermediate RH values

The viscoelastic creep components are shown in Figure 50. The creep power laws, $\varepsilon_{ve} = at^b$ (see Appendix for details), adopted are given in Table 29.

Table 29. Viscoelastic constants used to fit power creep law to test data at RH values 60% and 98%.

RH	*a*	*b*
60	1.41	0.223
98	2.51	0.135

The values of *a* and *b* are obtained using linear interpolation based on the change of moisture content that occurs in the adhesive film between the wet and dry states; see Section 0 for details. The strain velocity increment is then integrated numerically to obtain the viscoelastic creep values when the moisture changes. The increment is computed as, $\Delta\varepsilon_{ve}(t) = a(m)b(m)t^{b(m)-1}\Delta t$, and the viscoelastic creep computed as $\varepsilon_{ve}(t+\Delta t) = \varepsilon_{ve}(t) + \Delta\varepsilon_{ve}(t)$.

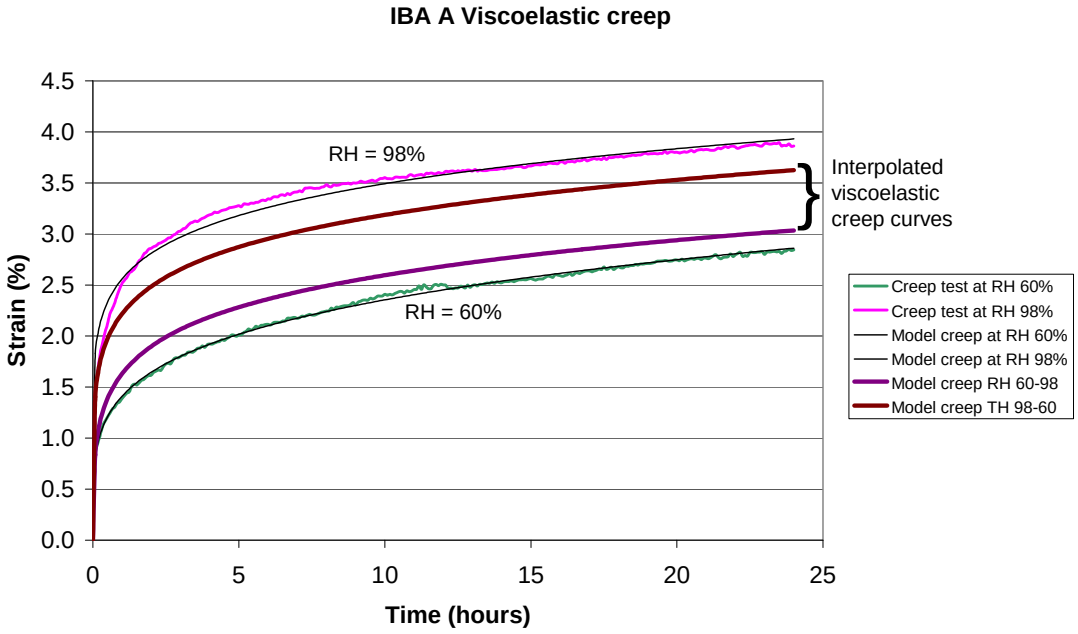

Figure 50. Viscoelastic creep at test RH, with a creep power law fit and the interpolated curves used when RH is varied between 60% and 98%.

Residual strain using the Muszynski et al (2002) model

The total strains for constant and varying creep are shown in Figure 51. There also exists a further strain component when the films are under varying moisture content, either going from RH 60% to RH 98% or RH 98% to RH 60%, see Figure 52. Muszynski et al (2002), in testing PRF resin (GP 4242 Resorsabond), on the basis of their test data were able to support the proposition that this residual strain had a mechano-sorptive character to it whereby strain arises as a consequence of applied stress and moisture change. For this to be the case it is necessary that once the moisture content ceases to change, around 4 hours after the commencement of the test, that this residual strain would not increase further with time, *t*. This did not occur with IBA A nor did it occur with the adhesives being tested by Irle and Bolton (1991). There is no law of nature that says that adhesives must have a mechano-sorptive component of strain. This highlights a difference between the PRF tested by Muszynski et al (2002) and IBA A. However, the comment is made against the background of the problems with Aramis and salt contamination.

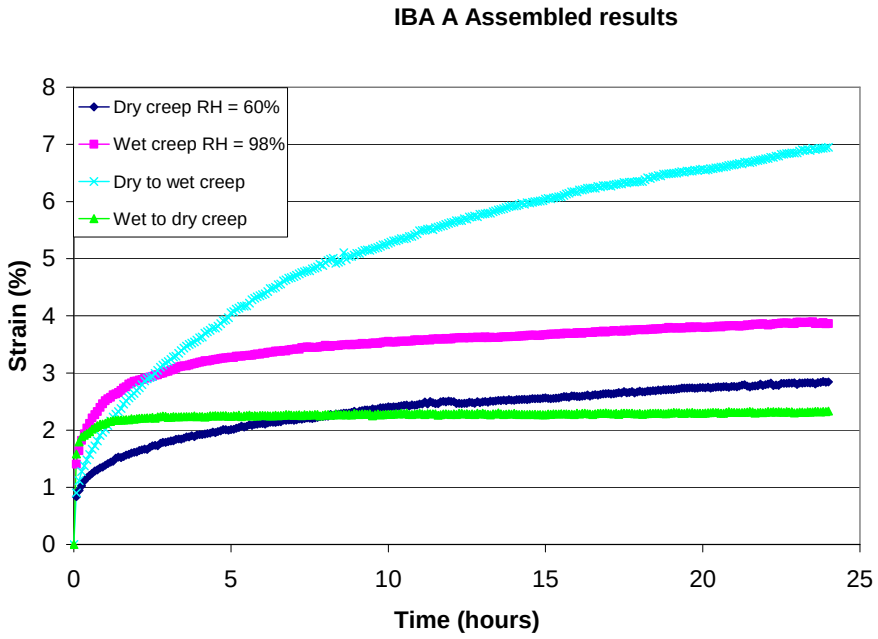

Figure 51. Strain observations for IBA A under load and varying moisture content.

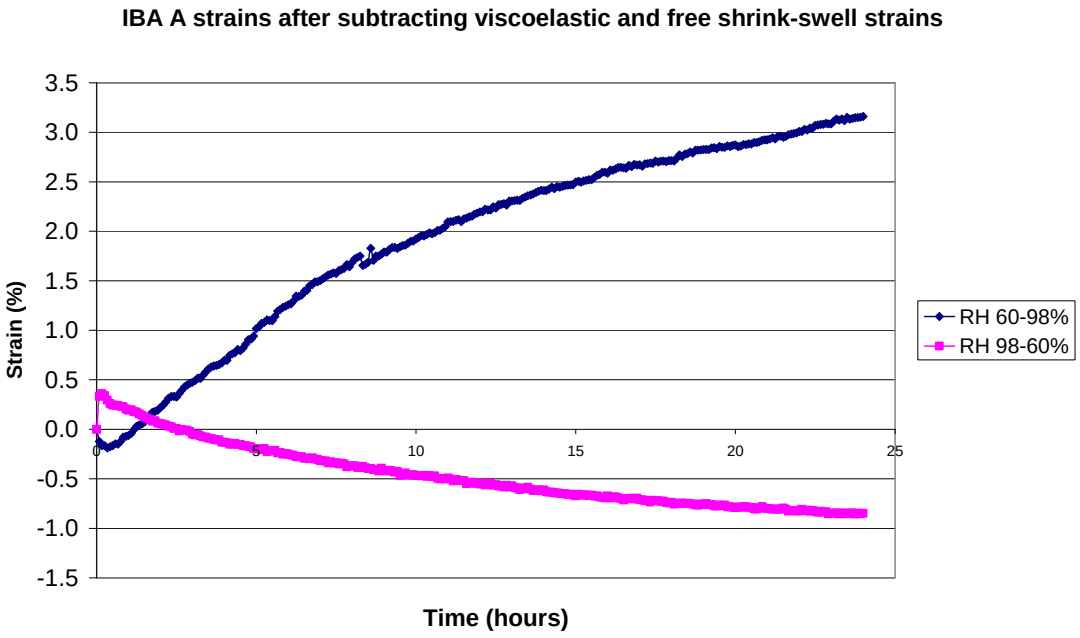

Figure 52. Strain other than viscoelastic and free shrink-swell.

IBA B results

The results for IBA B are provided without the detailed explanations given for IBA A. It is of interest that IBA B exhibited the same characteristic as IBA A in not having a mechano-sorptive component of strain. Chronologically, these tests were performed first.

Relative humidity and the specimen moisture content

IBA B was tested using K_2SO_4 to control the upper humidity level and LiCl to control the lower level. Chemical handbooks state that the RH with LiCl should approximate 11% over a wide temperature range but it was found with the particular chamber that a value of 20% only was achievable. The changes can be approximated by the following.

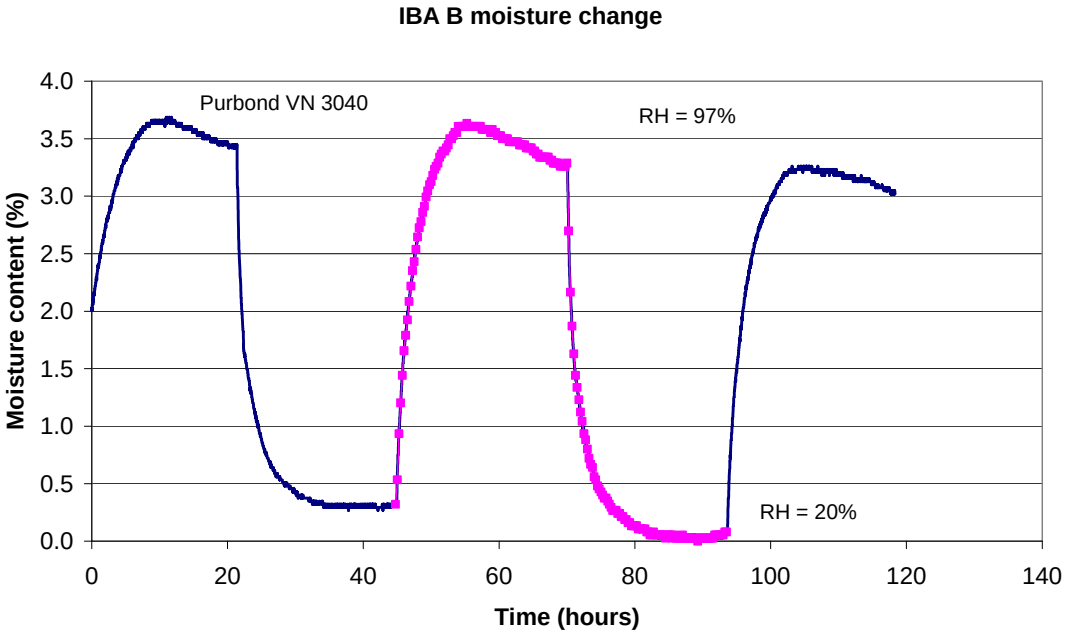

Figure 53. Variation of moisture content with time.

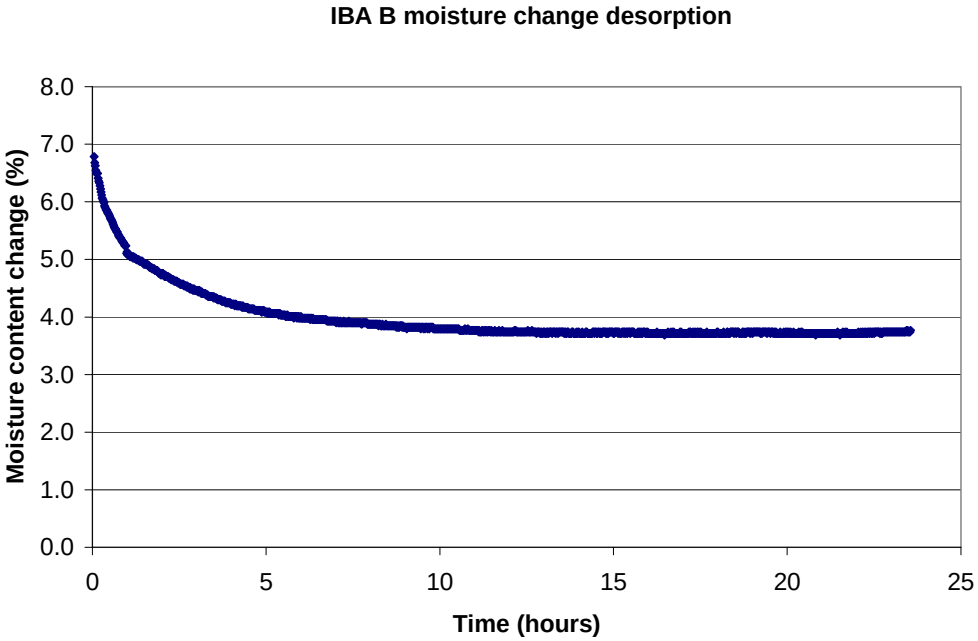

Figure 54. IBA B moisture content change during desorption.

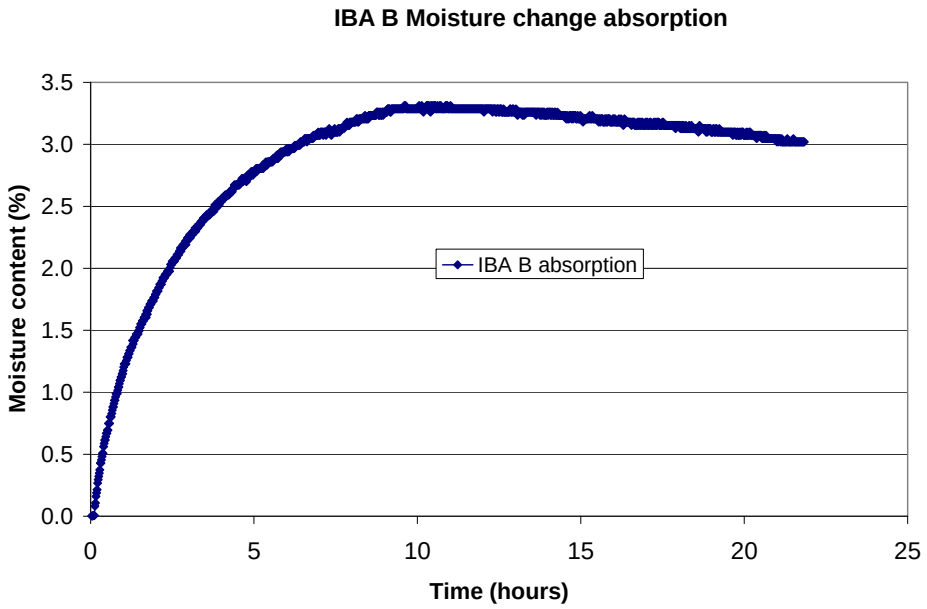

Figure 55. IBA B moisture content change during absorption.

Free shrink swell with RH and moisture content changes

The variations with both time and moisture content changes are given in Figure 56 - Figure 59. In this case the shrink-swell coefficients were closer to equal – 0.273 for shrinkage and 0.231 for swell. As the IBA B tests were performed first it led to misplaced confidence in the test protocols. However there is clearly a sharp difference between the performance of IBA A and IBA B in their free shrink-swell characteristics.

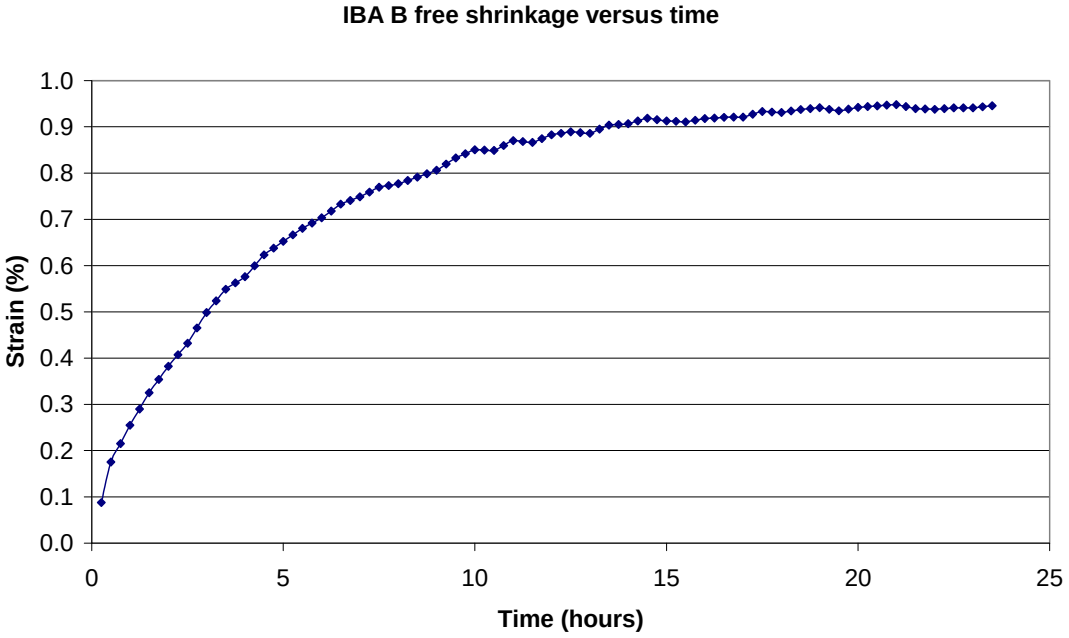

Figure 56. Variation of shrinkage with time.

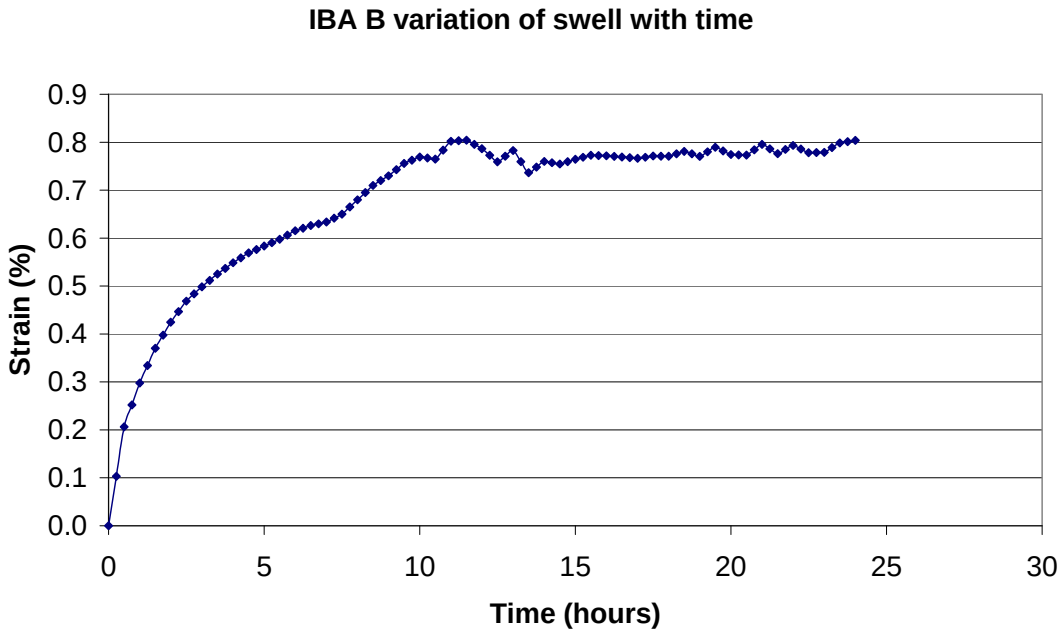

Figure 57. Variation of swell with time.

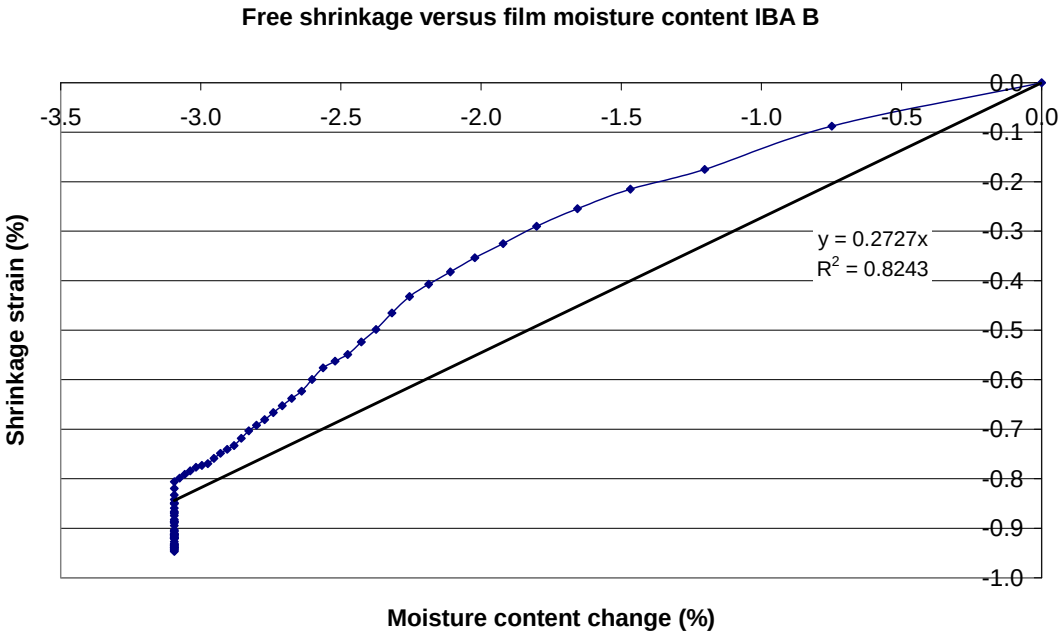

Figure 58. Variation of shrinkage with moisture content.

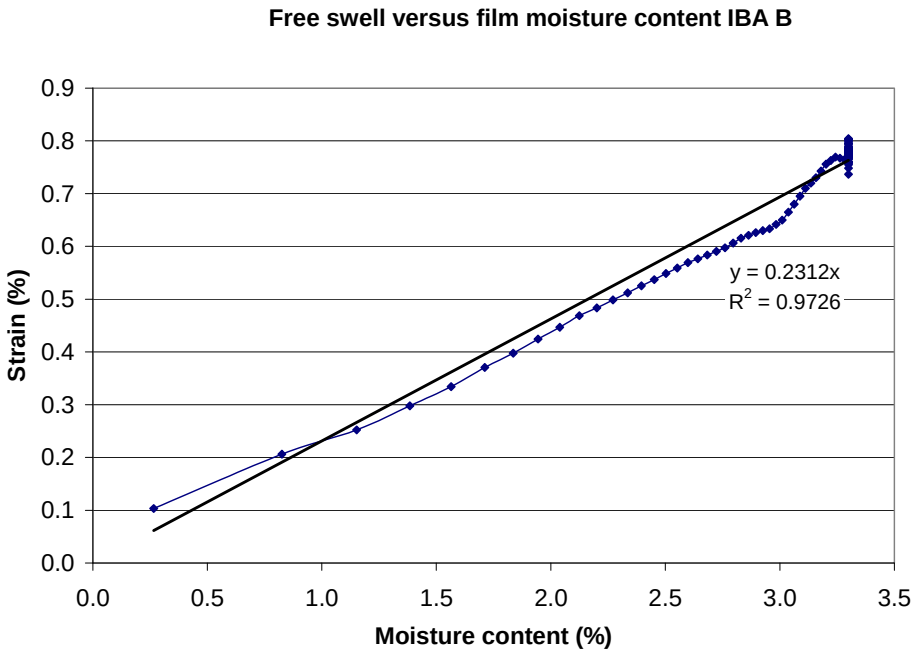

Figure 59. Variation of swell with moisture content.

Viscoelastic creep at test and intermediate moisture levels

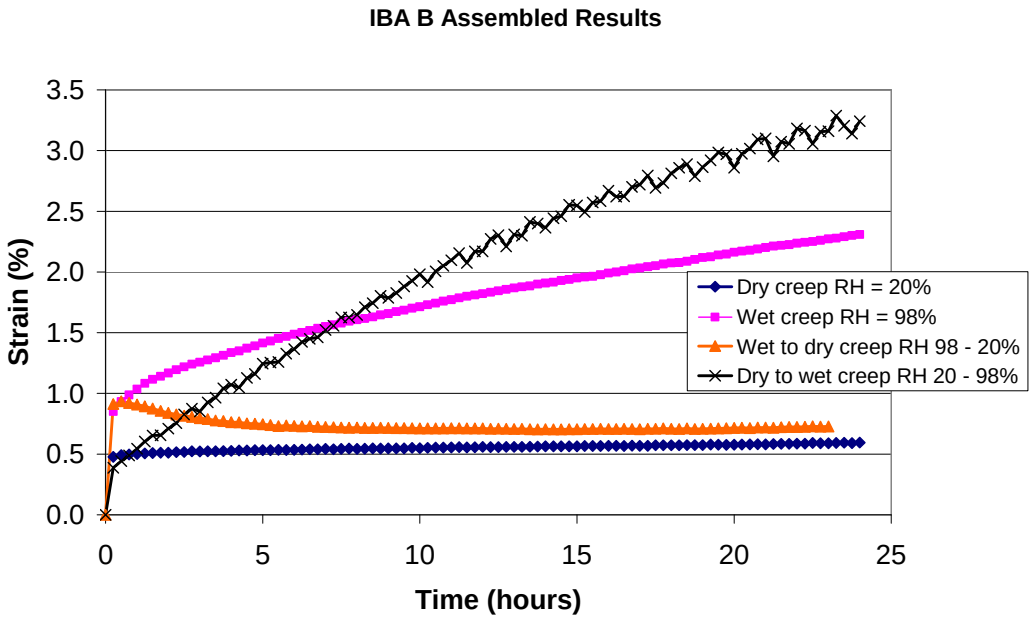

Figure 60. Strain observations for IBA B.

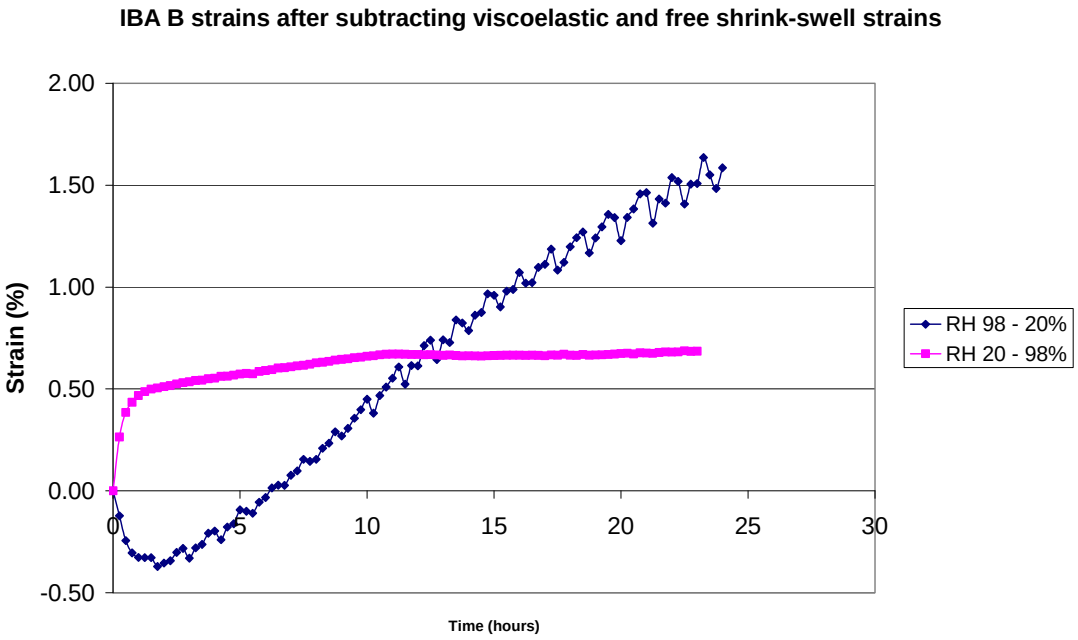

Figure 61. Strains other than viscoelastic and free shrink swell strains.

IBA D results

The results for IBA D are provided again without the detailed explanations given for IBA A.

Relative humidity and the specimen moisture content

IBA B was tested using K_2SO_4 to control the upper humidity level and NaBr to control the lower level giving a theoretical RH range between 98% and 60%. The problems encountered with what is believed to be a salt contamination problem show clearly in Figure 62. On using K_2SO_4 the humidity reached around 97% as expected and, on drying NaBr dropped to around 60% again as expected but the second wetting cycle the RH reached only 87%. Whether this is due to NaBr adhering to the specimen, the humidity sensor or to the sides of the test chamber is difficult to tell and highlights the need to revert to mechanical methods for controlling relative humidity.

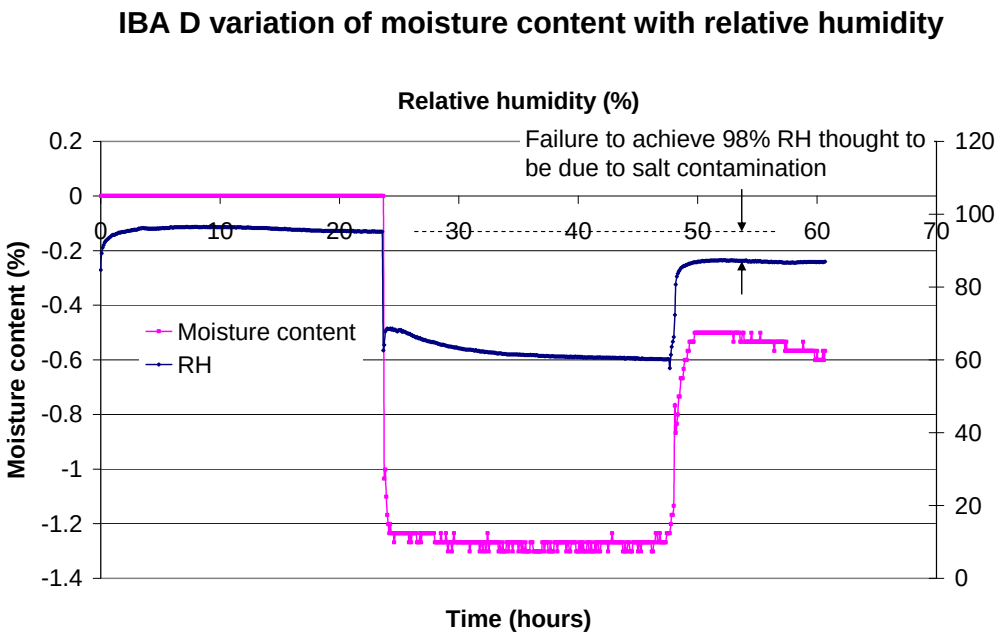

Figure 62. IBA B moisture content change during desorption.

Free shrink swell with RH and moisture content changes

The variations with time are given in Figure 63 - Figure 64. No attempt is made to determine the variation of shrink and swell with moisture content as by the time simultaneous weighing and Aramis measurements were attempted problems had emerged with the Aramis equipment.

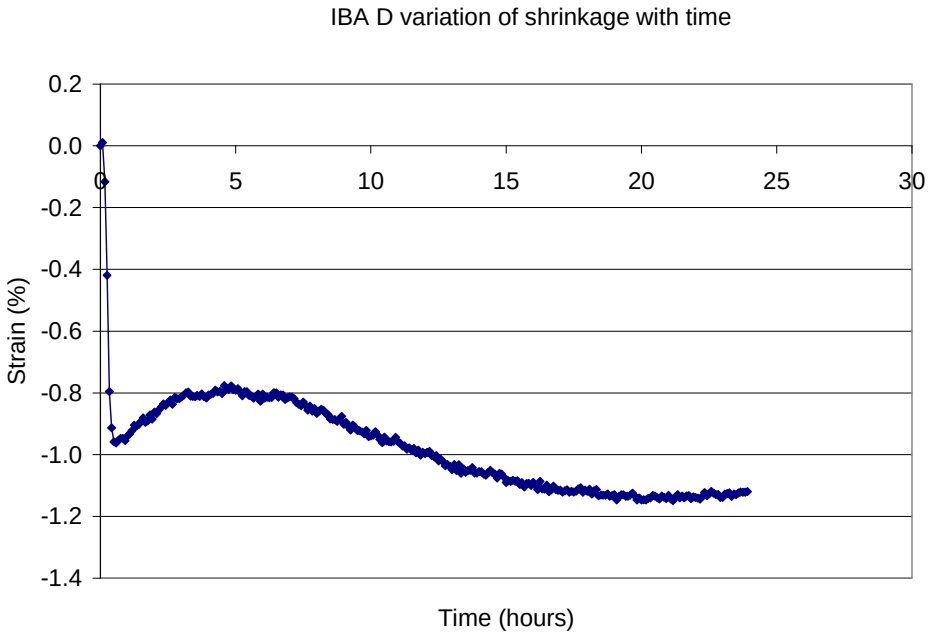

Figure 63. Variation of shrinkage with time.

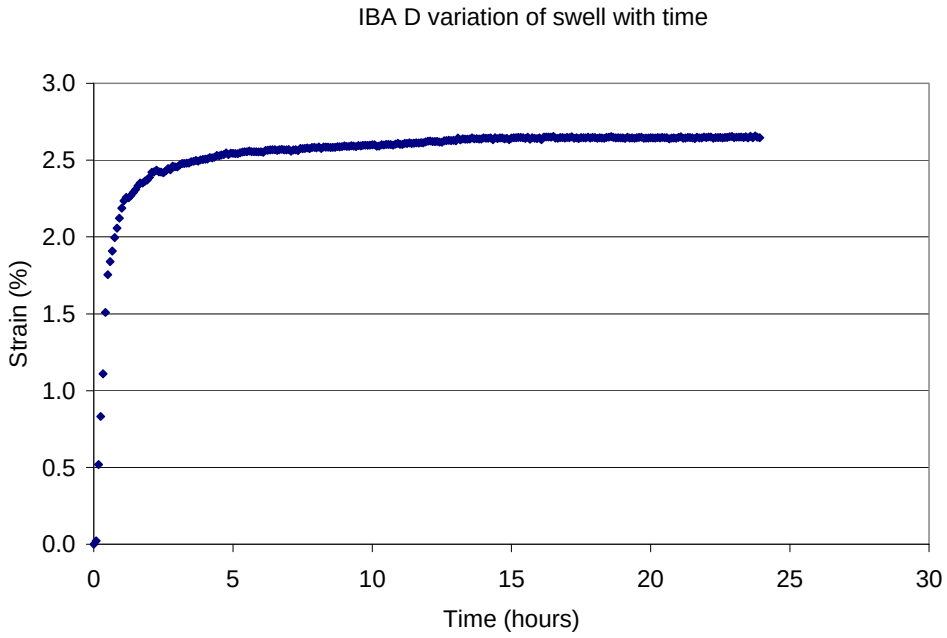

Figure 64. Variation of swell with time.

Viscoelastic creep at test and intermediate moisture levels

The most interesting result is the dominance of free shrinkage over the effect of the applied load estimated at 1 MPa in the wet to dry test. On load application a tensile strain appears to a level of 1.8% but this is reversed by the effect of the drying shrinkage over a total range of around 3% (1.8% to -1%). This is an anomalous result inconsistent with the free shrink change. As IBA D showed excellent performance even with spotted gum when dry (being the only adhesive to demonstrate high strength and wood fibre failure) it could well be that its drying shrinkage mitigates against its effectiveness after wetting and then subsequent drying.

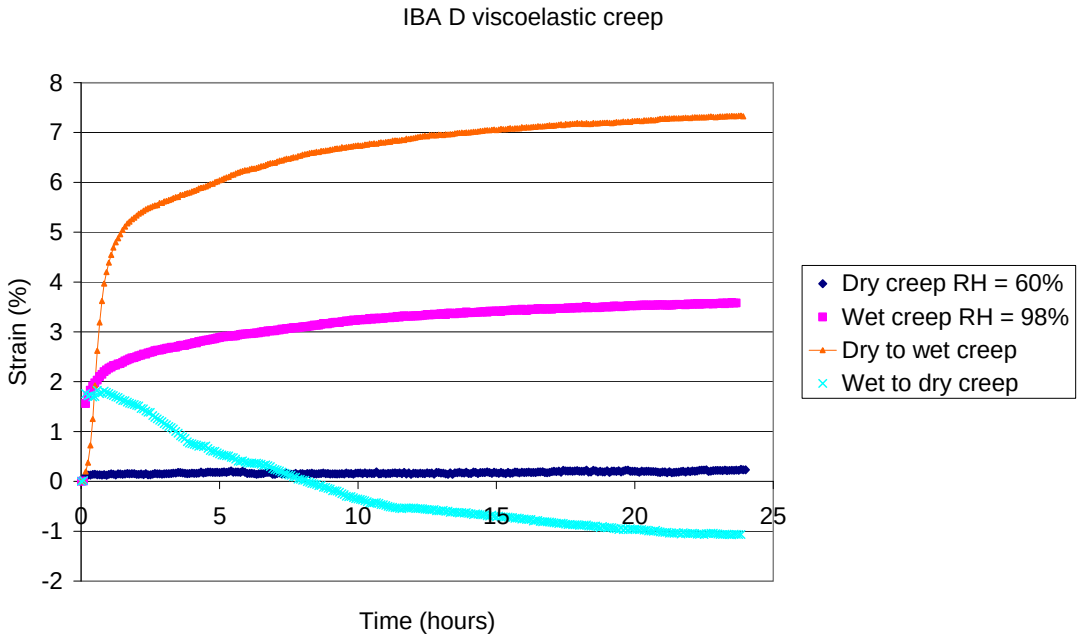

Figure 65. Strain observations for IBA D.

Results for PRF

Relative humidity and the specimen moisture content

Absolute values of moisture content were determined in this case. The dry weight was determined by the oven drying method, using a temperature of 103˚C. It is not actually necessary to know absolute moisture content values to undertake this study but it was of interest since values were available for comparison against the test results published by Muszynski et al. This showed they ranged between 12% and 18%, see Figure 66, compared with the Muszynski result in the range 13.5% to 20% for an identical change in relative humidity. The Monash measurements are somewhat unsatisfactory as can be seen by the fact that the RH in the humidity chamber was not controlled as it should have been. The graph suggests that either salt was deposited on the specimen or had adhered to the sides of the test chamber as discussed earlier. This problem would not arise with mechanical air conditioning.

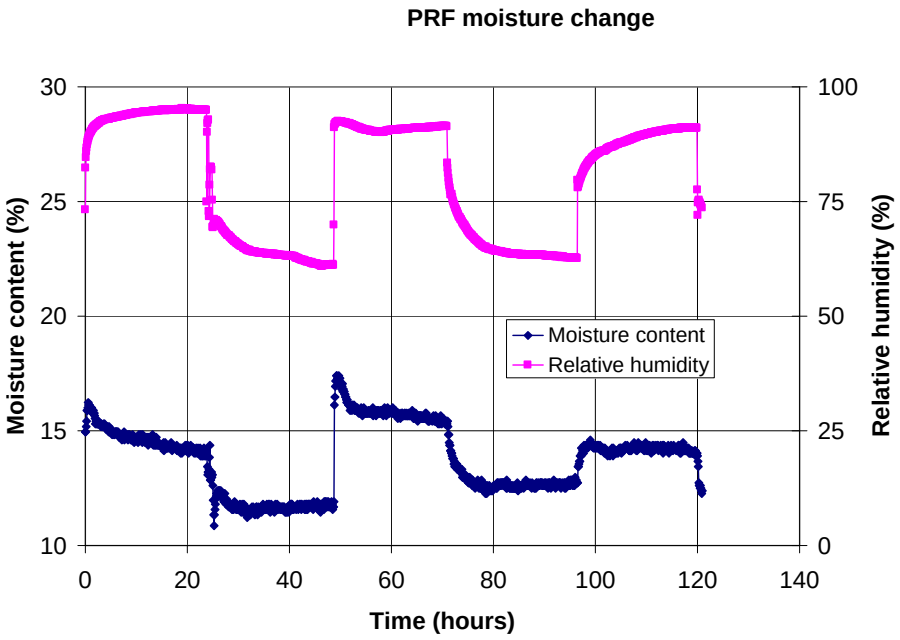

Figure 66. PRF variation of film moisture content with relative humidity.

Free shrink-swell with time

Figure 67 shows the response of three thin RF films tested simultaneously in slightly different positions in the test chamber and Figure 68 shows the mean result. The centre specimen had been through several loading cycles but the east and west specimens were in a virginal state. It is possible that the previous loadings have had an effect on the specimen response. If this result is repeated in future observations it will complicate observations as it implies that the response depends on load history. It will also mean that there are no unique long term properties that can be cited for PRFs. The PRF appeared to have sharply lower free shrink-swell characteristics but the results were unsatisfactory. It was at this time that problems appeared with the Aramis system so that the matter was unable to be resolved.

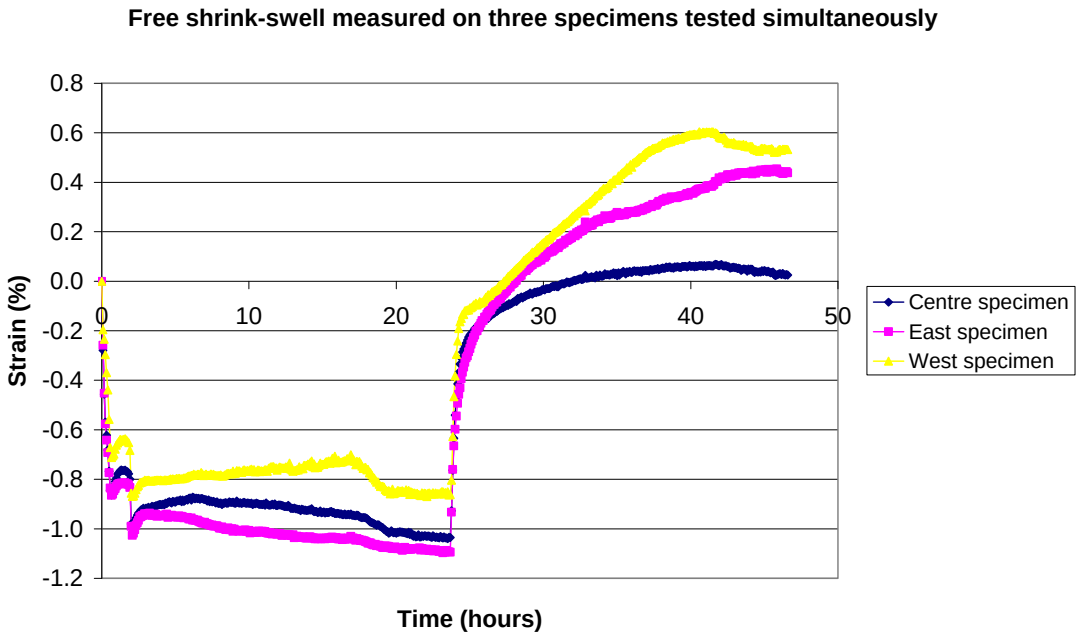

Figure 67. Free shrink-swell of three PRF specimens measured simultaneously.

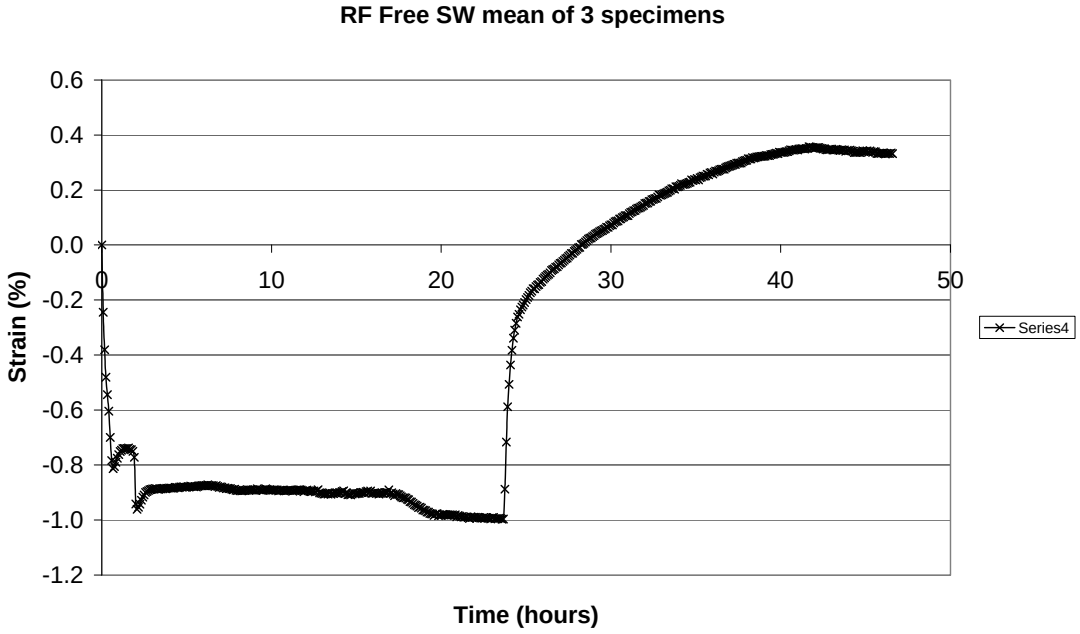

Figure 68. Mean free shrink-swell response of three PRF films.

Viscoelastic creep at test levels (RH 60% and RH 98%)

The viscoelastic creep at the test values shows very little differentiation between dry and wet conditions. This result is inconsistent the result obtained by Muszynski et al where wet creep resulted in strains that were 3 times those of the dry viscoelastic creep strains. More testing is required to confirm this result but it may simply reflect a characteristic difference between the two PRF adhesives.

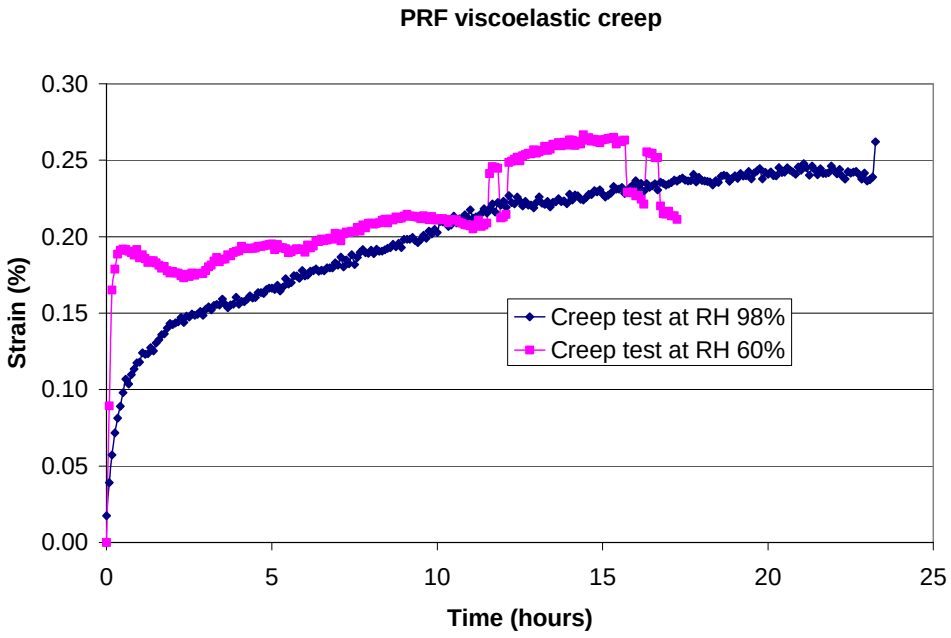

Figure 69. PRF viscoelastic creep at 60% and 98% relative humidity.

Total strains under varying RH

The results following repeated trials are shown in Figure 70.The result for RH 98% down to 60% showed negative strains due to the shrinkage exceeding those caused by the applied load. By way of contrast with the results cited by Muszynski et al, who used applied stress levels of 10 MPa as opposed to the 3 MPa used in these tests the low to high humidity tests show a delayed viscoelastic response. Note how the upper curve shows an increase in strain with time which may involve a mechano-sorptive response component but, because of the increase of strain with time, it is not entirely of this nature. Closer examination of the data published by Muszynski shows that, at 10 MPa, his thin films actually broke at around 8 hours. There is little point in further processing the data other than to note that delayed viscoelastic creep is less dominant in PRFs compared to IBAs A and B.

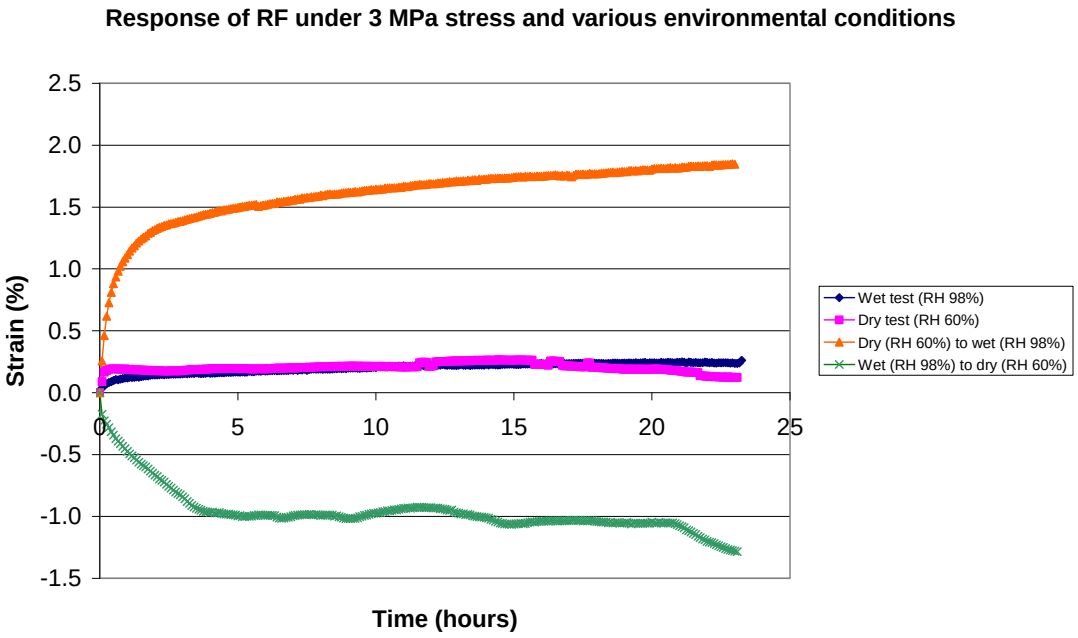

Figure 70. Response of RF under wet, dry wet to dry and dry to wet conditions.

Discussion and conclusions

Further testing of adhesives is required before drawing definitive conclusions but the following tentative remarks can be made.

1. The techniques of making PUR thin films has been mastered to the extent that it is now possible to study their hygro-mechanical response.
2. The Aramis system has proven, when functioning, to be a useful investigative tool and the problems associated with extracting data from the system processing it through Excel have been solved
3. Investigation is required into finding improved methods of controlling chamber RH. Muszynski claimed to have changed RH quite sharply but did not present logs of the RH change and independent enquiries led to the statement that the data was lost.
4. The data to date does not indicate that any of the adhesives exhibit a mechano-sorptive response but neither does it preclude that possibility. Recalling that mechano-sorptive strain is purely associated with moisture change and independent of time, the two strain (ε) versus time (t) curves for varying RH 60-98% and 98-60%, would need to flatten, $d\varepsilon/dt = 0$ since at later times the moisture content stabilises. This has not occurred for any of the adhesives examined to date nor does Muszynski's data for wet to dry conditions at the point where his film ruptured. The strain appears for wet to dry conditions appears to be more in the nature of a delayed viscoelastic response influenced by moisture change. It may well be necessary to develop alternative theoretical models to explain the hygro-mechanical response of adhesive films.
5. The viscoelastic response of IBAs are more affected by moisture change than PRFs.

MATERIALS AND METHODS

12 Month Exposure Test

Preparation of Test Beams

The timber used for this project was MGP10 grade radiata pine, F14 Victorian Ash and F27 Spotted Gum. The pine was purchased from Auspine, the Victorian Ash from Drouin West Timber and the Spotted Gum from Hyne and Son. The adhesives used in this study are listed in Table 2.

The preparation of the test beams was undertaken at Warrnambool Timber Industries Pty Ltd. Each adhesive manufacturer (Purbond, Ashland and Bostik) was involved in the preparation of the beams involving their adhesives using timber of dimensions of 90 x 45 mm for the pine and Victorian Ash samples and 90 x 35 mm for the spotted gum samples. Timber lengths length ranged from 4.5m to 6m. Two ply laminated beams were prepared for each wood adhesive combination by applying the adhesive onto one face of one of the beams to be bonded at a loading of approximately 250gsm. The IBA adhesives were applied by hand using an adhesive comb or coating rod. The PRF was applied using an industrial applicator. The beams were manufactured in the presence of technical representatives of each of the adhesive companies and under their supervision. Pressure was applied via a hydraulic hose and maintained for at least 8 hours. The beams were ripped in half lengthwise, dressed and docked to give test beams of 700 x 38 x 80mm (l *x* w *x* h) for the pine and Victorian Ash samples and 700 x 38 x 60mm for the spotted gum samples

Loaded Specimen - Loading Arrangement

The specimens were loaded in four point bending over a span of 600 mm at a level of loading approximately representative of working load conditions. The load span was one third of the support span, a particular case of four point bending also known as "third point" bending. The load configuration required the application of constant forces in the range of 2.6-4.5 kN to 240 individual test beams over exposure periods of 1 and 3 years. The large number of test beams and the loading durations limited the practical options for the application of the loads to the use of dead weights. If applied directly, dead weights totalling almost 90 tonnes would have been required to achieve the target forces. In view of the impracticality of handling such weight, loading fixtures employing a double lever arm load magnification system were designed and built. The load magnification system is illustrated in principle in Figure 71 and shown in more detail in Figure 72 and Figure 73. The system effectively magnifies a dead weight by a factor of up to 42, thereby allowing the required forces to be generated using whole (typically around 23 kg) or half lead ingots and reducing the total dead weight requirement to 3.6 tonnes. Half the test beams were placed in full outdoor exposure at a CSIRO site in Darwin, Northern Territory, Figure 74 and

the other half in an environment chamber at Monash University, Figure 75. The loading rigs themselves were designed in steel made up in 'knock-down' form, fabricated in Melbourne and finally assembled in by bolting in both Melbourne and Darwin. A disadvantage of the load magnification system employed is that any beam deflection is also magnified, the end of the lever to which the dead weight is attached descending a distance of up to 42 times the incremental beam deflection. To counter this, adjusting screws were placed between the spreader beam and the loading straps that apply the final load. These were adjusted periodically to keep the final lever arms within 10º of horizontal, maintaining loads within 1.5% of that initially applied in the horizontal position.

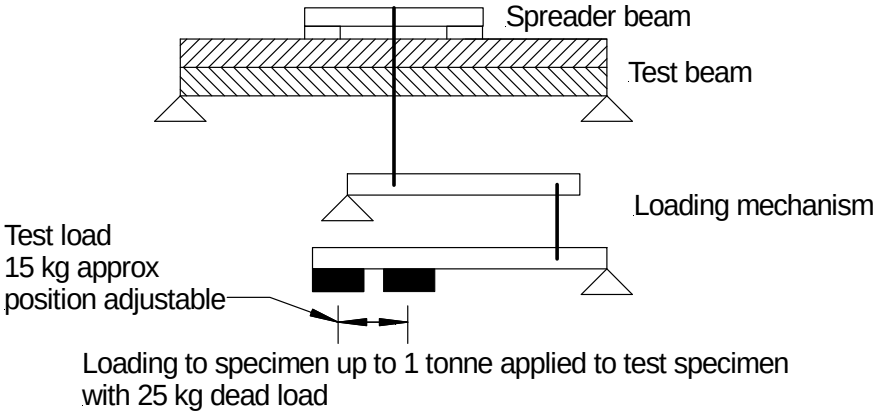

Figure 71. Conceptual details of the loading mechanism used to apply load to loaded specimens.

Because the masses of the lead ingots used as dead weights varied, and to allow for any dimensional variations in the loading mechanism, a purpose built calibration beam was employed in positioning the dead weights to accurately and reproducibly achieve target loads on individual test beams (Figure 76). Once in position, each ingot was fixed in place with hose clamps.

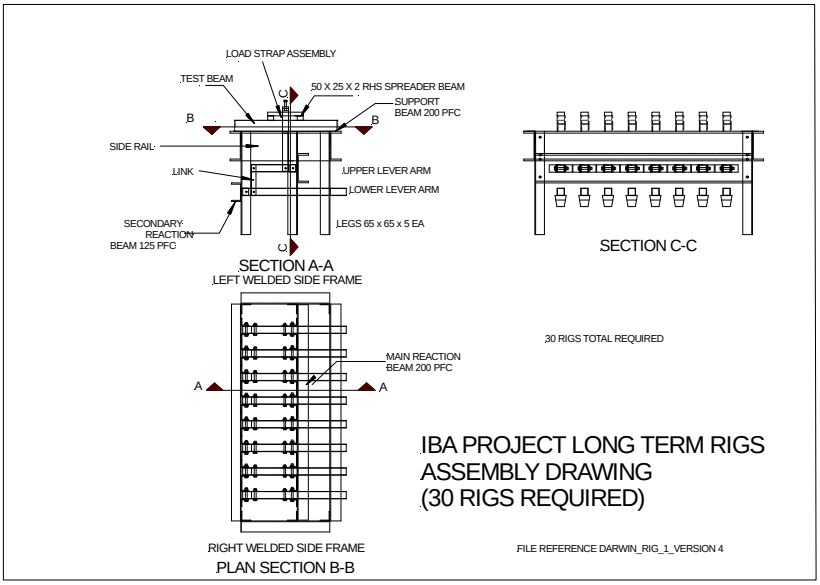

Figure 72. Assembly diagram of the test rigs as manufactured.

Figure 73. Double cantilever loading mechanism.

Figure 74. Pictures of the test rigs for the loaded beams at the outdoor exposure site, Darwin.

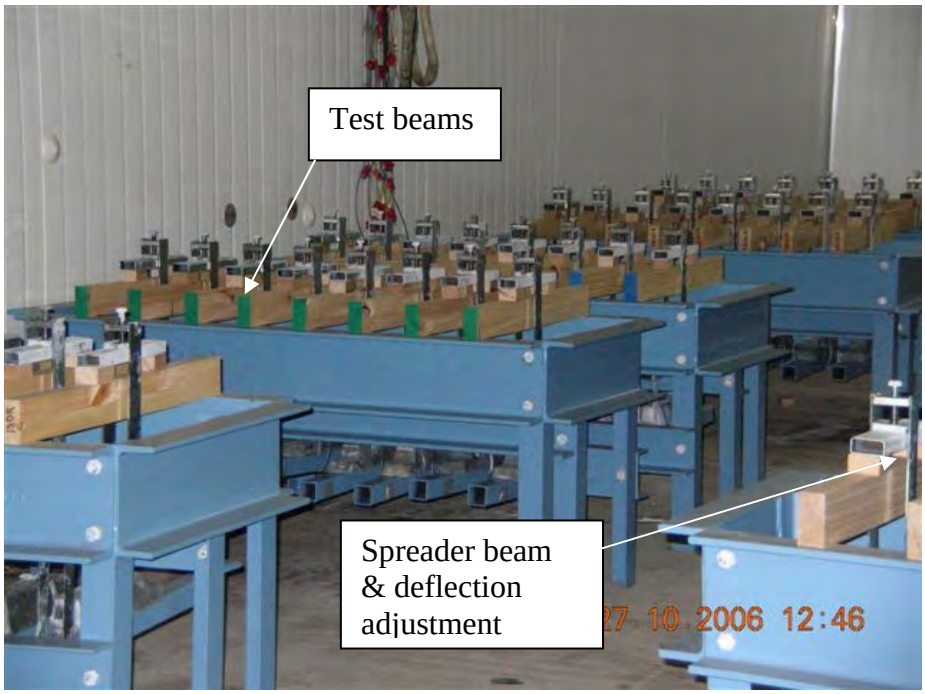

Figure 75. Test rigs with specimens in Monash University environment chamber.

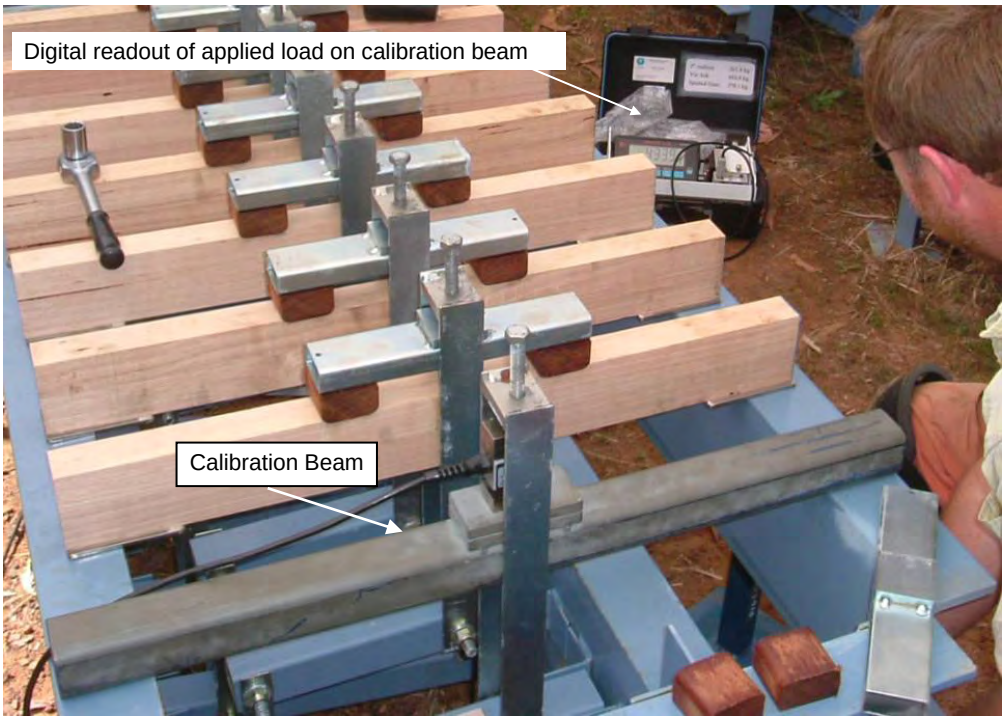

Figure 76. The calibration beam that was used to determine the correct position of the lead ingots to give the required load.

Specimen Loading

The test protocol within AITC 200-92 calls for loading of test beams at 1.5 x design bending strength as defined in US standards. Initially this was interpreted, in an Australian context, as 1.5 x basic working stress for working stress design as defined in Australian Standard AS1720.1 1997. This load level caused a number of failures in the timber that were totally unrelated to the issue of bond line performance; see Figure 77. Consequently, it was decided to fix loading along the following lines.

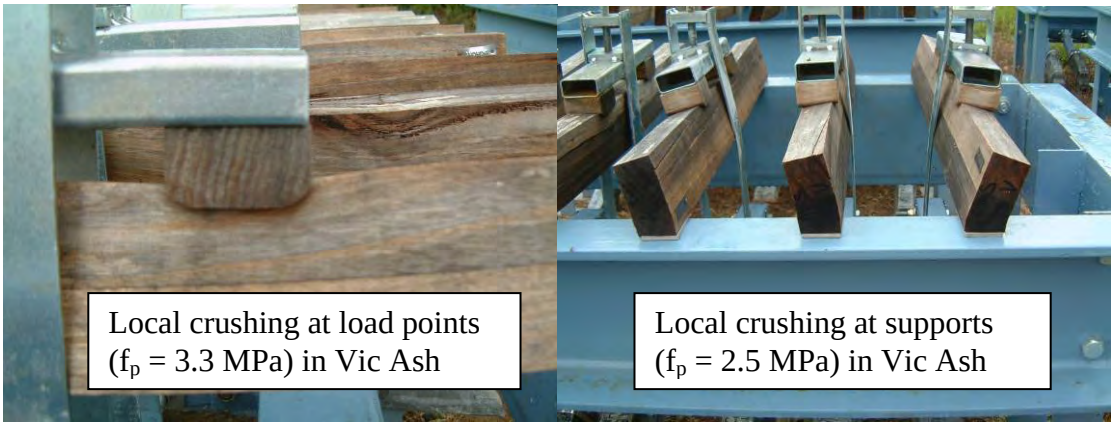

Figure 77. Early failure modes unrelated to bond line performance. This led to a decision to reduce load levels.

The bending stress level was computed according to

$$f_b = \phi k_1 k_4 k_6 f_b' \qquad 1$$

f_b = stress level to be applied during the test

ϕ = capacity factor taken as 0.9

k_1 = long term load factor = 0.6 for both 1 and 3 year specimens,

k_4 = moisture condition factor = 0.7

k_6 = temperature factor = 0.9

f' = characteristic strength values for GL grades given in AS1720.1:1997[20]

Lateral buckling was not considered a possibility given the dimensions of the test beams, depth/breadth = 80/38 ≈ 2 and slenderness coefficient $S_1 = 1.25(d/b)(L_{ay}/d)^{0.5}$ $= 1.25 \times 2 \times (700/80)^{0.5} = 7.4$. Taking the material constant $\rho_b = 1.15$ this leads to $\rho_b S_1 = 7.4 \times 1.15 = 8.5$ and $k_{12} = 1$.

Capacity factor

The capacity factor used by GLTAA members in domestic applications is 0.9.

Duration of load factor k_1

The duration of load factors given in AS1720.1:1997 are listed in Table 30.

Table 30. Values of duration of load factor k_1 extracted from AS1720.1:1997.

Type of load	Effective duration of peak load	k_1
Standard test	5 minutes	1.00
Short term	5 hours	0.97
Medium term	5 days	0.94
Long term	5 months	0.80
Permanent	50+ years	0.57

It is considered that 1 and 3 year exposure trials approximate permanent load conditions so therefore $k_1 = 0.57$. It is possible to interpolate between 0.57 (50 year value) and 0.8 (5 month value – floor loading which usually involves SC2 conditions) but the data on duration of load effects does not permit this level of refinement. There are no provisions in AS1720.1 that would encourage a designer to use a value higher than 0.57 for sustained (longer than 5 months) loading in SC3 conditions. Its value was rounded up to 0.6.

[20] Australian Standard AS1720.1:1997 Timber Structures Part 1: Design Methods

Moisture factor k_4

The moisture factor is based on the assumption of the very moist conditions that arise in Darwin. It is assumed that the wood moisture content will be at 25% giving $k_4 = 0.7$ according to AS1720.1:1997.

Temperature factor k_6

The latitude of Darwin and the temperature conditions used for much of the time in the Melbourne environment chamber justify taking $k_6 = 0.9$.

GL grade values

The use of GL grade values is based on the realistic expectation that high density timbers (above ADD 700-800 kg/m^3) cannot be adhesively bonded to the corresponding F values. The shear and bending characteristic strengths of the GL grades targeted are listed in Table 31; these have been taken from AS1720.1:1997 Table 7.1. The Radiata Pine was ordered as MGP10.

Table 31. Values of GL grades (MPa).

Species	**Grade**	f_b'	f_s'	***E***
Spotted Gum	GL18	50	5.0	18500
Victorian Ash	GL13	33	3.7	16700
Radiata pine	GL8	19	3.7	10000

1.35 safety factor on loads

Under Australian Standard AS1170.0 Part 0 an engineering designer is required to check a permanent load condition of 1.35G, that is, 1.35 x nominal dead load. The 1.35 value represents a partial factor of safety placed on dead loads to allow for errors in estimating load values such as might arise for a variety of reasons including miscalculation, dead load being added due to building additions etc. This was ignored, recognizing that the loading is 35% in excess of expected service loading.

The loading levels were set on the basis of bending stress levels shown in Table 32.

Table 32. Bending stress levels used for exposure stresses.

Species	GL grade	f'_b (MPa)		k_1	k_4	k_6	f_b (MPa)
P. radiata	8	19	0.9	0.6	0.7	0.9	6.5
Victorian Ash	13	33	0.9	0.6	0.7	0.9	11.2
Qld Hwd	18	50	0.9	0.6	0.7	0.9	17.0

Given the dimensions of the beams, their span (600 mm) and loading configuration (4 point bending) the corresponding shear stresses at the bond line were as stated in Table 33.

Table 33. Shear stresses on the bondlines during exposure.

Species	Beam dimensions (mm)				
	Depth, h	Width, b	Span, L	Applied load (N)	f_s (MPa)
P. radiata	80	38	600	2620	0.65
Victorian Ash	80	37.5	600	4491	1.12
Qld Hwd	59	37	600	3651	1.25

Determination of Bond Strength in Longitudinal Compressive Shear

The bond strengths of unexposed (control) test beams and residual bond strengths of exposed test beams were determined in longitudinal compressive shear. Tests were conducted in general accordance with the procedures specified by Mack.[21]

Four beams that had been under load and four beams that were unloaded for each wood/adhesive combination were tested from each exposure site (environmental chamber and Darwin exposure site). Test specimens were cut from the beams as shown in the following cutting plan:

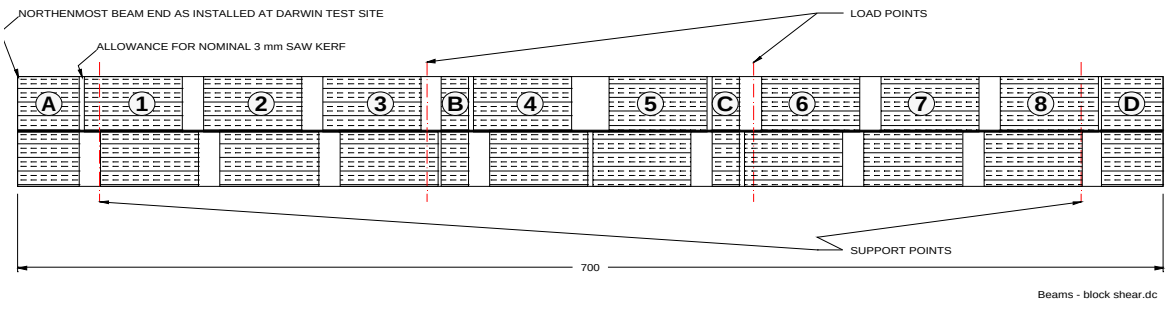

In the case of test beams loaded in third-point bending during exposure, specimens 1-3 and 6-8 lay in the areas of the beams that were subject to shear loads; specimens 4

[21] J. Mack, "Australian Methods for Mechanically Testing Small Clear Specimens of Timber." *CSIRO Division of Building Research Technical Paper (Second Series)* **No. 31**, (1979).

and 5 were considered to be potentially useful as controls for the determination of the effect of shear loading in the individual beams.

A 10 mm step either side of the glueline was incorporated at the loaded ends to assist in specimen positioning and stability. The effective glueline shear area was nominally 50 mm x beam width (~38 mm).
[The geometry and dimensions represent variations from those specified in the nominated procedure in that tests on clear wood are performed on 50 mm cubes which provide a shear area of 50 x 50 mm]

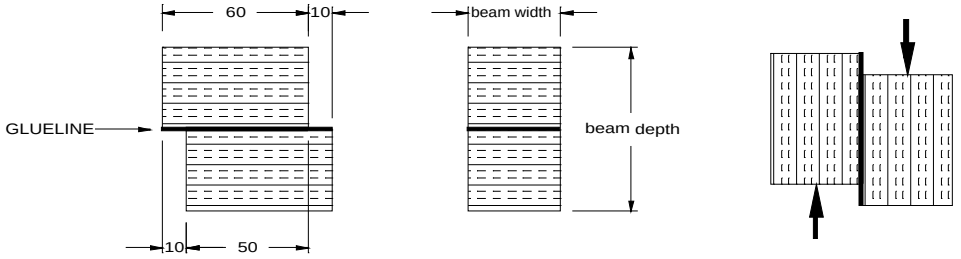

Beams - block shear.dc

The remaining sections of the beams, labelled A-D, were reserved for PALS (positron annihilation lifetime spectroscopy) analysis of the gluelines.

Cut test specimens were conditioned in an environment of 20 ±2°C and 65 ±5% RH for a minimum of two weeks immediately prior to testing.

Specimen gluelines were tested in longitudinal compressive shear using a roller guided block shear fixture of the type detailed in DRG No. 2144, *Shear Test Block – Roller Guided (Modified)*, Forest Products Research Laboratory, D.S.I.R. Princes Risborough, Bucks., 1930.

The glueline shear area of each specimen was determined from measurements (to the nearest 0.1 mm) of its overlap length and width. The specimen was then be loaded to failure at a constant crosshead displacement rate of 6 mm/min, and the failure load in Newtons recorded.

Glueline shear strength (MPa) = failure load (N) / glueline shear area (mm^2)

Specimens 2 and 6 from each beam were weighed (to the nearest 0.01 g) immediately following testing and after oven drying (103 ±2°C) to allow the determination of beam moisture content at the time of test.

AS/NZS 4364:1996 Delamination Test

This test is based on the experimental procedures as outlined in Appendix E of AS/NZS 4364:1996. The delamination test used was the high temperature procedure for type I adhesives. Radiata pine (MGP10) was purchased from Auspine, Victorian Ash (F17) was sourced from Drouin West Timber and Spotted Gum (F27) was purchased from Moxon Timbers. The timber was docked into 100 x 35 x 450 mm

pieces and conditioned for at least one month at 20°C and 65% relative humidity (RH).

Three bonded assemblies for each wood species-adhesive combination were prepared. Each assembly consisted of 6 lamellae. Prior to application of the adhesive, each lamellae was passed through a thicknesser such that it had two smooth faces and a final thickness of 27 mm. Adhesive application was made within one hour of planing the pine and Victorian Ash samples and within 2 minutes for the spotted gum samples.

The adhesive was prepared according to the manufacturer's instructions. Adhesive was applied on one side of the lamellae at a spread rate of 250 gsm. The lamellae were weighed before and after adhesive application to ensure correct coverage. Adhesive was spread using adhesive combs. Immediately after applying the adhesive, the assemblies were placed in clamps and a pressure of 1.0 MPa applied by tightening the clamp bolts to an appropriate torque. The clamps were retightened after 30 minutes and 1.5 hours. The assemblies were pressed for 22 hours at ambient laboratory conditions. After pressing, the bonded assemblies were allowed to condition for 3 weeks at 20°C and 65% RH prior to delamination testing.

After conditioning, 75 mm long test samples were cut from each beam. The cutting diagram is given in Figure 79. Three test pieces per beam (Test Pieces A, C and D) were used for the delamination test.

Figure 78. Preparing the bonded assemblies for the delamination test. (*top left*) the clamps used for manufacture; (*top middle*) applying the adhesive; (*top right*) spreading the adhesive; (*middle left*) assembling the glued lamellae in the clamps; (*middle right*) tightening the clamps to the correct pressure and (*bottom left*) the three bonded assemblies in the clamps; (*bottom right*) the vacuum-pressure vessel used for the water soak.

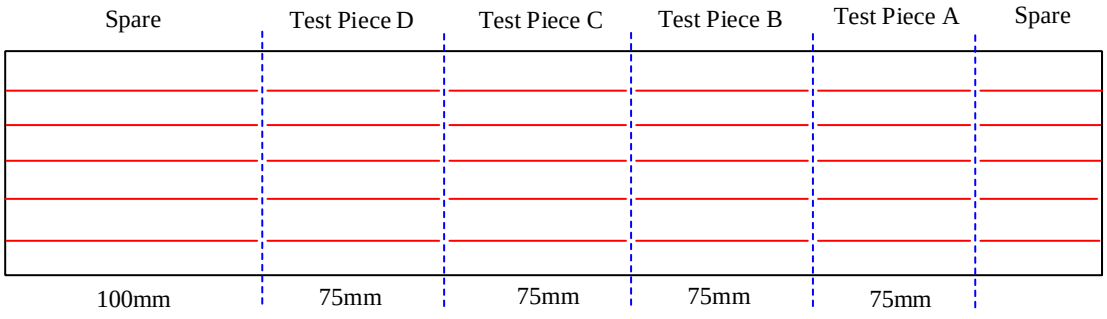

Figure 79. The cutting diagram and location of the test pieces within the manufactured beams for the AS/NZS 4364:1996 delamination test.

The test pieces were placed in a pressure vessel and immersed in water at a temperature of 15±5°C with care to ensure that they were fully immersed, not floating

and were separated by at least 5 mm to ensure that all the end grain surfaces were fully exposed to the water. A vacuum of 25±5 kPa (absolute) pressure was applied and maintained for 5 minutes. The vacuum was then released and a pressure of 600±25 kPa (absolute) pressure was applied and held for 1 hour. This vacuum pressure soak (VPS) was repeated once more to give a 2 cycle impregnation time of 130 minutes. After this VPS, the samples were immediately placed in a dehydrating oven and dried at 65°C for 22 hours. This VPS/dry routine was repeated twice more to give a 3 cycle VPS-dry regime that lasted a bit longer then 3 days. The mass of selected samples of all three wood species was recorded during this test to monitor water uptake and loss.

Immediately after the final drying period, the total length of open joints (delamination) on all the end grain surfaces was measured to the nearest millimetre. The delamination of the test sample was calculated as the ratio of the length of open end grain joints to the total length of end grain joints and expressed as a percentage.

CSA O112.9-04 Delamination Test

Test beams were manufactured in accordance with the methodology described in CSA O112.9. Just prior to bonding, the 140 x 19 mm laminates were dressed to fractionally below the standard limit and bonded with growth rings alternated in direction. After glue application, the specimens were clamped in the rig shown in Figure 80. Clamp pressure was maintained for 4 hours for all the IBAs and overnight for the PRF. Upon removal from the clamp, one side of the assembly was hand planed to produce a reference surface and a straight-line then cut on a 16 inch bench saw. The other side of the assembly was then cut to the final 130 mm width specified in the standard. Subsequently 75 mm sections were then cut for the actual test with a docking saw.

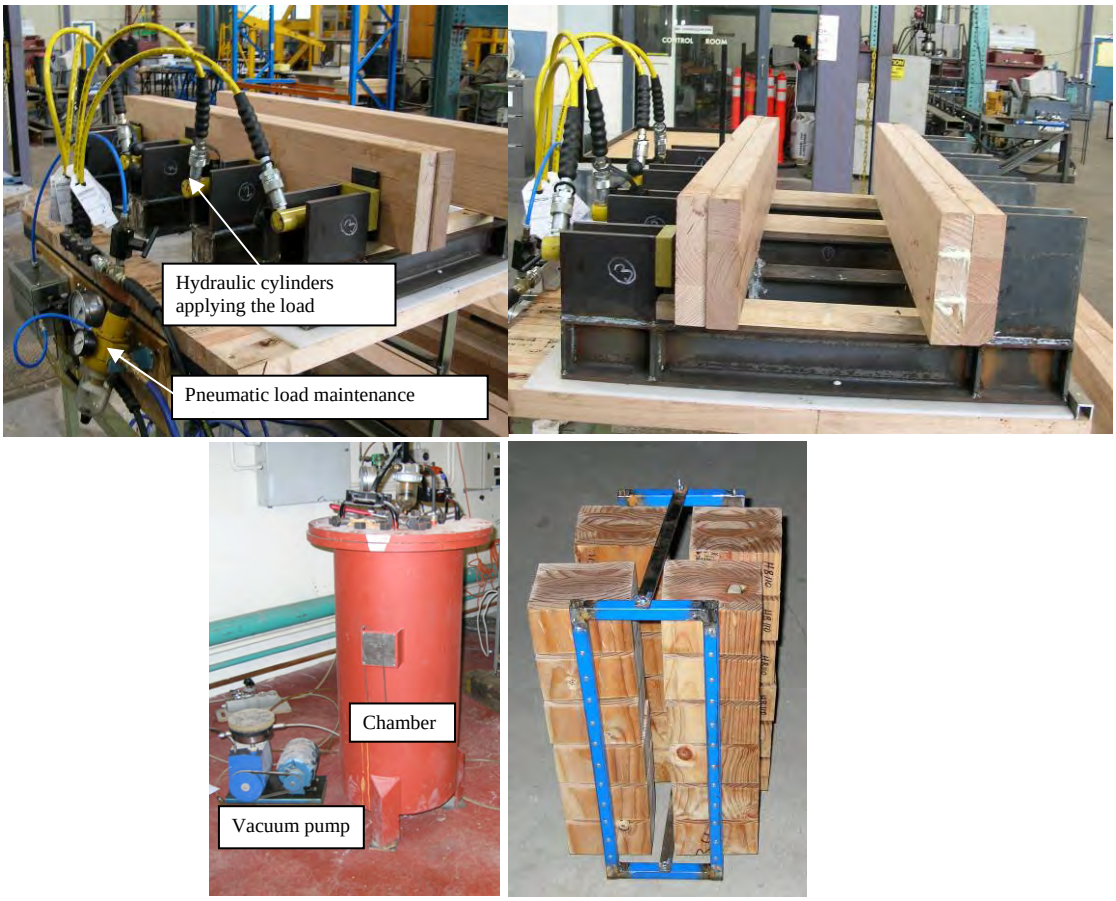

Figure 80.. (*top left*) Cramping rig used to make test specimens for cyclic delamination tests. The hydraulic cylinders have their load maintained by a pneumatic system. (*top right*) End view of cramping system showing the caul boards used to evenly distribute the cramping pressure. (*bottom left*) Test chamber used to apply vacuum and pressure to condition specimens. (*bottom right*) System used to separate specimens for cyclic delamination test. Screw fastening does not extend below outer laminate.

The test pieces were then placed into an autoclave and immersed in water at 22±5°C. Care was taken to ensure that samples were separated so that all of the end grain surfaces were freely exposed to the water. A vacuum of 25±10 kPa (relative to atmospheric conditions) was applied and held for 2 hours after which pressure (540±20 kPa) was applied for a further 2 hours. This was repeated once more to give a 2 cycle water impregnation of 8 hours duration. Immediately after the water impregnation, the samples were placed in an oven and dried for 88 hours at 28±2°C, taking care to ensure that the samples returned to within 10% of their original weight. This soak/dry cycle was repeated 2 more times to give a 3 cycle soak/dry test that lasted for 12 days. During the test, the samples were held within a metal frame (Figure 80). Three specimens were removed to monitor the weight loss during each drying period.

At the end of the final drying period, the length of delamination on each end grain bond line was measured to the nearest millimetre and expressed as a percentage of the total bond line length.

AS/NZS 1328.1:1998 Cleave Test

The cleave test was performed as described in Appendix B of AS/NZS 1328.1:1998. The wet and dry cleave tests were performed using spare beams from the long term exposure studies. Six beams from each wood-adhesive combination were used. Test pieces 35mm in length were cut from each beam. Five test pieces per beam were used to determine the dry wood fibre failure values and 9 test pieces were used to determine the wet cleave values. The positions of the test pieces in the beams are given in Figure 81. For guidance during cleaving, a notch 10mm deep was cut into the glue line on the end grain face for each sample, leaving the remaining 25mm length of the specimen in the bonded condition. The cleaving apart of the glue lines was achieved by using a bricklayer's bolster and a mallet. Wood fibre failure was visually assessed to the nearest 5%.

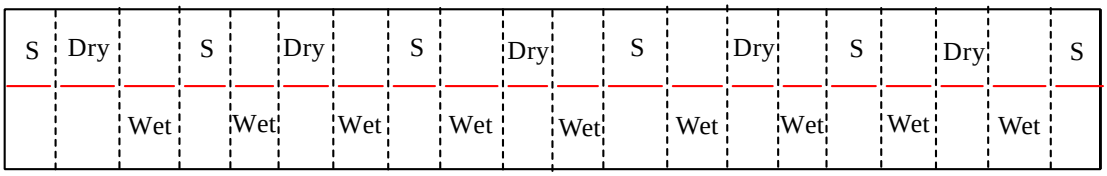

Figure 81. A schematic diagram showing the positions within each beam of test pieces for the dry cleave (*dry*) and wet cleave (*wet*). *"S"* denotes spare test pieces.

The dry samples were conditioned at 20°C and 65% RH for 4 weeks prior to being tested. The samples for the wet cleave were immersed in water at room temperature such that all of the end grain surfaces were exposed to the water. The samples were then subjected to a vacuum of 65 kPa for 1.5 hours followed by an applied pressure of 500 kPa for 1.5 hours. This cycle was repeated to give a 2 stage vacuum pressure soak. The samples were removed from the water and immediately cleaved apart. The cleaved samples were dried in an oven overnight before being assessed for wood fibre failure.

AS/NZS 4364:1996 Longitudinal Tensile Shear Test

Longitudinal tensile shear strength testing of the adhesive bonds were undertaken as described in Appendix D of AS/NZS 4364:1996. The wood used in this study was the same as that described in the AS/NZS 4364 delamination test (*vide supra*). The 35 mm thick pieces of timber were sliced lengthwise into thirds and conditioned for 1 month at 20°C and 65% RH for 1 month. Prior to application of the adhesive, each lamellae was passed through a thicknesser such that the timber had two smooth faces and a final thickness of 8 mm. Adhesive application was made within one hour of planing the Radiata Pine and Victorian Ash samples and within 2 minutes for the Spotted Gum samples. Ten panels for each adhesive/wood combination were prepared.

The adhesives were prepared according to the manufacturer's instructions. Adhesive was applied on one side of the lamellae at a spread rate of 250 gsm. The lamellae were weighed before and after adhesive application to ensure correct coverage. Adhesive was spread using adhesive combs. Immediately after applying the adhesive, the assemblies were placed in clamps and a pressure of 1.0 MPa applied by tightening the clamp bolts to an appropriate torque. The clamps were retightened after 30 minutes and 1.5 hours. The assemblies were pressed for 22 hours at ambient laboratory conditions (Figure 82). After pressing, the bonded assemblies were allowed to condition for at least 2 weeks at 20°C and 65% RH prior to cutting.

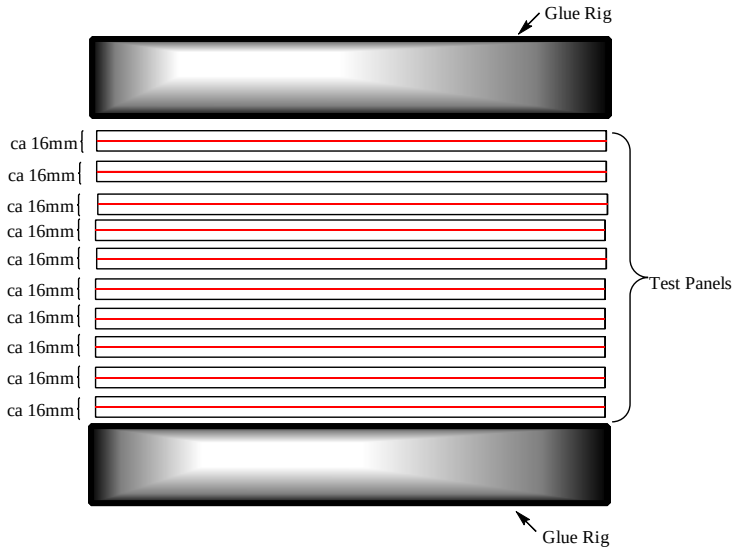

Figure 82. Schematic showing the assembly of the test panels in the press rig.

After conditioning, the panels were planed to a thickness of 10mm before test pieces were cut from the panels. The panels were trimmed on the long axis by 10mm and four 20mm strips were cut (Figure 83). These strips were then cut into thirds to give test strips of 20mm x 150mm. Two flat bottom cuts each 2.5mm in width were made in the bonded sections of each test piece. The cuts were made across the grain on opposite sides of the sample and displaced by 10 mm to give a test area of approximately 20 x 10mm (Figure 84). The cuts did not extend beyond the adhesive layer.

After preparing the test pieces, grouped lots of 20 test pieces per wood/adhesive combination were subjected to one of five treatments (Table 34) prior to tensile testing. After testing, the wood fibre failure values of each specimen were visually assessed.

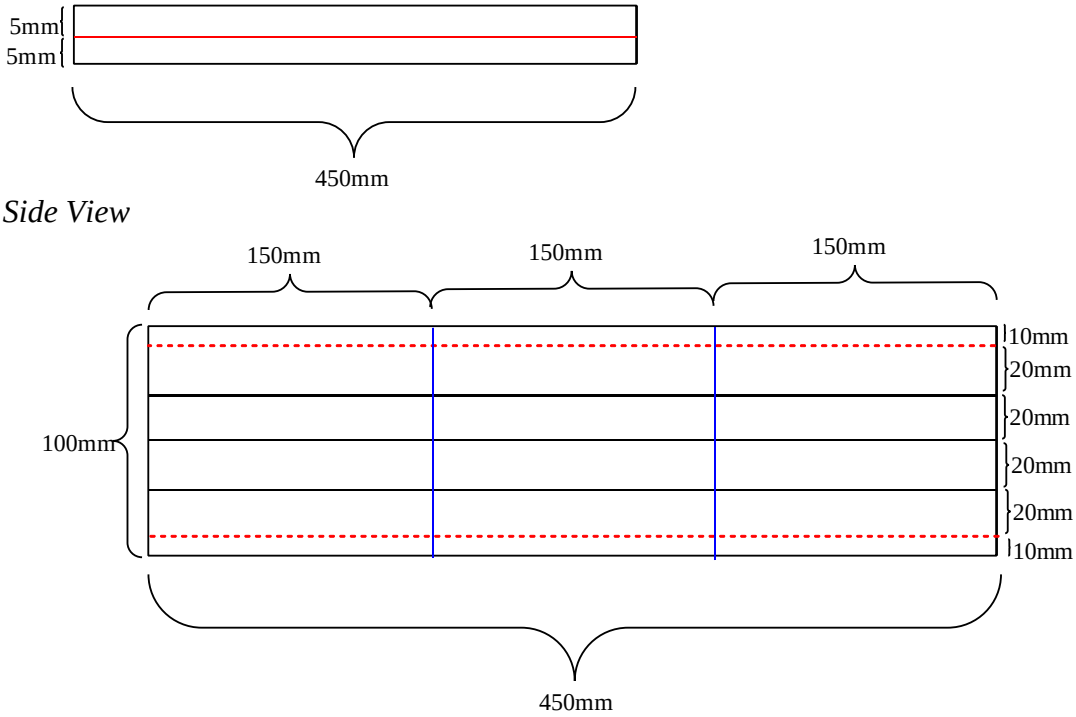

Figure 83. The test panels showing the divisions to give 12 test pieces per panel.

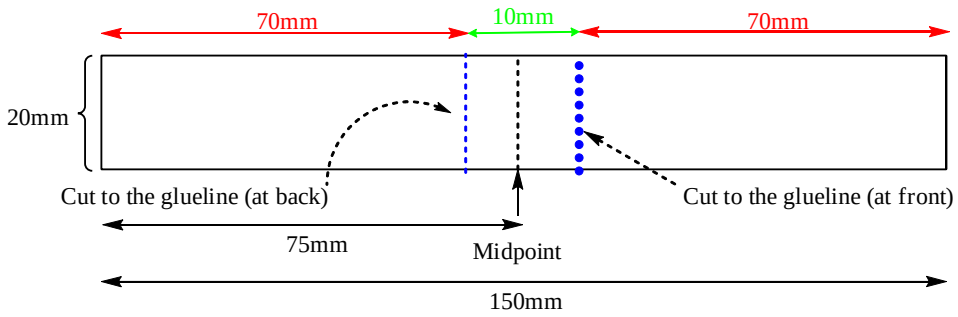

Figure 84. The test piece for the longitudinal tensile shear test showing the placement of cuts required to provide a 10 mm x 20 mm test area.

Table 34. The treatment conditions that the adhesives are exposed to prior to tensile shear testing.

Treatment Label	Treatment Description
A1	7 days conditioning at standard atmosphere[(1)]
A2	7 days conditioning at standard atmosphere 4 days soaking in water at 15±5°C Samples tested wet
A3	7 days conditioning at standard atmosphere 4 days soaking in water at 15±5°C Drying for 7 days at standard atmosphere Samples tested dry
A4	7 days conditioning at standard atmosphere 6 hours soaking in boiling water 2 hours soaking in water at 15±5°C Samples tested wet
A5	7 days conditioning at standard atmosphere 6 hours soaking in boiling water 2 hours soaking in water at 15±5°C Drying for 7 days at standard atmosphere Samples tested dry

[(1)] Standard atmosphere has been defined in the standard as a temperature of 20±2°C and a relative air humidity of 65±5%

ASTM D4502-92 Heat and Moisture Resistance Test

The determination of the resistance of the adhesives to heat and moisture were made using the methodology as outlined in ASTM D4502-92. Block shear specimens for all five adhesives were prepared using pine, Victorian Ash and Spotted gum substrates. For a more detailed description of the experimental set up and the issues arising from this test, please refer to the Results and Discussion section of this report.

Thin film methodology

Making observations on thin films

To make observations of strains on thin films which are less than 1 mm thick it is not possible to use contact strain measurement methods such as glued-on electrical resistance strain gauges as these would strongly influence the specimen behaviour. The technique employed was digital image correlation using Gom's Aramis system. This is a photogrammetric method that tracks overlapping image pairs and uses them in the same way that aerial topographic photographs are used. The image data in this case is taken digitally and read directly into a computer which processes the data all to provide displacement fields. Because most surfaces have no recognizable features these are provided by spraying a random speckle pattern that is then tracked in response to movement. The displacement gradients are given by a deformation tensor,

F, which is decomposed into a right stretch, **U**, and rotation, **R**, tensors as **F** = **R**·**U**. Strains are then extracted directly from the right stretch tensor, **U**.

The Aramis system itself consists of two cameras, Figure 85, and a computer based data collection system, Figure 86.

Figure 85. Aramis system digital cameras used to capture digital images.

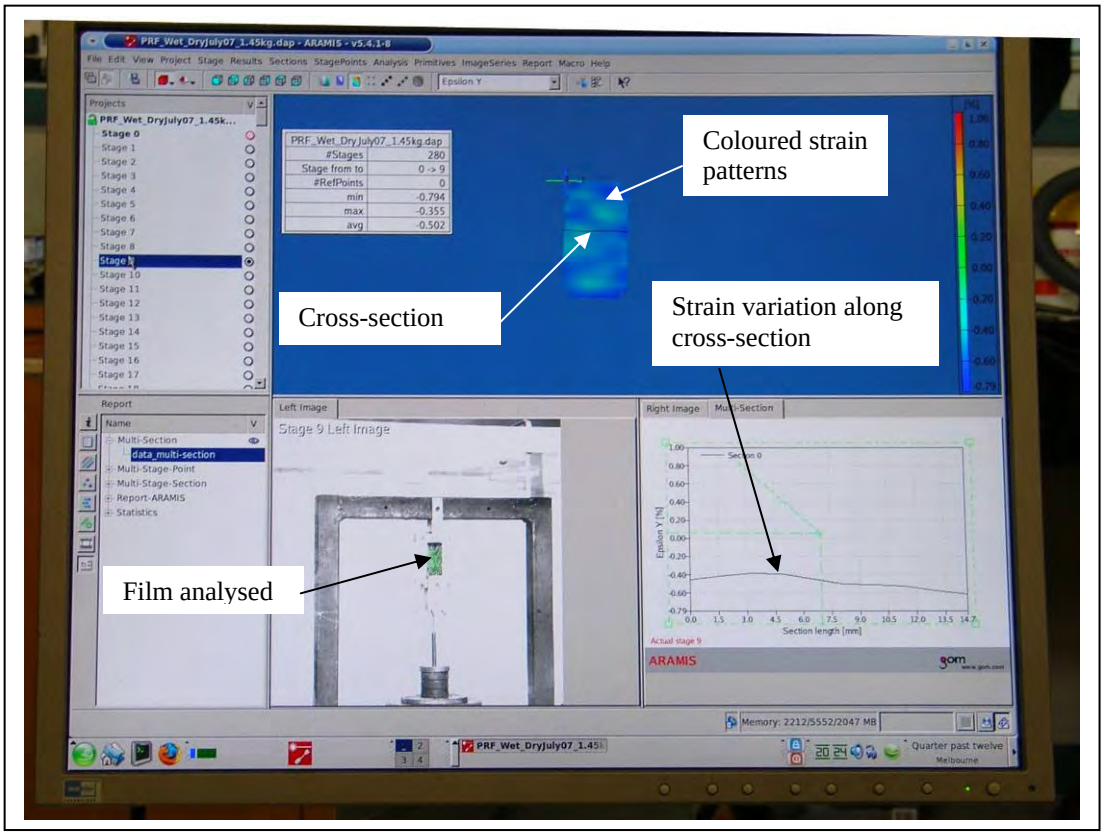

Figure 86. Screen images of computer based data collection system.

In the screen image, Figure 86, the "film analysed" refers to the object under study. The lower left window shows it coloured green which represents the area masked in as distinct from the whole window which represents the image area captured by the camera. The upper screen shows a coloured version of the masked area in which the colour coding is representative of the strain throughout the film. The cross-section line is the part of the film for which the strain is graphed in the bottom right image. The images are captured every 5 minutes over a 24 hour period; each image is called a "stage"; this stage data can be displayed by clicking on the stage number. In the example illustrated, Stage 9 has been selected.

The data from each stage is stored in a separate file by Aramis which makes it difficult to subsequently process. A system macro program has been written which enables the files to be concatenated into a single .txt file that can be read into Excel and processed into graphical output as shown later.

Making thin films

RF films

Making thin RF films is relatively straight forward. The adhesive is first mixed then de-gassed in a vacuum chamber for approximately 20 minutes. It is cast between two sheets of glass that have their surface coated with a thin film of a silicone based grease, Dow Corning 7 Release Compound. The glass sheets are separated by shims that enable a film of approximately 0.28 mm to be cast. At around 3 hours, the top

sheet of glass is removed and the semi-cured sheet is cut into strips approximately 15-20 mm wide and the glass is replaced; attempts to cut the films into strips when fully cured results in their shattering due to the brittle nature of cured RF resin. The films are then left to fully cure under the glass, see Figure 87. If the films finish their curing outside the glass there is a tendency for them to distort, Figure 87. Such films are not regarded as satisfactory for experimental purposes.

Figure 87. Thin films of PRF held between two glass sheets.

IBA films

The making of thin films of IBAs presents considerable technical difficulty due to the fact that the curing process results in the release of CO_2; this leads to formation of a large number of gas bubbles. The only method that was successful involved casting the films between stainless plates each covered with a sheet of plastic, in turn coated with the same Dow Corning 7 Release Compound used directly on the glass when casting the PRF films. The adhesive was mixed with water, 10% by weight, and stirred. It was then poured on to the lower plate plastic and placed in a vacuum chamber for sufficient time for most of the CO_2 to have formed and be drawn off, up to 40 minutes with the adhesives being investigated. The semi-solidified mass was kneaded and then compressed between the stainless plates to the finished thickness. Even by this method, CO_2 gas bubbles continue to form but these are small and dispersed. See Figure 88 for examples of films that are suitable and unsuitable for thin film studies. This particular problem was the reason that US researchers had given up on attempts to examine the stress-strain characteristics of IBA adhesives.

IBA films are quite flexible and can easily be cut with scissors from the sheets once the curing is complete.

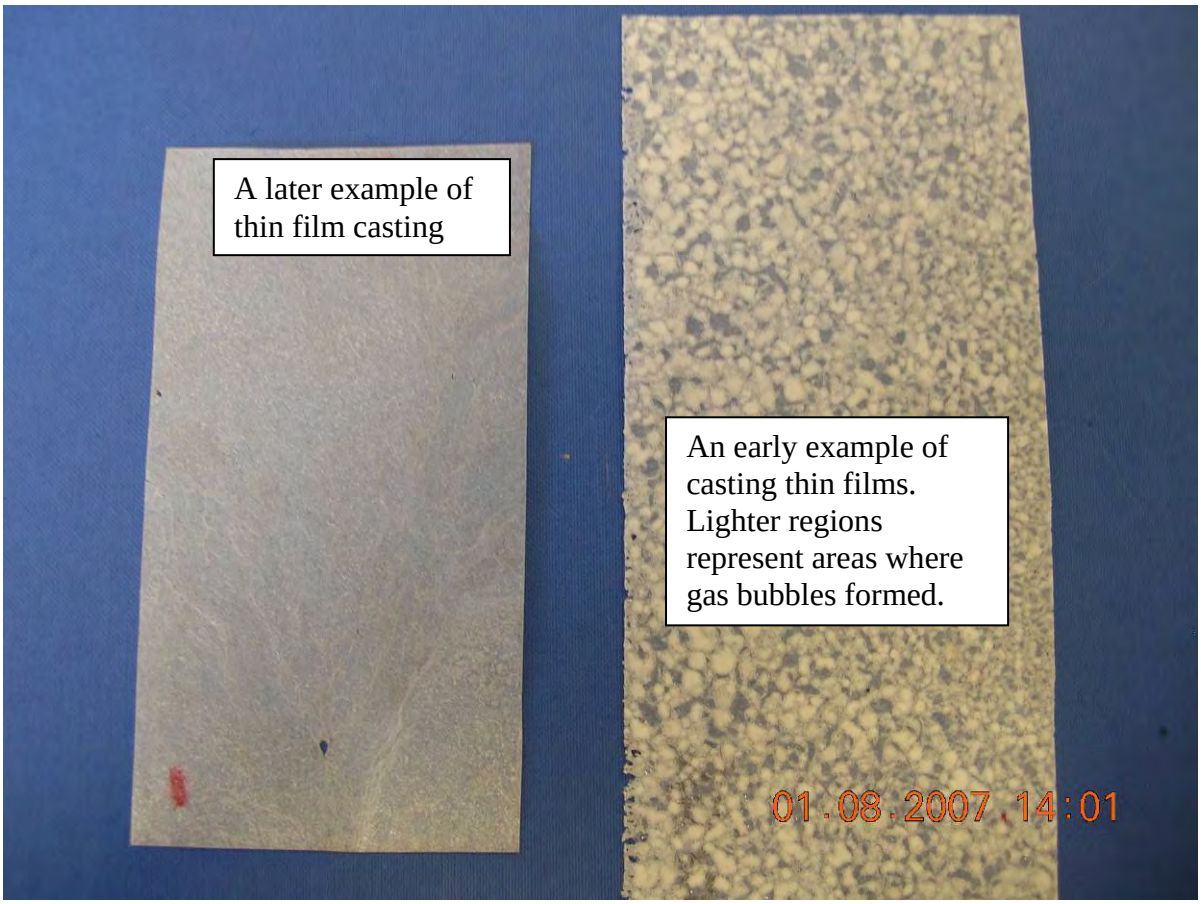

Figure 88. IBA film showing a large number of CO_2 gas bubbles.

Preparing thin films for observation

Paint spot patterns

The Aramis system determines deformations by following a random pattern of paint spots that are sprayed on the surface. The colour of the spots must contrast with that of the underlying adhesive film and a balance must be struck between the size of the spots and their density (the number of spots per unit area). Spraying on these spots is an art form and a rather hit-and-miss process. Given that observations are made over at least a 24 hour period it essential to have a trial run first to ensure that Aramis can actually make sense of the spot pattern. White artists' paint for PRF films, see Figure 88, and black or dark red for the whitish coloured IBA films. The Aramis system commences by detecting a reference pattern of speckles which it must be able to identify throughout the entire measuring process. Once this is possible the observations made can usually then be processed successfully, that is, the displacement field defined and strains extracted successfully through numerical processing of the strain tensors.

It actually takes a good deal of experience to spray effective speckle patterns. Acrylic paints were thought to have minimal effect on the film stiffness and its ability to absorb and desorb moisture.

Figure 89. PRF thin film with speckle pattern sprayed on the surface using an acrylic paint and clamped in the test rig.

Fixing the test specimen in the test rig

IBA adhesives are relatively simple to clamp between the test plates of the rig shown in Figure 89. The PRFs are more difficult to clamp as the clamping combined with the applied load, see Figure 89, and tend to cause a fracture at the edge of the clamp plate. It was found necessary to glue PRF films in place, using IBAs, to overcome this problem.

Temperature and humidity control

The observations were carried out in a temperature controlled room at 23ºC within a Perspex chamber in which saturated salt solutions were used to control humidity. A small personal fan was used to circulate air. Salts employed and expected humidity levels are given in Table 35. The use of LiCl was abandoned in the early stages given that it is difficult to handle.

Table 35. Saturated salt solutions used to control relative humidity at 20ºC and 25ºC.

Salt	Temperature and RH	
	20ºC	25ºC
Lithium chloride LiCl	11.3	11.3
Sodium bromide NaBr	59.1	57.6
Potassium sulphate K_2SO_4	97.6	97.3

Issues with controlling humidity change rate

Use of saturated salt solutions

A problem with the thin film study which has, to date, mitigated against obtaining accurate k_{sw} and k_{ms} values has been maintaining a consistent rate of relative humidity change when using saturated salt solutions. Ideally the change from low to high humidity and its converse should be instantaneous or, if this is not the case, occur at the same rates with respect to time. While saturated salt solutions ultimately provide precise RH levels the rates at which they do so can vary considerably for a variety of reasons. Thus adhering K_2SO_4 salt which leads to high humidity will build up on surfaces which means that when NaBr is introduced that there is, in reality a mix of the two of indeterminate proportions. The following statement was taken off the Internet and this refers to the simpler problem of maintaining a constant relative humidity not one where changes are required.

In practice there are some problems with saturated salt solutions. They are difficult to wash out of art objects after accidents. The salt tends to crystallise at the edges of the container. The crystals form a labyrinth that allows solution to rise by capillarity and crystallise further up the wall. Eventually the salt gets everywhere.

A less well known problem is that the salt solution is bad at dehumidifying. During this process the saturated solution begins to absorb water from the air. This dilutes the solution at the surface. The less dense surface solution is gravitationally stable and does not mix with the bulk of saturated solution, so the RH drifts upwards from the theoretical value for the saturated solution towards 100%. If the room temperature is unstable the salt solution behaves quite unpredictably, causing considerable errors when such solutions are used in experimental work to measure absorption isotherms or to calibrate instruments.

The situation can be improved by heaping up the solid salt in a cone, with just enough water to damp it. Extra solution formed by water absorption from the air will dribble down the outside of the cone, exposing a fresh crystal surface to grab more water from the air. Convective mixing can also be achieved by enclosing the saturated solution in a polymer sachet that is permeable to water molecules but not to charged ions. Thin silicone sheet is good for this purpose but now the job is so complicated that it is better to use another RH control method altogether.

Mechanical mixing is possible but messy and brings the extra uncertainty that the mixer adds heat to the solution, resulting in a higher than theoretical RH at the surface of the object being conditioned.

While data for the two IBAs seem plausible but inaccurate the PRF results are not meaningful. The matter is striking when performing the simple task determining the k_{sw} coefficients. Free shrink and free swell are usually regarded as varying linearly with changes moisture content and to be reversible. Therefore, if a linear approximation is applied to the test data, then we expect that the shrink and swell coefficients $k_{sw,swell} = -k_{sw,shrink}$ to reverse the process. This does not occur. Since k_{ms} is obtained by subtraction any errors in k_{sw} are carried forward to any determinations

made concerning k_{ms}. There exists a major problem with the salts themselves sticking to the test specimens and modifying not only the moisture content but altering specimen weight.

It is noted that Muszynski and his colleagues (see 0) at Oregon State University have reverted to mechanical air conditioning, presumably for the reasons cited in the preceding paragraphs.

Mitigation of the error and Aramis problems

The error can be minimised by performing the free shrinkage test in conjunction with the moisture gain test by placing, under zero load, on the balance. By the time this was attempted problems emerged with Aramis in that the cameras could not be focussed. Reference back to GOM in Germany, the manufacturers of the Aramis system, then required the expenditure of a further $50,000 to replace components and software which was not available meaning that this could not be undertaken. This is where the situation now sits. In addition, the closer examination of adhesives requires access to mechanical means of controlling relative humidity. What might be possible is to conduct the tests initially in a standard environment (temperature 23˚C, relative humidity 65%) with the test chamber open then to introduce moisture laden air with it closed.

Figure 90. Specimen under observation to observe weight changes.

Test program

Dealing with the mix of time and moisture varying phenomena

The test program outlined in Table 37 generally follows the overall approach by Muszynski et al (2002) but differs in some detail. All experimental observations are made by sampling data at either 5 or 15 minute time intervals and moisture content is tracked by inference. It was assumed that, provided the rate of change of relative

humidity is the same in all tests, the moisture content at any time after the commencement of the test means that it can be inferred from a separate test. The alternative approach used by Muszynski involves having a dummy specimen in the vicinity of the test specimen and to assume that its weight changes are the same as the actual test specimen. It is almost impossible to directly weigh and load a test specimen on a balance that is recording weight changes to 0.001 g. It would have been possible was to undertake the free shrink-swell test at the same time as recording weight changes but when this was attempted the Aramis equipment malfunctioned with a problem that is currently unresolved. This matter is currently being taken up with GOM who wish to replace major components of the system for a cost of around $50,000 which sum is not available.

Table 36. How time driven and pure moisture driven strain components are related in recording systems that are time based. Note that although $a(m)$, $b(m)$ are shown as constants they are regarded as functions of film moisture content.

Quantity	Physical law	How observed
ε_{sw}	$\Delta\varepsilon_{sw} = k_{sw}\Delta m$	Aramis observations, no load. Moisture content inferred separately.
ε_{ve}	$\Delta\varepsilon_{ve}(t) = a(m)b(m)t^{b(m)-1}\Delta t$	Moisture content constant thus true time varying phenomenon. Simply record strain against time.
$\varepsilon_{total} = \varepsilon_{ve} + \varepsilon_{sw} + \varepsilon_{ms}$	$\Delta\varepsilon_{ms} = \sigma\Delta m$ - mechano-sorptive component	There is a need to know how total strain varies with time and moisture content.

Details of test program

At constant RH values, tests 1 and 2, with the specimen under load only visco-elastic response is possible since the specimen will have a constant moisture level. With varying RH, tests 5 and 6, and no load the specimen will shrink or swell as it absorbs or desorbs moisture. Finally when under load and with varying moisture, tests 3 and 4, all deformation forms will be present including the elusive mechano-sorptive component which can only be obtained by a subtractive process. It is simply the strain that is left over after the other strain components have been taken out.

Table 37. Test program, temperature constant throughout.

	Conditioning (RH %)			Strain components		
Test	**Prior to test**	**Test conditions**	**Stress**	ε_{ve}	ε_{sw}	ε_{ms}
1. Creep at high RH	98	98		x		
2. Creep at low RH	20 or 60	20 or 60		x		
3. Creep low to high RH	20 or 60	98		x	x	x
4. Creep high to low RH	98	20 or 60		x	x	x
5. Free swell	20 or 60	98			x	
6. Free shrink	98	20 or 60			x	

In Table 37 the use of 20% or 60% RH reflects the fact that the original intention was to use LiCl to set the lower humidity limit. It was decided that this was too difficult as the humidity in the Perspex chamber would not drop rapidly enough. Subsequently, it was decided to limit the choice of lower humidity limit to 60% which can be achieved with NaBr.

Acknowledgements

The authors would like to acknowledge that this project has been made possible with the assistance of a large number of individuals and organizations. In particular, we would like to thank Purbond (in particular Stefan Gerber, David Macellari, Marcel Wursch, David Stewart and Darren Williams), Ashland (in particular Bill Gareis and Gary Walsworth) and Tim Goodall from Warrnambool Timbers

We would like to thank the following people from CSIRO who have assisted on the project; George Freischmidt, Muruga Muraganathan, Damien Scown, Jim Creffield, Kevin McCarthy, Mary Reilly and Gary Rabbett. We acknowledge that the PALS work was undertaken by Anita Hill, Cara Doherty, Kate Nairn, James Mardel and Tim Bastow.

Researcher’s Disclaimer

CSIRO advises that the information contained in this publication comprises general statements based on scientific research. The reader is advised and needs to be aware that such information may be incomplete or unable to be used in any specific situation. No reliance or actions must therefore be made on that information without seeking prior expert professional, scientific and technical advice. To the extent permitted by law, CSIRO (including its employees and consultants) excludes all liability to any person for any consequences, including but not limited to all losses, damages, costs, expenses and any other compensation, arising directly or indirectly from using this publication (in part or in whole) and any information or material contained in it.

Appendix A — Rate Process Method (ASTM D4502-92)

Basis of the rate process method

Stoichiometry

The reaction stoichiometry of "a" moles of adhesive A with "w" moles of water W to produce "x" moles of undesirable chemical X is represented by, Himmelblau (1962),

$$aA + wW \rightarrow xX \qquad 9.1$$

This equation is described as a second order reaction in that two molecules are involved in the reaction, A and W. The rate equation for a reaction is usually expressed in terms of molar concentrations which can be defined in the current context as the number of moles per unit area of bond line. If these concentrations are C_A and C_W the rate equation is given by

$$dC_A/dt = -k_1 C_A C_W \qquad 9.2$$

where k_1 = rate reaction constant determined by test, t = time. As implemented in ASTM D4502, it is further assumed that the water concentration is fixed. As water is used up it is replenished from the atmosphere which is effectively an unlimited supply although the concentration is fixed by the rate at which moisture can diffuse through the timber. This enables the writing of a quasi first order rate reaction equation

$$dC_A/dt = -k_2 C_A \qquad 9.3$$

Replacement of molar concentrations with shear strengths

Finally, the molar concentrations are replaced by shear stresses given the assumption that bond shear strength is directly proportional to the molar concentration. Hence, finally,

$$d\tau/dt = -k\tau \qquad 9.4$$

For an initial strength τ_0 (block shear) at time at time $t = 0$ equation 4 has the solution

$$\ln\tau = \ln\tau_0 - k(m,T)t \qquad 9.5$$

or

$$\ln(\tau/\tau_0) = -k(m,T)t \qquad 9.6$$

The constant, $k(m,T)$, where m = moisture content, T = temperature, depends on both the temperature and wood moisture content or molar concentration of water present. It is assumed that the moisture dependence is a linear one so that equation 9.6 can be rewritten, retaining the symbol, *k*, as

$$\ln(\tau/\tau_0) = -mk(T)t \qquad 9.7$$

Application of the test method to obtain the rate constants, k, for given aging temperature and moisture concentration

The test is carried out at two different moisture levels (m_1 , m_2) and at two or preferably three different temperatures (T_1, T_2, T_3) for each of the two moisture levels. To simplify the test procedure having the two moisture levels chosen are usually:

- dry or at very low moisture concentrations when temperatures in the range 100-160ºC can be used,
- fully immersed in water at atmospheric pressure when temperatures in the range 60-100ºC are available.

For fixed temperature and wood moisture content, equation 9.5 is written as $\log_{10} y = \log_{10} a + kt$ in ASTM D4502 equation 1. Given the ready availability of natural logarithms (ln) and exponential functions (exp) in Excel, it is simpler to work with these. If $t_{0.75,i,j}$ = time for strength to drop to $0.75\tau_0$ at moisture content m_i and temperature T_j from which, using equation 9.7,

$$t_{0.75,i,j} = \frac{\ln(\tau_{0.75,i,j}/\tau_0)}{m_i k(T_j)} \qquad 9.8$$

In the main text it is explained in more detail that $t_{0.75,i,j}$ is extracted after applying a least squares fit to the time versus strength data with the regression line forced through zero at time, $t = 0$. The value of $m_i k(T_j)$ is the slope of the regression line and $\ln(\tau_{0.75,i,j}/\tau_0) = \ln(0.75) = -0.2877$.

Adjustment for moisture level

Unless the moisture content of the wood under test is at 20% the estimate of $t_{0.75,i,j}$ will require adjustment. For example, if the wet test is carried out fully saturated, the moisture content is typically around 120%. Thus a corrected value of the rate constant needs to be determined, call this estimate of the time to lose 25% of initial strength $t_{0.75,j}$ which is given by

$$t_{0.75,j} = t_{0.75,i,j}(m_{test}/m_{life-estimate}) = \frac{\ln(0.75)}{k(T_j)} \qquad 9.9$$

where m_{test} = moisture content at which the wet test is conducted, $m_{life-estimate}$ = moisture content at the Service Class conditions defined in the standard. This proposal relies on the assumption that the degradation rate is linearly dependent on the wood moisture content and it also assumes that

Adjustment by the Arrhenius Law to typical service conditions

The Arrhenius Law describes the manner by which the reaction rate is affected by temperature. It takes the generalized form $k = ae^{-B/T}$ where T = absolute temperature in $^{\circ}K$ and a, B = constants. Substituting into equation 9.9 leads to

$$t_{0.75,j} = \frac{\ln(0.75)}{a} e^{B/T_j} = be^{B/T_j} \qquad 9.10$$

where $b = \ln(0.75)/a$. Taking logarithms of both sides and writing $A = \ln(b)$, leads to the essence of equation 2 of ASTM D4502, namely,

$$\ln t_{0.75,j} = A + B/T \qquad 9.11$$

By fitting the observed data to this equation, we can arrive at the time to lose 25% of the original bond strength as a function of temperature. In applying the ASTM D4502 method chemical degradation is accelerated by testing at high temperatures and this degradation rate is then used to estimate the degradation rates at lower temperatures.

Appendix B — A theoretical framework for adhesive bond line response

Basic constitutive relationship for strain increment

The basic constitutive relationship takes the incremental form

$$\varepsilon = \varepsilon_{ve} + \varepsilon_{sw} + \varepsilon_{ms} \qquad 10.1$$

ε = strain increment, ε_{ve} = visco-elastic strain increment, ε_{sw} = free shrink-swell strain increment, ε_{ms} = mechano-sorptive strain increment

Visco-elastic increment

Creep power law adopted

The visco-elastic component will be undertaken by fitting to a model having the form

$$\varepsilon_{ve}(t,m) = \varepsilon_e + \sigma a(m) t^{b(m)} \qquad 10.2$$

ε_e = elastic (immediate) strain, σ = stress level, $a(m)$, $b(m)$ = constants that depend on moisture content only, t = time, m = moisture content

Muszynski rewrites equation 10.2 as

$$\varepsilon_{ve}(t_j, m_j) = \varepsilon_e + \sigma \sum_{i=1}^{j} a(m_i) t^{b(m_i)} = \varepsilon_e + \sigma \sum_{i=1}^{j} \Delta J(t_i, m_i) \qquad 10.3$$

Viscoelastic creep at intermediate moisture levels

Viscoelastic creep is measured by observing the thin film under constant load or stress and conditions of constant moisture content and temperature, but only at the moisture levels corresponding to RH60% and RH 98%. When the RH changes the film moisture level does not change immediately and there will be periods during which there are intermediate moisture levels. At the intermediate moisture levels the a and b values are obtained by linear interpolation against the change of moisture content.

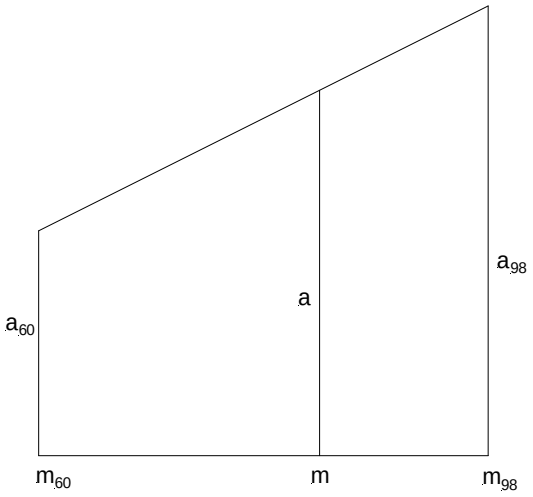

Thus $a = a_{60}\left(1 - \frac{m}{m_{98} - m_{60}}\right) + a_{98}\frac{m}{m_{98} - m_{60}}$ where m = amount by which the moisture content exceeds m_{60}. A similar interpolation is used to obtain the b value.

Free moisture shrink-swell

Free moisture shrink swell

$$\varepsilon_{sw} = k_{sw}\Delta m \qquad 10.4$$

It is measured under conditions of near zero stress $(\sigma = 0)$ at constant 23˚C and varying RH 60% → 98% and RH 98% → 60%.

Mechano-sorptive response

The basic law is given as

$$\Delta\varepsilon_{ms} = \sigma k_{ms}|\Delta u| \qquad 10.5$$

where $|\Delta u|$ = absolute value of the moisture changes.

For monotonic changes of moisture the expression simplifies to

$$\Delta\varepsilon_{ms} = \sigma k_{ms}\Delta M \qquad 10.6$$

It is measured under load at constant 23˚C and varying RH 60% → 98% and RH 98% → 60%.

Temperature and humidity

Muszynski and Shaler conducted tests at 23˚C and two humidity levels as follows:

- 23˚C and 60% RH which can be achieved in an air-conditioned room in an enclosed chamber with a saturated solution of sodium bromide
- 23˚C and 98% RH which can be achieved in an air-conditioned room in an enclosed chamber with a saturated solution of potassium sulphate

Measurement method

The mechanosorptive component of strain cannot be measured directly. Details of a testing regime that enables the mechanosorptive component to be extracted are given in Table 37. The viscoelastic free shrink swell components are measured in separate tests and the mechanosorptive component is measured by subtraction under a test environment in which all three strain components are active.

$$\varepsilon_{ms} = \varepsilon - \varepsilon_{ve} - \varepsilon_{sw} \qquad 10.7$$

Appendix C — What is achievable with stress analysis once the film properties are established?

Analysis types and indicative results

The ultimate objective of the thin studies is to provide data that is useful in stress analysis techniques specifically directed at assessing glue line performance under changing environmental conditions. Comparing the performance of PURs with PRFs could well provide insights into performance differences under long term conditions and, if successful, set objectives for adhesive manufacturers to follow in adhesive development. Two distinct physical phenomena are involved, moisture diffusion and stress analysis. The moisture diffusion analysis provides information on the depth to which changes in relative humidity produce changes in wood moisture and the depth to which these changes penetrate and the stress analysis, when used in conjunction with the data gleaned from the thin film studies and processed in an appropriate manner against mathematical models, provides information on the internal stresses such moisture changes induce.

The preliminary analyses that follow were undertaken to provide some analytical background to thin film studies taken at Monash University in connection with the project *Durability of isocyanate-based adhesives in engineered wood products*. It does not form part of the original contract which involved only the experimental observations but it does give an insight to what is achievable and the methods that need to be used in analysing the data.

Finite element analysis

Both moisture diffusion and stress analysis can be undertaken using the finite element package, Strand7. The finite element method grew out of stress analysis methods employed in aeronautical and structural design but it was quickly realised that the same differential equations governed other problems of mathematical physics, eg, stress analysis can be reduced to solutions of the biharmonic equation. Moisture diffusion analysis is only indirectly available in Strand7 which deals with the analogous problem of heat transfer in that it is mathematically modelled by the same partial differential equation. Strand7 requires data be provided in heat transfer terms.

As the Strand7 theoretical manual points out, steady state heat transfer is governed by the Laplace equation,

$$\frac{\partial}{\partial x}\left(k_x \frac{\partial \phi}{\partial x}\right)+\frac{\partial}{\partial y}\left(k_y \frac{\partial \phi}{\partial y}\right)+\frac{\partial}{\partial z}\left(k_z \frac{\partial \phi}{\partial z}\right)=0$$

This sometimes written in the more compact form $\nabla k\phi = 0$. Strand7 goes to point out that, with diffusion problems, the following analogies apply relative to heat transfer.

Field Problem	**Unknown**	k_x, k_y, k_z
Heat transfer	Temperature $(\phi = T)$	Thermal conductivity
Gas diffusion	Concentration $(\phi = C)$	Diffusion coefficient

With transient heat transfer, which is relevant to the movement of moisture through wood during diurnal and seasonal changes in relative humidity, there is an additional term on the right side of equation 1 so it becomes, replacing ϕ with T,

$$\frac{\partial}{\partial x}\left(k_x \frac{\partial T}{\partial x}\right)+\frac{\partial}{\partial y}\left(k_y \frac{\partial T}{\partial y}\right)+\frac{\partial}{\partial z}\left(k_z \frac{\partial T}{\partial z}\right)=\rho c \frac{\partial T}{\partial t}$$

T = temperature

ρ = density

c = specific heat or the amount of heat that a unit volume requires to raise its temperature by unit temperature (˚C or ˚K)

k_x, k_y, k_z = thermal conductivity

In an isotropic, homogeneous material, equation 2 reduces to

$$k\left(\frac{\partial^2 T}{\partial x^2}+\frac{\partial^2 T}{\partial y^2}+\frac{\partial^2 T}{\partial z^2}\right)=\rho c \frac{\partial T}{\partial t}$$

Moisture diffusion analysis

Moisture diffusion analysis is used to determine the ingress of moisture during diurnal and seasonal variations of atmospheric changes in relative humidity since it is basically this phenomenon that leads to movements in both glue lines and the underlying wood substrates. The underlying differential equation describing this phenomenon is Ficks Law second law which that the flow of mass by diffusion (flux), across a plane, is proportional to the concentration gradient or moisture content in the problem under consideration. It takes the general forms:

<u>for orthotropic, non-homogeneous materials</u>

$$\frac{\partial}{\partial x}\left(D_x \frac{\partial C}{\partial x}\right)+\frac{\partial}{\partial y}\left(D_y \frac{\partial C}{\partial y}\right)+\frac{\partial}{\partial z}\left(D_z \frac{\partial C}{\partial z}\right)=\frac{\partial C}{\partial t}$$

<u>for isotropic, homogeneous materials,</u>

$$D\left(\frac{\partial^2 C}{\partial x^2}+\frac{\partial^2 C}{\partial y^2}+\frac{\partial^2 C}{\partial z^2}\right)=\frac{\partial C}{\partial t}$$

C = moisture concentration (gm/gm), also the moisture content $m = M_{moisture} / M_{wood}$

D = diffusion coefficient units $mm^2 s^{-1}$

Strand7 can analyse diffusion in 2 and 3 dimensions according to equation 4.

Although diffusion rates vary for the longitudinal, radial and tangential grain directions the data is not readily available so that a simple isotropic analysis is carried out. The model analysed, Figure 91, may be thought of as a typical section of a beam subjected to environment chamber exposure at Monash and outdoor exposure at CSIRO, Darwin. Because of symmetry only one-quarter is subject to analysis with a specified moisture increment along the exposed faces, OA and AB and with no moisture transfer across the symmetric faces, BC and CO. The face BC represents the glue line. Thus the boundary conditions are

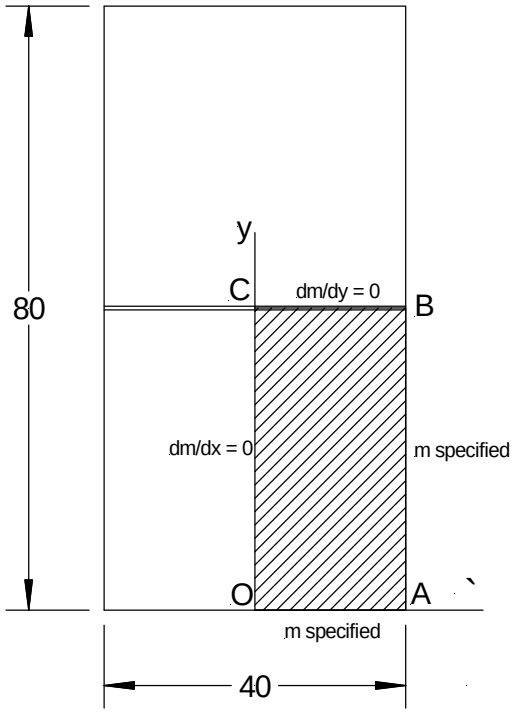

Figure 91. Typical beam subject to moisture diffusion analysis.

Typical moisture diffusion coefficients for wood

One study by Liu and Simpson[22] (1999) suggests that; with red oak (*quercus rubra*), diffusion coefficients are of the order of $D_{wood} = 0.3 mm^2/h$. No data is available for adhesives so that it is assumed at this stage that $D_{adhesive} = 0.3 mm^2/h$. It may well be and this seems to be suggested by the weight studies undertaken in conjunction with the Aramis observations that moisture diffusion rates may be both greater and less than those of some wood species. If diffusion rates are greater, then bondlines may well be a pathway along which higher moisture fluxes occur. One method for obtaining such values is described in ASTM E96-80 but did not form part of the current project.

Input of data into Strand7

Strand7, in its analysis of heat transfer, requires data to be entered separately for ρ and c in equation 3. To make the system analyse moisture diffusion the simplest approach is to enter unit density and specific heat and then use the moisture diffusion coefficients as commonly understood and as cited above.

Typical analyses of a two dimensional problem

A two dimensional analysis has been completed for the section shown in Figure 91 with a 10% increase in moisture content applied along boundaries OA and AB and a

[22] Liu, JY and Simpson, WT, (1999) Inverse determination of diffusion coefficient for moisture diffusion in wood, Proceedings of 33rd ASME National Heat Transfer Conference: Heat and Mass Transfer in Porous Media, Albuquerque, New Mexico.

zero moisture gradient across BC and CO the time steps with small ones been taken initially. This analysis has to be regarded only as indicative of the way in which moisture spreads through a cross-section in beam. Results of moisture distribution are shown for 3, 12, 24 days. This analysis implies that moisture diffusion will occur at twice the rate in the adhesive which is a pure guess. No hard data is available for diffusion coefficients of adhesives.

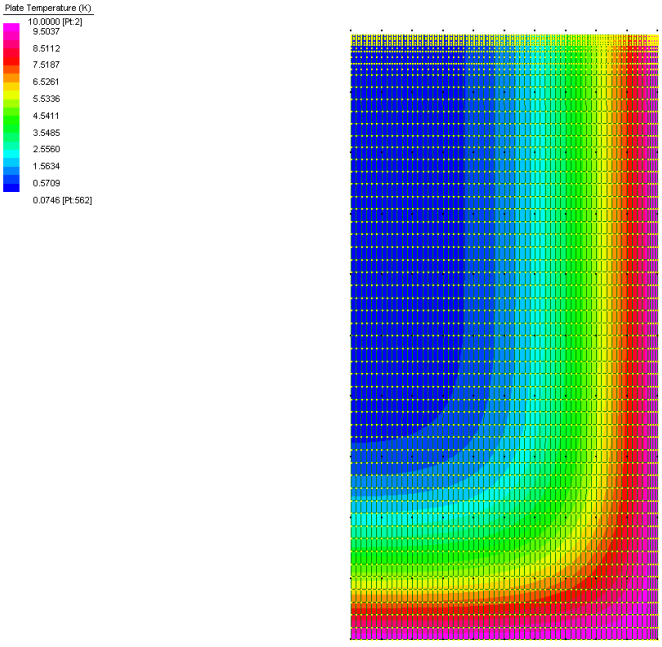

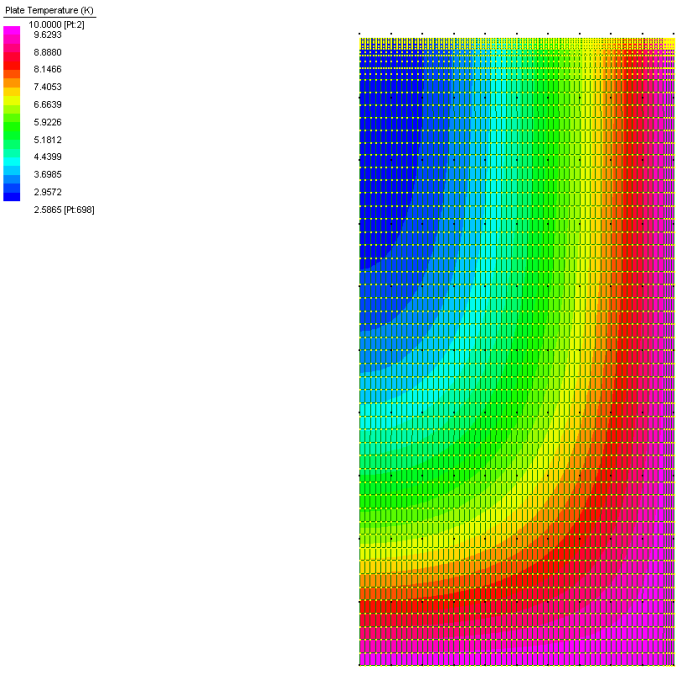

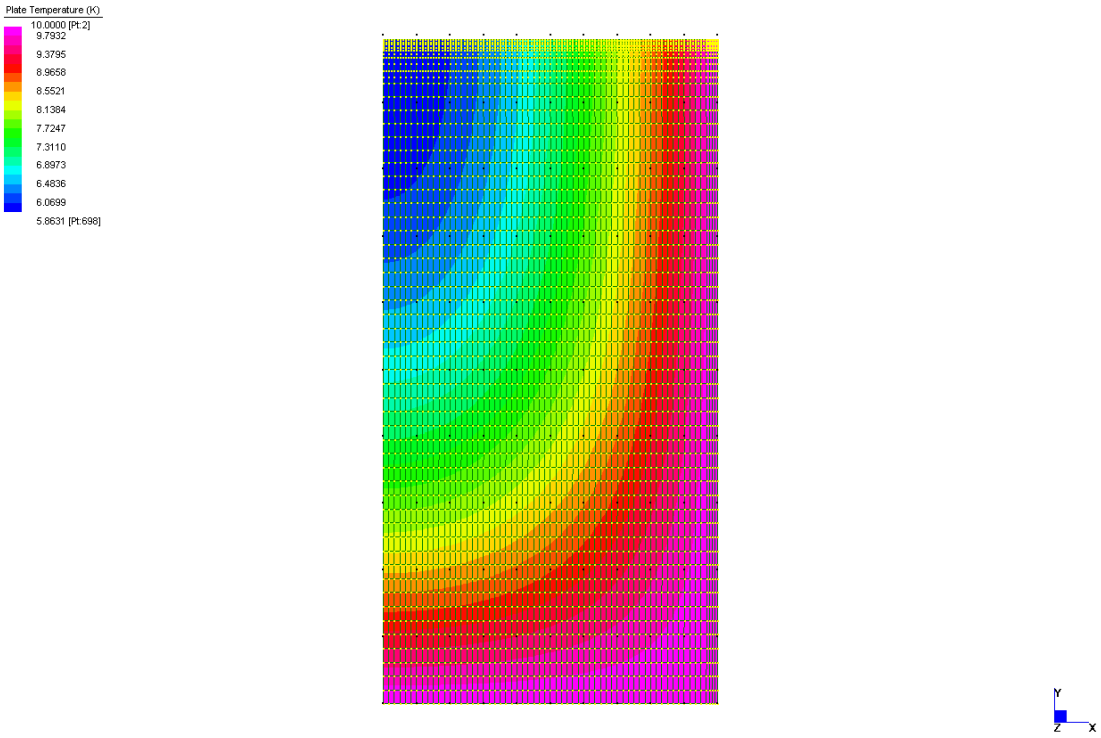

Figure 92. Diffusion contours (wood moisture content) at 3, 12, 24 days following a 10% jump in moisture content along edges OA and AB. Note that the temperature designation has to be interpreted as moisture content given that it is essentially a heat transfer analysis performed by Strand7.

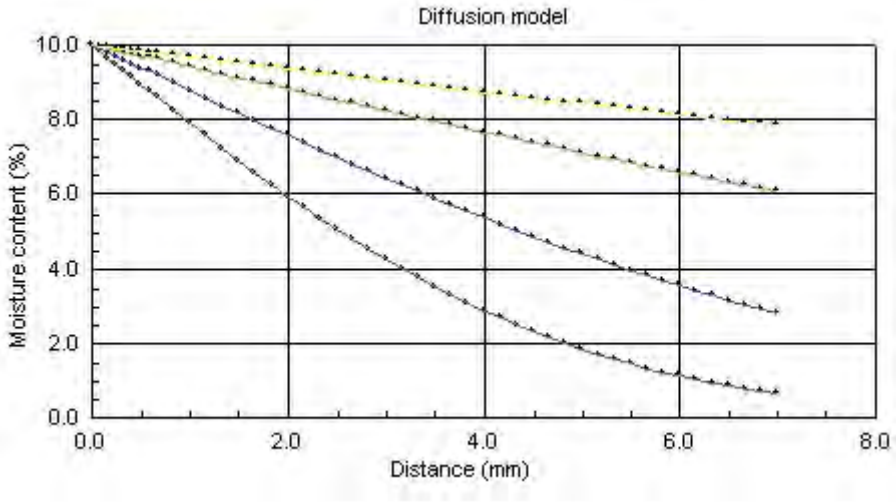

Figure 93. Variation of moisture in penetration the bond line at 1, 3, 12, 24 days.

Further developments

Further developments of the moisture diffusion study will require the collection of data on diffusion coefficients for timbers used in glulam production and for other engineered wood products. It will also require data on variation of relative humidity in various major centres. Some, if not all, of this data is expected to be available from CSIRO or Government meteorology centres. This would fed into Strand7 which has the capacity to specify specific time sequences.

Stress analysis

Because direct coupling of diffusion and stress analyses is not possible within Strand7 the analyses will need to be undertaken sequentially rather than in parallel. By direct coupling is meant that, following a time increment, a stress analysis is automatically performed followed by yet more time increments without any actions being required by the analyst. Indirect coupling requires that this action be taken manually and is not practical without exorbitant labour. For accurate analysis account has to be taken of the creep characteristics (both visco-elastic and mechano-sorptive) of both the wood and adhesive, the service environment (weather and loading) and the conditions of manufacture. At this time it must be assumed that there is zero stress at the time of manufacture, dubious assumption.

Material properties

The thin film studies were undertaken to provide a description of the physical response of thin films to changes in moisture in the presence of externally applied load with a view to their use in stress analysis. To provide a testing methodology it was decided that the Muszynski et al proposal be adopted which presumes that there are separate strain components consisting of the following form:

- free shrink-swell which is the expansion and contraction due to moisture absorption and desorption in the absence of applied external load,
- viscoelastic creep which is a combination of the strain expected according to Hooke's law but describes the later additional strains that arise with the effluxion of time,
- mechanosorptive creep which requires both applied external loads and moisture cycling and differs from viscoelactic creep in that it is not time dependent but simply depends on the number of moisture cycles.

$$\varepsilon\left(\sigma, t, MC, \Delta MC\right) = \varepsilon_{sw} + \varepsilon_{ve} + \varepsilon_{ms}$$

ε = total strain

ε_{ve} = visco-elastic strain,

ε_{sw} = free shrink-swell strain,

ε_{ms} = mechano-sorptive strain

σ = stress level, t = time,

MC , ΔMC = moisture content, moisture content increment.

The laws adopted by Muszynski et al are stated in strain velocity terms but are presented here in incremental format and take the forms

$$\Delta\varepsilon_{ve}(t) = a(m)b(m)t^{b(m)-1}\Delta t$$
$$\Delta\varepsilon_{sw} = k_{sw}\Delta m$$
$$\Delta\varepsilon_{ms} = k_{ms}\sigma\left|\Delta m\right|$$

where it is acknowledged that the constants a and b are themselves functions of moisture content.

The observations made in the thin film study used a methodology that permitted the equation 6 components of strain to be extracted. From a Strand7 perspective this cannot be readily implemented. What is more convenient is a suggestion by Bolton and Irle[23,24,25] who used a simple 4 element creep model in describing the behaviour of formaldehyde resins (PF, LAPF and UF) which takes the form

$$\varepsilon = \frac{\sigma}{E_1} + \frac{\sigma}{E_2}\left[1 - \exp\left(\frac{E_2 t}{\eta_2}\right)\right] + \frac{\sigma t}{\eta_3}$$

E_1, E_2, η_2, η_3 are all experimental constants.

Irrespective of the material constitutive relationships, if Strand7 is to be used, the only applicable analyses available are linear elastic and time varying non-linear elastic followed by a "Transient heat flow" analysis. The latter can be used to analyse visco-elastic creep and by transforming the Δm's to Δt's mechano-sorptive and free shrink-swell analysis can be included as is illustrated by Bolton and Irle. Even simpler forms of creep expressions are possible such as the expression proposed by Clouser[26]

$$\varepsilon = \frac{\sigma}{E_{t=0}}\left(1 + at^b\right)$$

Within Strand7 this is modelled by setting $E = E_{t=0} \Big/ \left(1 + at^b\right)$ varying with time, that is, the value of E becomes time varying. The initial strains caused by humidity changes are modelled as temperature changes and then to follow this with a transient heat analysis. The problem is treated as one of plain strain with a constitutive relationship of the form

$$\begin{Bmatrix} \sigma_{xx} \\ \sigma_{yy} \\ \sigma_{xy} \end{Bmatrix} = \frac{\left(E_{t=0} \Big/ \left(1 + at^b\right)\right)(1-\nu)}{(1+\nu)(1-2\nu)} \begin{pmatrix} 1 & \frac{\nu}{1-\nu} & 0 \\ \frac{\nu}{1-\nu} & 1 & 0 \\ 0 & 0 & \frac{1-2\nu}{2(1-\nu)} \end{pmatrix} \begin{Bmatrix} \varepsilon_{xx} \\ \varepsilon_{yy} \\ \varepsilon_{xy} \end{Bmatrix} - (1+\nu)\Delta m \begin{Bmatrix} \alpha \\ \alpha \\ 0 \end{Bmatrix}$$

where Δm is interpreted as a temperature change $\left(\Delta m \equiv \Delta T\right)$, α taken as a coefficient of thermal expansion which, multiplied with Δm, generates the desired level of initial strain. What is always inevitable in bonded wood products is that the wood and adhesive will always respond differently to the service environment,

[23] A. Bolton, M Irle, "Physical aspects of wood adhesive bond formation with formaldehyde adhesives. Part 1. The effect of curing conditions on the physical properties of urea formaldehyde films", *Holzforschung*, **41(3)**, 1987, 155.
[24] A. Bolton, M Irle, "Physical aspects of wood adhesive bond formation with formaldehyde adhesives. Part 2. Binder physical properties and particleboard durability", *Holzforschung*, **42(1)**, 1991, 53.
[25] A. Bolton, M Irle, "Physical aspects of wood adhesive bond formation with formaldehyde adhesives. Part 3. The creep behaviour of formaldehyde based resins at different relative humidities", *Holzforschung*, **45(1)**, 1991, 69.
[26] Clouser, WS, "Creep of small wood beams under constant bending load", Report 2150 Forest Service, Forest Products Laboratory, Madison, Wisconson, 1959.

whatever the source of initial strain. It is always possible to undertake a linear elastic analysis as given by equation 13 as an alternative to one based on equation 12.

$$\begin{Bmatrix}\sigma_{xx}\\ \sigma_{yy}\\ \sigma_{xy}\end{Bmatrix}=\frac{E(1-\nu)}{(1+\nu)(1-2\nu)}\begin{pmatrix}1 & \frac{\nu}{1-\nu} & 0\\ \frac{\nu}{1-\nu} & 1 & 0\\ 0 & 0 & \frac{1-2\nu}{2(1-\nu)}\end{pmatrix}\begin{Bmatrix}\varepsilon_{xx}\\ \varepsilon_{yy}\\ \varepsilon_{xy}\end{Bmatrix}-(1+\nu)\Delta m\begin{Bmatrix}\alpha\\ \alpha\\ 0\end{Bmatrix}$$

Whether or not a linear elastic or a visco-elastic analysis is conducted is unlikely to make much difference to the conclusions about the desirable features of the physical response to changing humidity of wood adhesives.

Analysis objective

A mathematical analysis has been carried out using finite elements analysis which involves examining what happens with thin bonded lines when a simulated "initial strain" is introduced. Whatever hypothesis is put forward to explain bond strength must be compatible with observed behaviour.

What are the most observable characteristics of glue debonding

For the mathematical analysis to be of any merit it must reflect what is observed in practice with specific reference to glued laminated timber (glulam). The observable facts are detailed in what follows.

What is observable at the macro-level?

Lamination separation

What is typically seen on the side of a glulam member undergoing debonding is lamination separation. This separation is probably seen more frequently to be occurring at the wood adhesive interface or close by. While this may be described as both an adhesive or cohesive failure the most usual feature is that it occurs close to the interface. Thus it could be expected that any stress analysis would show the stress levels close to the interface are greater than those that occur within the middle part of the glue line. The reason that it is seen more closely along the edges is because this is where the greatest moisture changes occur.

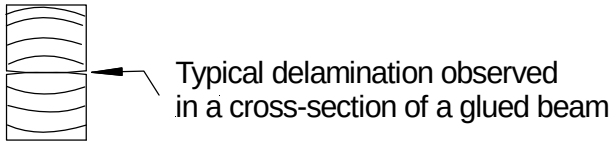

Figure 94. Bondline separation.

Shear failure

Another failure that is less common is a shear failure that occurs near supports brought about by external load application in conjunction with varying moisture levels. Loaded beams were observed to fail in shear which was identified by a step that occurred at beam ends although no such failures were observed in unloaded beams.

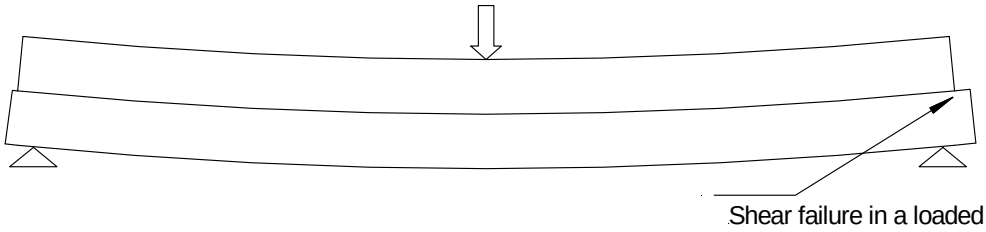

Figure 95. Outward physical sign of shear failure in a glue line as a result of applied external load in varying environmental conditions.

What is observable at the micro-level?

At the micro-level, defined in this case as what happens at the 100 micron level, is that fracture paths are most often observed close to the glue to wood interface. Using conventional language such failures can be what are described as adhesive (detachment of the adhesive from the adherend) or cohesive (rupture within the bond line itself). A further traditional classification involves failures that proceed into the adherend.

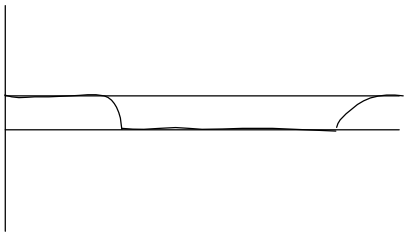

Figure 96. Typical failure observed in glue lines when debonding occurs.

Model details

Two models were investigated one with and one without creep effects included according to $E = E_0 \big/ \left(1 + 0.109 t^{0.24}\right)$. The other parameters are given in

.

Table 38. Values used in stress analysis.

Item	Analysis no creep	Analysis with creep
Model depth (mm)	80	As opposite but with both wood and adhesive governed by the creep equation: $E = E_0 \big/ \left(1 + 0.109 t^{0.24}\right)$
Model width (mm)	40	
Glue line thickness (mm)	0.5	
Wood modulus of elasticity - isotropic (MPa)	1 000	
Wood Poisson's ratio	0.2	
Glue modulus of elasticity (MPa)	200	
Glue Poisson's ratio	0.2	
Glue coefficient of thermal expansion ($/^{\circ}K$)	0.001	
Glue temperature increment ($^{\circ}K$)	-20 to 0 over 6 mm	
Maximum glue initial shrinkage strain	$-20 \times 0.001 \times 100 = -2\%$	
Wood initial shrinkage strain	0	

The model itself is shown in Figure 97 with moisture being extracted from the glue line to a depth of 6 mm and creating an initial shrinkage strain of 2% at the face exposed to a drying atmosphere. The wood itself is deemed not to shrink so that the 2% initial strain represents a glue strain that is 2% less than that of the wood strain. The beam size is close to the cross-section of beams subjected to long term tests at

Darwin and in the Monash University environmental chamber. It will be seen that the shrinkage initial strains (be these from conventional shrinkage or from mechano-sorptive action) cause highly localised effects and therefore the same model. The depth of moisture penetration, varying in a linear manner as shown in Figure 7, corresponds to the analysis result obtained in the diffusion analysis.

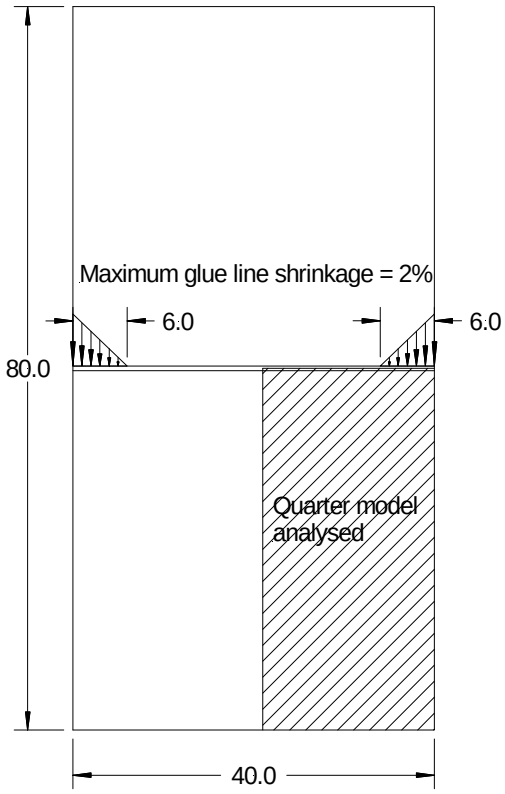

Figure 97. Full finite element model shown in "wire frame" format. The dark blue blocks represent nodes that have been allocated temperatures intended to simulate moisture penetration of the glue line to a depth of 6 mm.

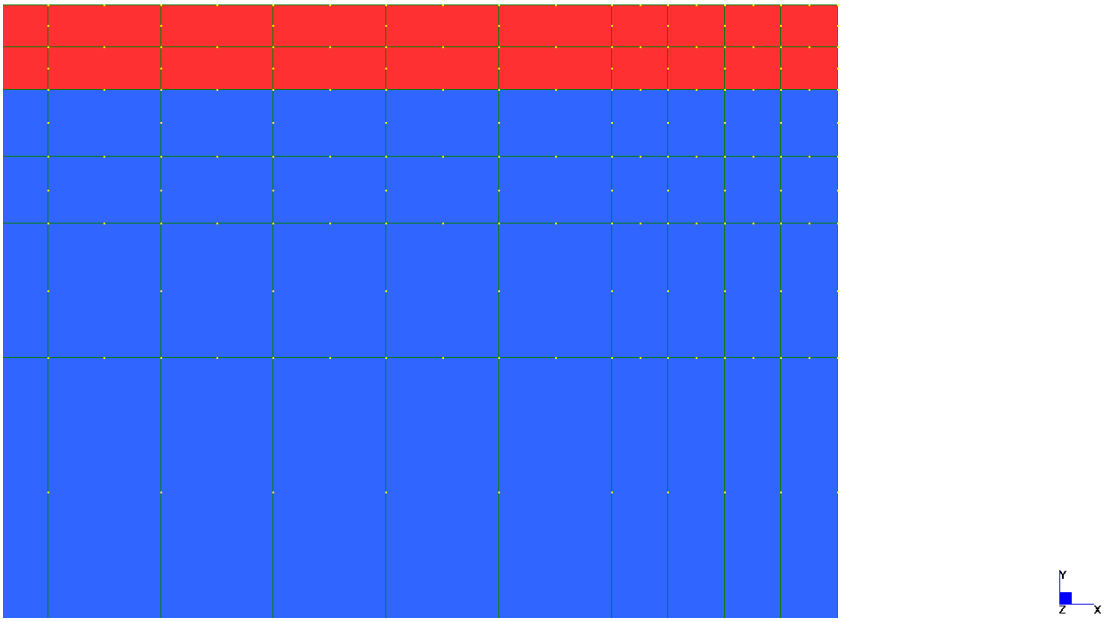

Figure 98. The model graphics in the vicinity of the top right corner of the quarter model. Blue represents wood and red the bond layer.

Analysis results

Linear analysis – "no creep"

The linear elastic solution shows high shear stress at the point D in Figure 6.

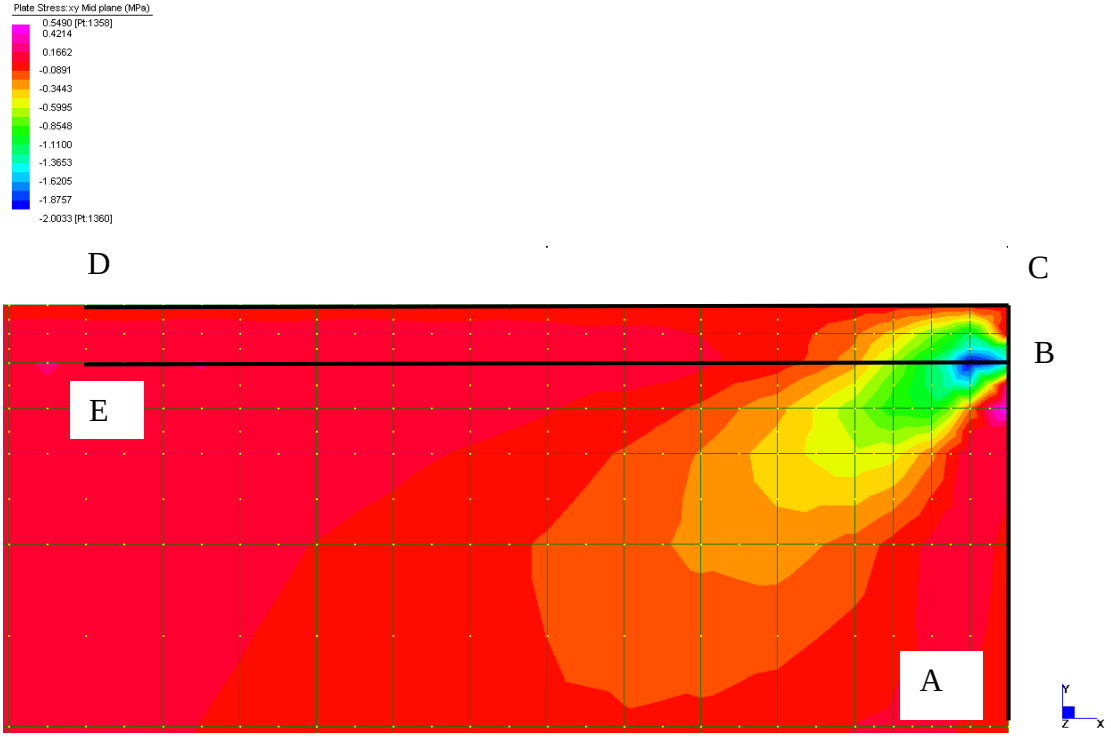

Figure 99. Shear stress contours obtained from a "no-creep" solution showing high stress regions at the outer ends.

Shear stress distribution

The shear stress distribution along B to E and C to D is shown in Figure 9. Note that the shear stress at distance 0.0mm, points B and C should be zero. The reason for this not occurring is that the finite element method lacks the capacity to record such a result. The similarity of the result along line B to E to that predicted by Volkersen[27] theory is obvious to those familiar with such theory but the low level of shear stress at the centre of the bond line is not predicted. The result is obvious given that the effect of differential movements of wood and adhesive must lead to low shear stresses along the adhesive bond line.

[27] Volkersen, O, (1938) Die niektraftverteilung in zugbeanspruchten mit konstanten laschenquerschritten. Luftfahrtforschung 15, pp41-47.

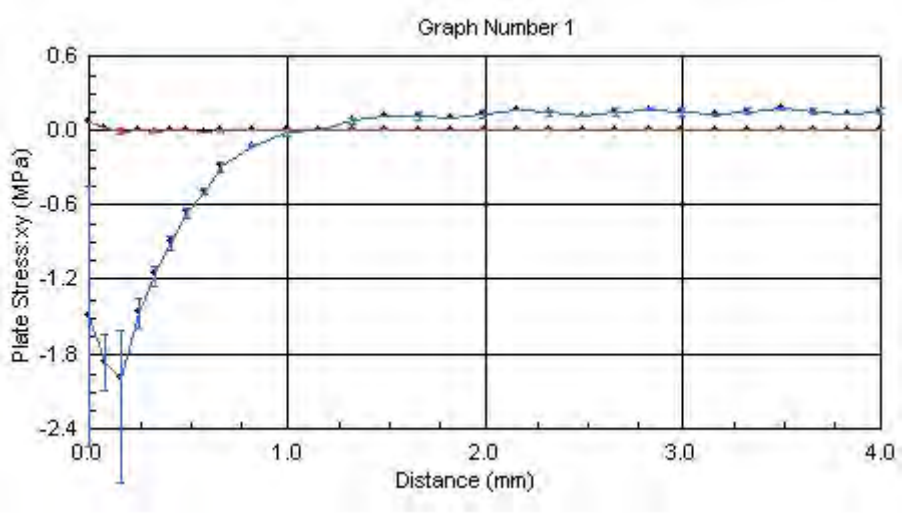

Figure 100. Shear stress along lines B to D and E to F. The line EF represents the stresses of the adhesive midway between the two adherends.

Tension stress distribution perpendicular to the glue line

The tension stress perpendicular to the grain along C to A is shown in Figure 10. It it relevant that there is a combination of both high tension and shear stress in the region of point B.

.

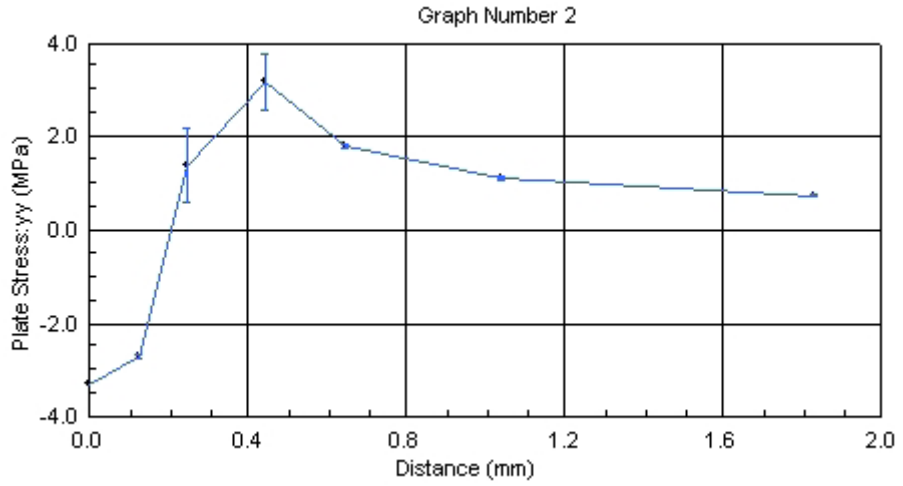

Figure 101. Tension stress perpendicular to the grain along line C to A.

Non-linear analysis – "with creep"

Creep plays a critical role in stress relief as is shown by undertaking the same stress analysis with a creep function included. The creep expression used in this analysis, $E = E_0 / \left(1 + 0.109 t^{0.24}\right)$, is taken from Soltis et al[28] and is one of many results that could have been used based on observations on Douglas Fir. The test data is fitted to an expression of the form, for relative creep, $= at^b$, observed over a 150 day period. The correlation coefficient was 0.95, which sounds excellent but it may not fit the 3 and 4 day data quite so well. Thus the analysis results should only be seen as

[28] Soltis, LA, Nelson, W, Hillis, JL, (1989) Creep in structural timber, Proceedings, Second Pacific Timber Engineering Conference, Auckland, New Zealand, pp215-221.

indicative, not absolute. The same creep function is applied to the adhesive in this indicative analysis. The chief merit of this analysis rests with it being indicative of what is important in the Aramis thin film studies.

Shear stress distribution

The shear stresses distribution along B to E is shown in Figure 11 at times 1 minute and 1 day after the simulated humidity change. Note that these stresses are significantly lower.

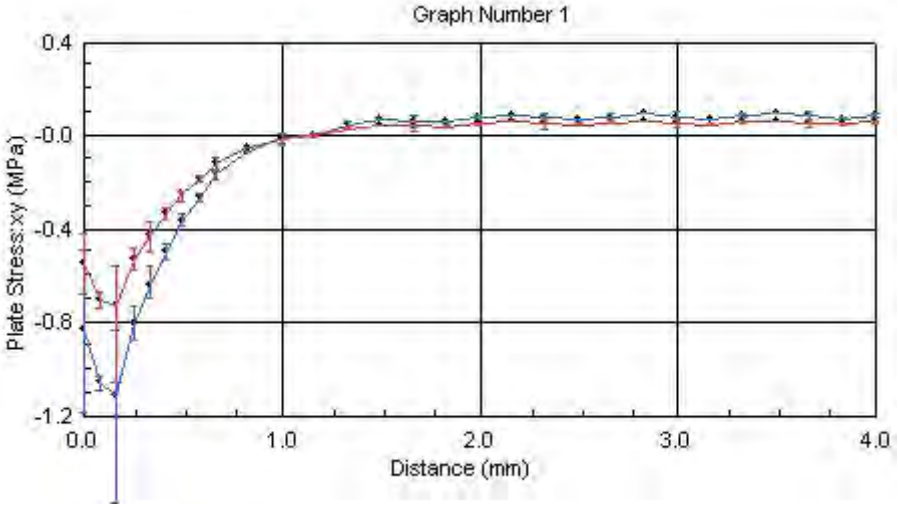

Figure 102. Shear stresses along line B to E at 1 minute and 1 day after an abrupt humidity change of the adhesive only. The wood and adhesive both creep according to at^b

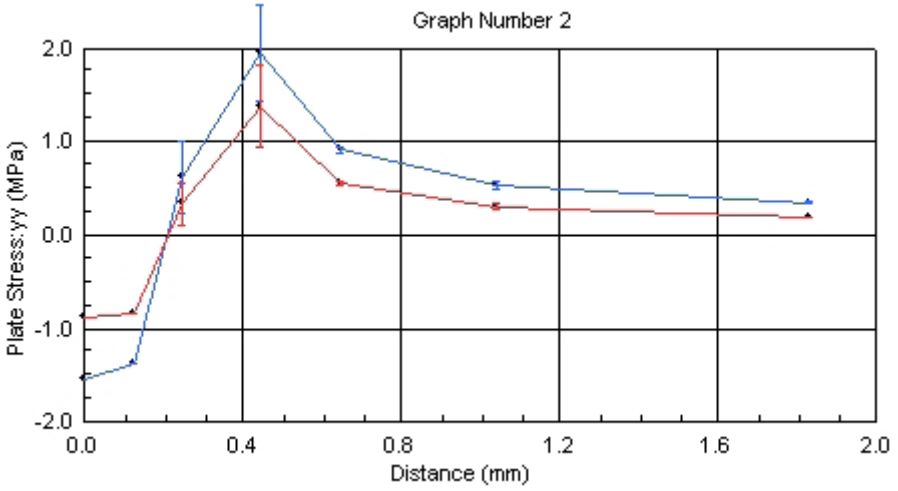

Figure 103. Tension stresses along line C to A at 1 minute and 1 day after an abrupt humidity change of the adhesive only. The wood and adhesive both creep according to at^b.

Appendix D — Box and Whisker Plots

One way of plotting data is by box and whisker plots.[29] This is a useful way of graphically depicting the distribution of data by giving 5 number summaries; the upper quartile (75th percentile), the median, the lower quartile (25th percentile) and maximum and minimum observations.

Throughout the report, the box plots are constructed as shown below. The two whiskers represent the 5-95% data range.

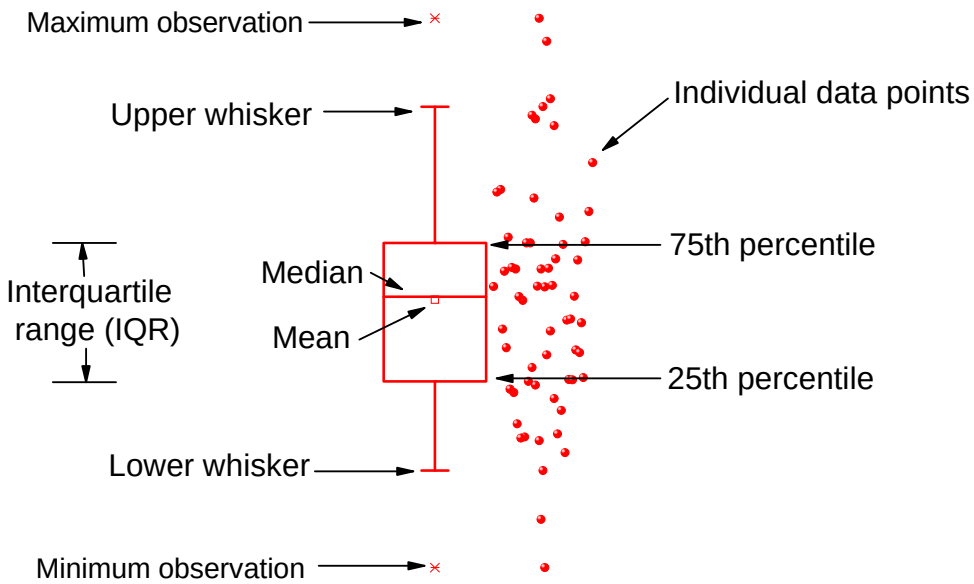

[29] See for example http://en.wikipedia.org/wiki/box_plot

Appendix E- Background on the PALS technique

PALS has been developed as a powerful tool over the past few decades for the detection and quantification of material free volume, ranging from defects on the atomic scale up to free volume elements in polymers and porosity in microporous and mesoporous amorphous and crystalline solids. In PALS, positrons (e^+), the antiparticle of the electron, are generated by an unstable isotope, typically ^{22}Na, which is marked by the simultaneous release of a positron and a 1.28 MeV gamma ray (detected as the positron birth). The positron then enters the material to be probed and in a matter of a few picoseconds reaches a thermalised state through elastic and inelastic collisions (small compared to the overall positron lifetime). Some of the positrons form positronium, an electron – positron bound state, which can exist as either ortho-positronium where the spins of the electron and positron are parallel, or para-positronium where the spins are anti parallel. The positron will eventually annihilate with an electron and its mass is converted to two 0.511 MeV gamma rays (detected as its death).

The lifetime of the positron or positronium is longer when it is localised in spaces of lower electron density, such as pores and voids. In a vacuum, the ortho-positronium lifetime is 142 nanoseconds, but in a porous material with a certain electron density, the ortho-positronium (oPs) will annihilate by pick off with an electron from the solid with the opposite spin, with the reduction in the lifetime being a function of the electron density and consequently the pore size. The intensity of this lifetime reflects the relative number of the pores. It is worth noting that the PALS technique is able to probe the porosity considered to be closed to other porosity measurement techniques, such as nitrogen adsorption, due to two features (i) oPs has a Bohr radius of 0.53Å or a van der Waals radius of 1.3Å so pores too small for N_2 are accessible to oPs and (ii) positrons are injected into the material where oPs is subsequently formed; therefore, oPs can probe internal pores that are closed to the external surface (and hence closed to N_2 adsorption). Hence PALS gives a measure of the size and number of free volume elements in the material. As the material physically ages the number of pores decreases and this is detected as a decrease in the oPs intensity (I_3). As the adhesive chemically ages due to UV degradation free radicals are produced and these inhibit oPs formation which also results in a decrease in the I_3 parameter. Hence degradation of polymers or adhesives is usually detected by a decrease in I_3.

PALS spectra consist of various exponential components, each of them due to a specific positron annihilation mode. The shortest lifetime can be attributed to para-positronium self annihilation (~0.125 ns), the second lifetime to free and trapped positron annihilation (~0.3 - 0.9 ns) and the longest lifetime or lifetimes to ortho-positronium pickoff annihilation. The average lifetimes (..and intensities (I) of the different components are obtained by applying nonlinear fit routines to the obtained spectra as a weighted sum of discrete exponentials:

$$N(t) = \sum_{i=1}^{k+1} \frac{I_i}{\tau_i} e^{(-\lambda_i t)}$$

where $_i$ is the decay rate, the reciprocal of the lifetime ($_i$). In a half logarithmic plot of the lifetime spectra, the different lifetimes are noticeable as linear fractions with different slopes.

The conversion of the lifetime to a pore size is often carried out via the quantum mechanical model of Tao and Eldrup:

$$\lambda = 2\left(1 + \frac{R}{R + \Delta R} + \frac{1}{2\pi}\sin\frac{2\pi R}{R + \Delta R}\right)$$

where R is the radius of the potential well or the pore radius and R has been found empirically to be 0.17 nm. The model of Tao and Eldrup is limited to pores of a few nanometres or less such as are typically found in polymers and adhesives.

It has been suggested that one reason why chemists are not generally aware of the extensive research on positron annihilation or the opportunities for its applications in various fields of science and technology is that most of this work is done by physicists and published in physics orientated journals.